Modelling Microbial Interactions and Food Structure in Predictive Microbiology

Promotor:

dr. ir. K van 't Riet

Voormalig hoogleraar in de Levensmiddelenproceskunde bij het departement Agrotechnologie en Voedingswetenschappen aan Wageningen Universiteit thans werkzaam als Adjunct Directeur, TNO Strategie en Programma, Delft.

Co-promotor:

dr. ir. M.H. Zwietering

Voormalig universitair hoofddocent bij het departement Agrotechnologie en Voedingswetenschappen, sectie proceskunde, thans werkzaam als Senior Researcher bij Danone Vitapole, Le Plessis Robinson, Frankrijk.

Samenstelling promotiecommissie:

Prof. dr. ir. R.M. Boom (Wageningen Universiteit)

Prof. dr. ir. F.M. Rombouts (Wageningen Universiteit)

Prof. dr. ir. M. van Schothorst (Wageningen Universiteit)

T.F. Brocklehurst (Inst. Food Research, Norwich, Engeland)

PRADEEP K. MALAKAR

Modelling Microbial Interactions and Food Structure in Predictive Microbiology

Proefschrift

ter verkrijging van de graad van doctor
op gezag van the rector magnificus
van Wageningen Universiteit, prof.dr.ir. L. Speelman
in het openbaar te verdedigen op maandag 25 februari 2002
des namiddags te half twee in de Aula.

Malakar, P.K.

Modelling Microbial Interactions and Food Structure in Predictive Microbiology

Thesis Wageningen University – with summary in Dutch

ISBN 90-5808-579-1

Abstract

Malakar, P.K. (2002) Modelling Microbial Interactions and Food Structure in Predictive Microbiology. Ph.D. thesis, Wageningen University (148 pp., English and Dutch summaries)

Keywords: modelling, dynamic models, microbial interactions, diffusion, microgradients, colony growth, predictive microbiology.

Growth response of microorganisms in foods is a complex process. Innovations in food production and preservation techniques have resulted in adoption of new technologies to ensure food quality and safety. Predictive microbiology is one such technology, where growth responses of homogenous pure broth cultures of microorganism to the environment are quantified. In this thesis an extension to this technology is investigated, where the effects of microbial interactions and food structure on the growth of microorganisms is quantified.

Microbial interactions in broth culture were studied in a model system consisting of a lactic acid bacterium and an enterobacter. Knowledge of the kinetics of pure culture growth of these microorganisms was used to simulate growth of these microorganisms in a mixed culture. These simulations were performed using a set of coupled differential equations, and the simulations compared to experimental results. Both simulations and experimental data showed that microbial interactions only started to affect growth at high population levels (> 10^8 cfu.ml^{-1}).

The effect of food structure was studied by investigating bacterial colony growth of a lactic acid bacterium. Diffusion is an important transport mechanism for colony growth and a non-invasive technique for measuring lactic acid concentration in a colony was developed. Further, the same technique was used for measuring an effective diffusion coefficient of lactic acid in a gel system capable of supporting bacterial colony growth. This diffusion coefficient was used for simulation of growth of bacterial colonies, in which growth and transport processes were adequately characterized by a set of coupled partial differential equations.

These simulations were also compared to experimental results. Both simulations and experimental data showed that transport limitations only affected growth in large colonies made up of more than 10^6 cells. These large colonies arise from low initial contamination levels.

The models and techniques developed in this thesis will be of importance to predicting microbial safety and quality of foods.

Contents

INTRODUCTION:

Modelling microbial interactions and food structure in predictive microbiolgy

1. Motivation

Progress and change go hand in hand. The present market place has changed considerably since the turn of the 20th century. Improvements in transportation meant that foods could be distributed over longer distances, increasing availability to consumers. This has then driven technological innovations to keep this valuable commodity from spoiling, have an acceptable shelf life and still make profits for the food manufacturers, food distributors and supermarkets. This in turn heightened the expectations of the consumer, which in turn led to further innovations.

Since Pasteur demonstrated quantitatively that certain microorganisms spoilt foods, we have managed to continually improve microbial food quality and safety using combinations of physical, chemical and biological (fermentation) means. Now the trends are moving towards more convenience (ease of preparation, satisfactory shelf life) and less processed foods. These foods must be of higher quality, having better flavour, texture and appearance. Another important factor is freshness and use of less artificial additives. And last but not least, it has to be safe.

These changes in consumer preferences pose challenges to food manufacturers. Traditionally, the intrinsic and extrinsic hurdles built into foods allowed the food manufacturers to have confidence in achieving their food safety objectives. Catering to these new trends may lead to an ineffectiveness of one or more of these safety factors. One response from food manufacturers has been to incorporate milder processing steps and to rely on new and novel combination of

hurdles (Leistner 1994) to microbial growth, to control and stop microbial proliferation in foods. Some of the hurdles currently in use are *pH*, water activity, bacteriocins, low temperature and modified atmosphere packaging. Table 1 summarizes some of the major existing and new technologies for food preservation. Food design is an iterative process and Leistner (1994) demonstrates how this can be done using an integrated approach. He proposes the following tools, namely hurdle technology, predictive microbiology and HACCP principles.

In this thesis we will concentrate on predictive microbiology and trying to question the validity of some of its intrinsic assumptions. Current models in predictive microbiology often do not incorporate the effects of microbial ecology and food structure. Under certain conditions, these factors may play an important role in determining the safety of a food product

Table 1: Major existing and new technologies for food preservation (Gould 1995)

Restriction of access of microorganisms to products
Aseptic packaging of thermally processed foods
Packaging
Inactivation of microorganisms in products
Heat pasteurization and sterilization
Ionizing radiation
Addition of enzymes (e.g. lysozyme)
Application of high hydrostatic pressure
Electric shock treatments
Slowing down or prevention of growth of microorganisms in products
Lowered temperature-chilling and freezing
Reduced water activity-curing, conserving, drying
Acidification
Fermentation
Vacuum and modified atmosphere packaging
Addition of preservatives
Microstructure control in water-in-oil emulsions

2. Microorganism growth

2.1. Predictive microbiology

Traditionally the data on growth and survival of microorgansims in foods were quantitatively limited and only relevant to the food system under investigation. An exception was the thermal death kinetics of spores, which is still extensively used in the canning industry. Here the concept of D, z and F values is used routinely to ensure product safety. In foods, which do not undergo such severe heat treatment, challenge testing was the preferred method to assess microbial safety. However there are many problems associated with this method. These problems include the choice of strains to use, the history of the innoculum and innoculation method and counting methods.

Challenge testing is also time consuming as well as an expensive procedure. Nowadays, most of the novel and new foods in the market place are not shelf stable and require low temperatures to ensure safety and adequate shelf life. These foods also have additional hurdles built into them. Challenge testing for all ranges of these hurdles will be prohibitive if it needs to be done for every new food.

Predictive microbiology is a more structured manner of doing the same type of analysis. It offers a quantitative, transparent and systematic approach to predicting growth and survival of microorganisms in foods. Predictive microbiology also requires a multidisciplinary effort. It brings together expertise in microbiology, mathematics, computer science, food science and engineering. There are now extensive databases available for the growth and survival of pathogens in foods (McClure et al. 1994). These databases can be easily accessed by researchers worldwide and are increasingly being used in the development of hazard analysis critical control points (HACCP) programs (Baker 1995). HACCP programs are becoming mandatory in many countries.

These quantitative predictions are also being used in quantitative microbial risk assessment studies to assess the probability of being ill from consuming certain foods. Another exciting area is the development of computer expert systems, which combine both the quantitative data from predictive microbiology

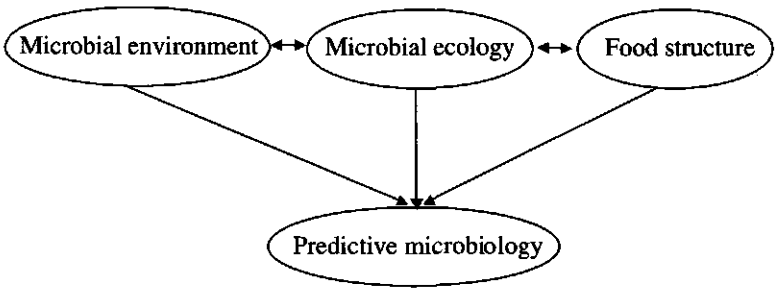

Fig. 1: Present domain of predictive microbiology. Knowledge of the microbial environment, microbial ecology and food structure specifies the growth response of a microorganism. However there are also complex dependencies between these variables. The type of nutrients available (microbial environment) determines which microorganisms (microbial ecology) can grow in a food. The type of food (food structure) determines the strains of microorganisms that can colonize the food. The microbial environment on the surface of a food is different from that inside a food.

and expertise of food microbiologists. Fig. 1 shows the current domains of predictive microbiology. We assume that if we can specify the microbial environment, the microbial ecology and food structure, it would be possible to predict the future behaviour of the microorganism.

The microbial environment consists of the initial state of the intrinsic and extrinsic variables of the environment (Jay 2000) where a microorganism is found. Intrinsic variables are the natural condition of the food. These can be the *pH*, water activity and nutrient content of the food. The extrinsic variables are the ones that are imposed on the food. These can be the temperature, atmospheric gaseous composition and relative humidity.

Microbial ecology is the study of the presence and interactions of the variety of microorganisms that can grow in or on the food. The food structure controls how the environmental variables act on the microorganisms. Growth in broth culture is different from growth on the surface of the food. At present the knowledge of the effects of microbial ecology and food structure is limited. Fig. 1

also shows that microbial growth in foods is a complex phenomenon, with dependencies among all the variables. In predictive microbiology, this complexity has been reduced by the use of simplifying generalizations.

2.2. Microbial environment

Currently we assume microbial growth can be quantified by the effect of the environmental conditions only. This interaction is summarized by mathematical equations where these conditions act as the independent variables. The current environmental variables built into these models are temperature, aw and *pH*. In some cases, nitrite and lactic acid concentration and gas composition data are also included. Roberts (1995) states that this strategy has worked quite well, when validated against growth in real foods. The deviations from using these models in practice compared favourably to deviations measured in microbiological experiments.

These models do have predictive ability as we can perform interpolation to analyse growth in conditions not tested for. However care must be taken when interpolating near the edge of the domain of the models (Baranyi et al. 1996). These models are very useful in giving first estimates of microbial growth (order of magnitude calculations) and can also be used for the planning of challenge tests if required. Product development time can be shortened, which means savings to food manufacturers. These empirical models are, however not only useful to food manufacturers and researchers. They can also serve as an education tool for students, food handlers and the public. One can show easily how certain practices will allow the proliferation of pathogens. This is especially important as inappropriate handling after leaving the factory causes many food poisoning cases. So, by only considering these environmental variables, these models are able to provide for better management of food safety.

2.3 Microbial ecology

The complex diversity of microbial interactions is often not taken into account in predictive microbiology. Foods are generally able to support a

diversified microbial ecosystem. It is also a complex material in most cases and is nutrient rich. As in all scientific endeavours, this complexity has to be reduced in order to explore the underlying trends.

This idealization involves the use of pure cultures or a cocktail of the same species in a homogenous environment. This homogenous environment is the semi-defined or defined laboratory medium, where conditions are optimal for the growth and enumeration of the particular pure culture. Given this idealized situation, we are then able to test the responses of the microorganism to various environments. The main reason for using this method is the reproducibility of the results. Given a certain set of growth conditions, the growth response of the microorganism will always be the same within a certain time interval. The reproducibility of results allows for structured analysis, whereby different phases of growth may be studied independently.

We then extrapolate this type of behaviour to mixed growth conditions in real foods. Some researchers have raised some objections to this practice (Fleet 1999, Kilsby 1999). There is abundant evidence in literature to show that microbial interactions modify the growth of microorganisms. One of the oldest is the fermentation of foods. Fredericson and Stephanopoulos (1981) give a very succinct summary of the various types of interactions occurring between microorgansims and Table 2 gives the description of some of these modes of interactions. Most of these interactions have been extensively studied in continuous cultures. One typical study is the dynamic analysis of two bacterial populations in a chemostat responding to changes in operational conditions by Yoshida et al. (1979)

Most of the studies in foods on microbial interactions are geared towards the elucidation of the mechanism of interactions. Two populations are grown together and the growth in the mixed culture is compared to growth in pure culture and if interaction occurs the compound that causes the interaction is isolated. This is usually the end point of the investigation (Gram and Melchiorsen 1996). Other authors investigated further the effect of these compounds on the growth rate of either population (Beal et al. 1994, Breidt and Fleming 1998). Quantitative data on the multi dimensional effects of the environmental variable on microbial

interactions is however quite sparse. Thomas and Wimpenny (1993) showed an interesting method of investigating competition between bacteria as a function of the temperature, salt concentration and *pH*.

The following are two recent quantitative studies of microbial competition as a function of the environment. Buchanan and Bagi (1997) modelled the decrease of the maximum population density of *Listeria monocytogenes* by *Carnobacterium piscicola* as a function of the *pH*, temperature and NaCl concentration. They concluded that the extent of suppression was dependent on the relative growth

Table 2: A few types of interaction found in mixed populations of microorganisms

Interaction	Description	Comments
Competition	Growth of two or more populations, mutually exclusive as they strive for a common factor required for growth	Usually leads to the establishment of a population of single species.
Neutralism	When the growth of two species has no effect on each other	Examples of neutralism have not been documented to occur in nature but this type of interaction has been demonstrated in the laboratory
Amensalism	This interaction occurs when one species retards the growth of another species	Inhibition of growth on one species by another can be the result of a number of factors such as excretion of toxic products or change of culture environment. Does not lead to stable mixed cultures
Mutualism	The growth of each species in the mixed culture is promoted by the other	Interactions range from a symbiotic relationship where two species are totally dependent on one another up to a loose cooperative relationship. Commonly found in mixed cultures used for single cell protein from methanol and methane and in yoghurt fermentation

rates of the individual species. If *L. monocytogenes* grew faster under a set of environmental conditions, the extent of suppression was smaller.

Pin and Baranyi (1998) compared the growth response of some groups of bacteria found on meat as a function of the *pH* and temperature when grown in isolation and grown together. They used a statistical *F* test to show if the difference in the growth rates in mixed cultures were significant. This allowed them to identify which strains were dominant under certain sets of *pH* and temperature.

2.4.Food structure

Many food products are not homogenous. Predictive modelling is generally performed using homogenous broth cultures. We assume every cell in the broth culture is exposed to the same conditions. Any changes in the broth are transmitted instantaneously either by diffusion or with the help of physical agitation. However, not all foods are amenable to these conditions. Most foods have physical structures, which entrap microorganisms and retard diffusion.

In sausages, a solid matrix will bind bacteria initially found on the surface of meat. In these conditions colony formation takes place and in time, gradients of substrates and products will occur. These gradients will eventually have an impact on the growth rates of the microorganisms in the colony.

In water in oil emulsions, the microorganisms can be entrapped in the water fractions. The resulting microenvironment and its changes in time will also have an impact on the growth of microorganisms.

3. Aim of thesis

Complexity was reduced in predictive modelling to give a workable model, where the contributions of the microbial ecology and structure are neglected. It is questionable if this is a justified assumption or just an experimental expediency. In food microbiology, the numbers of microorganism present in foods are used as an indicator of quality and safety within a specified maximal level. If microbial ecology and structure only show an appreciable effect on the growth of a microorganism after this level is reached, then the above assumption is justified.

Ross and McMeekin (1994) cite a number of cases where microorganisms only affect the growth of other microorganisms at high population densities. So, the question to be answered is when do interactions occur and are they relevant for predicting either food safety or food spoilage.

In this thesis, we will attempt to quantify when microbial interactions and gradient effects occur. We define that interaction takes place when the growth rate of one of the microorganisms deviates by 10 % from its maximum growth rate given the product environmental conditions. To measure the effect of microbial ecology we will follow the growth of two model microorganisms and quantify when the growth of one of them differs by 10% from its maximal rate.

To measure the effect of food structure, we will study the diffusion of nutrients into bacterial colonies and diffusion of byproducts of bacterial metabolism out of the colonies. Eventually these transport processes will create a concentration gradient across a colony resulting in a range of growth rates within. Here we will follow the growth of bacterial colonies in a model solid substrate and attempt to quantify when growth also deviates by 10% from the maximal rate.

4. Outline of thesis

In the first part of this thesis (Chapter 2 and 3), the microbial interactions of two model microorganisms will be investigated in a broth culture. These microorganisms are *Enterobacter cloacae* and *Lactobacillus curvatus*. In this mixed culture system *L. curvatus* produces lactic acid, which will inhibit the growth of *E. cloacae*.

Chapter 2 deals with the growth kinetics of pure cultures of these microorganisms. Here growth will be modelled as a function of the environmental factors in a broth culture. These are the substrate concentration (glucose), the *pH* and the lactic acid concentration. The temperature will be kept constant.

The growth kinetics of these two microorganisms will be then used for predicting the growth of these microorganisms together in a mixed broth culture in Chapter 3. The growth of these two microorganisms will be characterized by a series of differential equations. These differential equations will be solved

analytically and numerically and for both methods, the numbers and time when interaction occurs will be compared to experimental results.

In the second part of the thesis (Chapter 4, 5 and 6), colony growth of *L. curvatus* in a model solid medium will be investigated. *L. curvatus* cells will be immobilised in growth media with agar or gelatine as the gelling agent. A non-invasive method using fluorescence ratio imaging will be used to confirm that gradients of *pH* do form in colonies. This technique will be the topic of Chapter 4.

In Chapter 5, the diffusion of lactic acid in a buffered system will be investigated. In Chapter 6, growth, lactic acid production and concurrent diffusion of lactic acid in a colony will be modelled by a set of partial differential equations. A pseudo steady state approach will be compared to the numerical solutions and experimental results.

The thesis will end with a general discussion and summary of the research.

5. Reference

1. Baker,D.A. 1995. Application of modelling in HACCP plan development. Int. J. Food Microbiol. 25: 251-261.
2. Baranyi,J., Ross,T., McMeekin,T.A., Roberts,T.A. 1996. Effects of parameterization on the performance of empirical models in predictive microbiology. Food Microbiol. 13: 83-91.
3. Beal,C., Spinnler,H.E., Corrieu,G. 1994. Comparison of growth, acidification and productivity of pure and mixed cultures of *Streptococcus salivaius* subsp. *thermophilus* 404 and *Lactobacillus delbrueckii* subsp. *bulgaricus* 398. Appl. Micobiol. Biotechnol. 41: 95-98.
4. Breidt,F., Fleming,H.P. 1998. Modeling of the competitive growth of *Listeria monocytogenes* and *Lactococcus lactis* in vegetable broth. Appl. Environ. Microbiol. 64: 3159-3165.
5. Buchanan,R.L., Bagi,L.K. 1997. Microbial competition: Effect of culture conditions on the suppression of *Listeria monocytogenes* Scott A by *Carnobacterium piscicola.* J. Food Protect. 60: 254-261.
6. Fleet,G.H. 1999. Microorganisms in food ecosystems. Int. J. Food Microbiol. 50: 101-117.

7. Fredrickson,A.G., Stephanopoulos,G. 1981. Microbial competition. Science 213: 972-979.
8. Gould,G.W. (ed) 1995. New methods in food preservation. Chapman and Hall, London.
9. Gram,L., Melchiorsen,J. 1996. Interaction between fish spoilage bacteria *Pseudomonas* sp. and *Shewanellla putrefaciens* in fish extracts and on fish tissue. J. Appl. Bacteriol. 80: 589-595.
10. Jay,J.M. 2000. Modern food microbiology. Aspen publishers, Inc. Maryland, USA.
11. Kilsby,D.C. 1999. Food microbiology: the challenges for the future. Int. J. Food Microbiol. 50: 59-63.
12. Leistner,L. 1994. In: Food Preservation by combined Processes, (ed) Leistner, L. and Gorris, L.G.M. Final report of FLAIR concerted action no.7, Sub-group B, EUR 15776 EN p.1.
13. McClure,P.J., Blackburn,C.D., Cole,M.B., Curtis,P.S., Jones,J.E., Legan,J.D., Ogden,I.D., Peck,M.W., Roberts,T.A., Sutherland,J.P., Walker,S.J. 1994. Modelling the growth, survival and death of microorganisms in foods: the UK Food Micromodel approach. Int. J. Food Microbiol. 23: 265-275.
14. Pin,C., Baranyi,J. 1998. Predictive models as means to quantify the interactions of spoilage organisms. Int. J. Food Microbiol. 41: 59-72.
15. Roberts,T.A. 1995. Microbial growth and survival: Developments in predictive modelling. Int. Biodeterioration & Biodegradation. 36: 297-309.
16. Ross,T., McMeekin,T.A. 1994. Predictive microbiology. Int. J. Food Microbiol. 23: 241-264.
17. Thomas,L.V., Wimpenny,J.W.T. 1993. Method for investigation of competition between bacteria as a function of three environmental factors varied simultaneously. Appl. Environ. Microbiol. 59: 1991-1997.
18. Yoshida,T., Rao,B.S.M., Ohasa,S., Taguchi,H. 1979. Dynamic analysis of a mixed culture in chemostat. J. Ferment. Technol. 57: 546-553.

Modelling the interaction between *Lactobacillus curvatus* and *Enterobacter cloacae*: Part I: Individual growth kinetics

Abstract

Mixed cultures of *Lactobacillus curvatus* and *Enterobacter cloacae* were chosen as a model system to quantitatively study microbial interactions involved in food spoilage and food preservation. In this paper models were developed to predict the individual behaviour of *L. curvatus* and *E. cloacae* in pure suspension cultures as a function of the glucose and lactate concentration and the *pH*. In a second paper these models will be used to predict the moment of interaction in mixed suspension cultures and the cell concentrations at this moment.

The effect of *pH* on the maximum specific growth rate could be described by a parabolic equation for *L. curvatus* and *E. cloacae*. *E. cloacae* is clearly more sensitive to a *pH* decrease than *L. curvatus*, as may be concluded from the theoretical minimum *pH* for growth of 5.6 for *E. cloacae* and 4.3 for *L. curvatus*. For both organisms no effect of glucose on the maximum specific growth rate could be detected and Monod kinetics with a low Monod constant was assumed. For *L. curvatus* the effect of lactate on the maximum specific growth rate at different initial *pH* values could be described by a linear relationship. For *E. cloacae* a slight effect of lactate on the maximum specific growth rate could only be detected at *pH* 7. However, this effect was negligible compared to the effect of the *pH*. For both organisms the lag time was modelled by the inverse of the specific growth rate. It can be concluded that, with regard to interactions between *L. curvatus* and *E. cloacae*, the *pH* is likely to be the most important factor in case *L. curvatus* is the dominant organism. Substrate limitation is likely to become

Published: Int. J. Food Microbiol. 1999. 51:53-65
Authors: Martens,D.E., Beal,C., Malakar,P.K., Zwietering,M.H., van 't Riet,K.

important in the case *E. cloacae* is the dominant organism or for media with a high buffer capacity.

1. Introduction

In food microbiology, the growth of microorganisms is often described by empirical models. In general, these models relate the natural logarithm of the number of cells over time at a given set of initial environmental conditions to a number of parameters like the lag time, the maximum specific growth rate and the final level of microorganisms reached. By modelling the effect of the relevant factors as for instance the *pH*, temperature and water activity on these parameters the effect of different initial environmental conditions is incorporated (McMeekin et al. 1993, Ross and McMeekin 1994, Baranyi and Roberts 1995, McMeekin and Ross 1996). This procedure may only be applied if the change in initial values of the relevant factors during growth is negligible. Consequently, the influence of the growing organisms on their environment must be negligible, which will be the case for low contamination levels. Furthermore, the models are generally developed to describe the growth of only one single strain in homogeneous suspension cultures. However, many microbiological processes in food processing and food storage deal with solid foods and with mixed populations (for example, Driessen 1981, Béal et al. 1994, Choi and Beuchat 1994, Ha et al. 1994, Julliard and Richard 1994, Robinson et al. 1994, Giraffa et al. 1995, Lambropoulou et al. 1996, Thomas and Wimpenny 1996). Interactions between the various types of microorganisms present may result in the emergence of spoiler organisms, which normally would not grow. Furthermore, they may bring about different growth behaviour for individual species as compared to pure cultures of these species. Consequently, these interactions may be important for predicting the shelf life of a product (McMeekin and Ross 1996).

Interaction between two organisms is assumed to occur as soon as the presence of one organism influences the growth of the other. Interactions may be direct, through physical contact, or indirect. Indirect interactions are mediated through a change of the environment (Frederickson 1977) and can be specific as is

the case with bacteriocins (Choi and Beuchat 1994, Hansen 1994, Giraffa et al. 1995, Casla et al. 1996) or more a-specific as is the case with inhibition by acids and competition for substrate (Ha et al. 1994, Houtsma et al. 1994, Greer and Dilts 1995, Gram and Melchiorsen 1996, Houtsma et al. 1996).

The objective of this study is to calculate at which moment in time and at which microorganism levels interactions between the microorganisms of different species start to occur. Comparison of the microorganism levels at the moment of interaction with spoilage levels and safety levels gives information whether microbial interactions can be of importance for the safety of foods. As an experimental model system the interactions between *Lactobacillus curvatus* and *Enterobacter cloacae*, which are typical spoilage organisms of meat products, are studied. *L. curvatus* is a facultative heterofermentative organism. In media containing hexoses in excess it produces mainly lactic acid. In addition, small amounts of other organic acids, certain diols and peroxide may be produced. Furthermore, *L. curvatus* strains are known to produce bacteriocins (Holt et al. 1984-1989, Casla et al. 1996). *E. cloacae* is a facultative anaerobic organism that can grow on a variety of carbon sources and produces a number of acids under anaerobic conditions (Holt et al. 1984-1989). Each compound consumed or produced by one of the organisms can in principle influence the growth of the other organism. The main compounds through which interaction may occur under aerobic conditions are then presumably glucose and lactic acid. Both organisms may compete for the available glucose. Furthermore, the lactate produced by *L. curvatus* may inhibit the growth of *E. cloacae* either directly through the lactate molecule or indirectly through a decrease in *pH*. Since the other products excreted by *L. curvatus* are produced in small amounts compared to lactic acid, their effect on the growth of *E. cloacae* is neglected. Last, *E. cloacae* is a gram negative organism and thus probably not affected by the bacteriocin potentially produced by *L. curvatus* (Hansen 1994).

The aim of this first paper is to develop mathematical models that describe the effect of glucose, lactate and *pH* on the behaviour of *E. cloacae* and *L. curvatus* in pure suspension cultures. In a second paper these models will be used to predict

and validate experimentally the point of interaction in mixed cultures in terms of time and microorganism levels.

2. Theory

For each microorganism the specific growth rate μ (h^{-1}) is determined as a function of the initial glucose (S) and lactate (P) concentration ($mol.m^{-3}$) and the initial pH in suspension cultures ($\mu=f(S,P,pH)$). The growth rate, r_X ($cell.m^{-3}.h^{-1}$), can be calculated from the specific growth rate according to:

$$r_X = \mu X \qquad 1 \qquad (cell.m^{-3}.h^{-1})$$

where X is the cell concentration ($cell.m^{-3}$). The glucose consumption rate, r_S ($mol.m^{-3}.h^{-1}$), can be calculated according to Pirt (1965):

$$r_S = (\frac{\mu}{Y_{XS}} + m_S)X \qquad 2 \qquad (mol.m^{-3}.h^{-1})$$

where Y_{XS} is the yield of cells on glucose ($cell.mol^{-1}$) and m_S is the maintenance coefficient for glucose ($mol.cell^{-1}.h^{-1}$). The lactic-acid production rate, r_P, ($mol.m^{-3}.h^{-1}$) for *L. curvatus* is given by:

$$r_P = (\frac{\mu}{Y_{XP}} + m_P)X \qquad 3 \qquad (mol.m^{-3}.h^{-1})$$

where Y_{XP} is the yield of cells on lactic acid ($cell.mol^{-1}$) and m_P is the maintenance coefficient for lactic acid ($mol.cell^{-1}.h^{-1}$). The pH of the medium can next be obtained from a titration curve of the medium with lactic acid. The titration curve can be described by:

$$pH = \frac{pH_0 + a_1[P]}{1 + a_2[P]} \qquad 4$$

where pH_0 is the initial pH, and a_1 and a_2 are fit parameters ($m^3.mol^{-1}$). It should be realised that equations 1 to 3 are developed for constant environmental conditions. Since interaction can solely occur due to a change in environmental conditions, the models are in principle only valid until the start of interaction. In this first paper, models will be developed for both organisms regarding the relation between the specific growth rate and the lactate and glucose concentration and the pH. In

addition, the value of the parameters in equations 1 to 3 will be determined for both individual organisms.

3. Material and methods

3.1. Bacterial strains

L. curvatus was isolated from spoiled vacuum-packed cooked ham (Muermans et al. 1993). *E. cloacae* was kindly provided by the section of Food Microbiology of Wageningen Agricultural University. Before storage, pure cultures of each strain in MRS broth at *pH* 7.0 were recovered at the end of the exponential phase. Glycerol (100 $g.L^{-1}$) was added to the bacterial suspension, which was frozen and stored at –18 °C. Before the experiments the cultures were thawed and precultured for 22 hours.

3.2 Culture conditions

Pure cultures of *L. curvatus* and *E. cloacae* were conducted at a constant temperature of 30 °C in 250 ml Erlenmeyers filled with 80 ml standard MRS broth (Merck). The *pH* was adjusted to the desired value using 2 $mol.L^{-1}$ HCl or 2 $mol.L^{-1}$ NaOH. For the experiments at different initial lactate concentrations, two times concentrated solutions of MRS and DL-lactic acid (Janssen Chimica, Belgium, 85% (wt/wt) original concentration) were prepared. After adjusting the *pH* to the desired value, both solutions were sterilised separately to avoid Maillard reactions (MRS 15 minutes at 118 °C, lactic acid 20 minutes at 121 °C). The two solutions were next brought together and the *pH* was adjusted if required. For the experiments at varying glucose concentrations the MRS medium was reconstituted from its original components except for glucose. Glucose was next added to the desired concentration and the medium was sterilised for 15 minutes at 118 °C. The *pH* was adjusted to the desired value before the experiment. The cultures were inoculated form the preculture to an initial density of about 10^3 $cfu.ml^{-1}$.

3.3. Analysis

Samples of 1 ml were taken at appropriate time intervals and the number of cfu.ml^{-1} was determined using the pour-plating method. For *L. curvatus* MRS agar (Oxoid) medium and for *E. cloacae* VRBG (Oxoid) medium was used. The plates were incubated aerobically at 30 °C for one day in the case of *E. cloacae* and for two days in the case of *L. curvatus* before counting. For some experiments additional samples of 1 ml were taken for determination of the glucose and lactate concentrations. After filter sterilisation (0.45 μm), these samples were stored at -20 °C until analysis.

Glucose and lactate concentrations were measured by HPLC (Spectra Physics) with a Aminex HPX-87H column (Biorad). 0.005 mol.L^{-1} of degassed H_2SO_4 was used as eluent. The detection limit of the method is 1 g.L^{-1}. Calibration was done with D-glucose monohydrate (Merck) and DL-lactic acid (Janssen Chimica Belgium).

3.4. Modelling the growth curves

The growth curves obtained at different initial conditions were described by the modified Gompertz equation:

$$\ln\left(\frac{X(t)}{X(0)}\right) = A\exp\left\{-\exp\left[\frac{\mu_m e}{A}(\lambda - t) + 1\right]\right\} \qquad 5$$

Where A is the is the maximum value reached ($=ln[X(\infty)/X(0)]$), μ_m is the maximum specific growth rate (h^{-1}), λ is the lag time (h), and e is exp(1). Regressions were carried out using standard statistical software (TableCurve 2D for Windows V2.03, least-square non-linear regression, Gaussian errors). For a reliable estimation of growth parameters, experimental growth curves were only used for model construction if they satisfied the following objective criteria:

1) There should be at least three datum points in the lag phase, which should be minimally 1 hour apart. For lag times shorter than three hours 1 or 2 datum points are required.

2) There should be at least four datum points in the exponential phase, that are at least 1 hour and 1 ln unit apart.
3) There should be at least three datum points in the stationary phase, that are at least 1 hour apart.

Because the individual datum points of the rejected growth curves were reliable measurements, the data of these experiments were nevertheless included in the final evaluation of the performance of the models.

4. Results

4.1. Modelling the growth of L. curvatus

The relation between the maximum specific growth rate of *L. curvatus* and the temperature and *pH* has been extensively examined by Wijtzes et al. (1995). They found the next relation:

$$\mu_m = b_1 (T - T_{\min})^2 (pH_{\max} - pH)(pH - pH_{\min}) \qquad 6 \qquad (h^{-1})$$

where μ_m is the maximum specific growth rate as estimated using equation 5, b_1 ($h^{-1}.°C^{-2}$) is a regression parameter, $T_{\min}$ (°C) is the theoretical minimum temperature for growth, and $pH_{\min}$ and $pH_{\max}$ are the theoretical minimum and maximum *pH* for growth, respectively. The parameter values found by Wijtzes et al. (1995) are given in Table 1. At a fixed temperature equation 6 may be simplified to:

$$\mu_m = 4\mu_{opt1} \frac{(pH - pH_{\min})(pH_{\max} - pH)}{(pH_{\max} - pH_{\min})^2} \qquad 7 \qquad (h^{-1})$$

where μ_{opt1} (h^{-1}) is the maximum growth rate at the optimal *pH* and the prevailing conditions. The value for μ_{opt1} at a temperature of 30 °C is given in Table 1. In Fig. 1 the maximum specific growth rate as predicted by equation 6 and the parameter values given in Table 1 are shown for a temperature of 30 °C together with the experimental data measured in this work. For comparison the experimental data measured at 29 °C by Wijtzes et al. (1995) are also shown after having been transformed to a temperature of 30 °C using equation 6 and the parameter values in Table 1 ($\mu_{30}=\mu_{29}\cdot(30-T_{\min})^2/(29-T_{\min})^2$). From the growth rates measured at 29 °C

Table 1: Parameter values for *L. curvatus* (Equations 6 and 7).

Parameter	Value	95% Confidence interval	
b_1 ($h^{-1}.°C^{-2}$)[a]	$1.26 \cdot 10^{-4}$	$1.05 \cdot 10^{-4}$	$1.47 \cdot 10^{-4}$
T_{min} (°C)[a]	-3.27	-4.48	-2.06
μ_{opt1} (h^{-1}) at 30 °C[b]	1.06	1.01	1.11
pH_{min}[a]	4.26	4.13	4.38
pH_{max}[a]	9.77	9.53	10.01

[a]: fitted parameters obtained from Wijtzes et al. (1995)

[b]: predicted optimal growth rate at 30 °C ($= 0.25 \cdot b_1 \cdot (30-T_{min})^2 \cdot (pH_{max}-pH_{min})^2$)

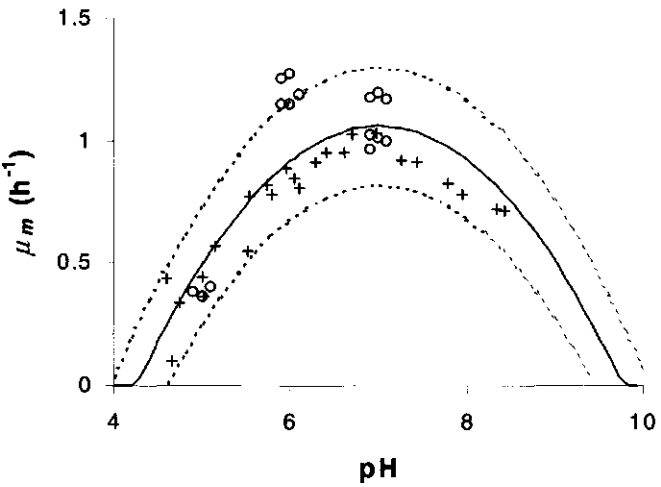

Fig. 1: Maximum specific growth rates as a function of *pH* for *L. curvatus*. (O) Datum points determined in this work. (+) Datum points of Wijtzes et al. (1995) transformed from a temperature of 29 °C to a temperature of 30 °C using equation 6. The solid line represents the predicted curve obtained from Wijtzes et al. (1995) (equation 6). The dashed lines represent the 95% prediction intervals. Parameter values are given in Table 1.

the standard error was calculated, which was used in turn to calculate the 95% prediction intervals shown in Fig. 1. At *pH* 6 the measured specific growth rates are significantly higher than predicted by the model of Wijtzes et al. (1995). The

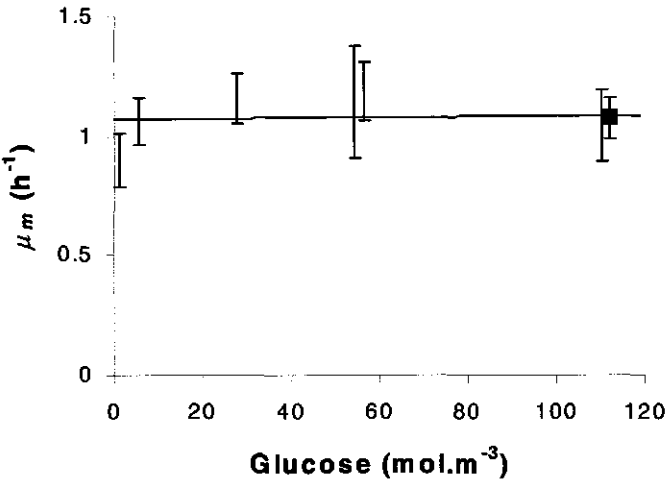

Fig. 2: Maximum specific growth rate of *L. curvatus* as a function of the glucose concentration at *pH* 7.0 and 30 °C. The open squares represent the datum points obtained in reconstituted medium with the error bars representing the 95% confidence intervals for the intra-experiment variation. The filled square represents the average value of 6 measurements in standard MRS at *pH* 7.0 with the error bar representing the 95% confidence interval calculated with the between experiment variation.

cause of this observed difference remains unknown. However, it may be due to slight differences in the sterilisation procedure (20 min at 121 °C by Wijtzes et al. 1995 compared to 15 min 118 °C in this work) and preculture method (two precultures by Wijtzes et al. 1995 compared to one in this work).

The effect of the glucose concentration in the range of 0-111 $mol.m^{-3}$ is shown in Fig. 2. As can be seen there was no statistically significant difference between the mean maximum growth rate obtained in the commercial available MRS (filled square at 111 $mol.m^{-3}$) and the maximum growth rate obtained in the reconstituted medium (open square at 111 $mol.m^{-3}$). For the determination of the least-square regression line shown in Fig. 2, the 6 individual datum points were used and not the average value. The slope of the least-square regression line through the datum points was not significantly different from zero (Table 2).

Table 2: Intercept and slope of the least-square regression line shown in Fig. 2 and parameters of equation 10, μ_{opt3} and slope, b_2, from the least-square regression line shown in Fig. 3 for *L. curvatus*.

Experiment	Parameter	Value	95% confidence interval	
Glucose	Intercept (h^{-1})	1.07	0.96	1.18
	Slope ($m^3.mol^{-1}.h^{-1}$)	0.00015	-0.0011	0.0014
Lactate *pH* 7	μ_{opt3} (h^{-1})	1.05	0.94	1.17
	b_2 ($m^3.mol^{-1}.h^{-1}$)	0.0010	0.00010	0.0019
Lactate *pH* 6	μ_{opt3} (h^{-1})	1.19	1.14	1.25
	b_2 ($m^3.mol^{-1}.h^{-1}$)	0.0019	0.0016	0.0022
Lactate *pH* 5	μ_{opt3} (h^{-1})	0.39	0.36	0.43
	b_2 ($m^3.mol^{-1}.h^{-1}$)	0.0014	0.0011	0.0017

It is thus concluded that there was no effect of the initial glucose concentration on the maximum specific growth rate. Even if no glucose was added the maximum growth rate was comparable to the maximum growth rate with the addition of 111 $mol.m^{-3}$ glucose. This may have been due to small amounts of consumable sugars present in the yeast and meat extract, that were necessary for the cultivation of *L. curvatus*. On the basis of these results, Monod kinetics with a very low Monod constant, K_S ($mol.m^{-3}$), was assumed as given by:

$$\mu_m = \mu_{opt2} \cdot \frac{S}{K_S + S} \qquad 8 \qquad (h^{-1})$$

The Monod constant was obtained from literature (general value for *E. coli* on glucose, van 't Riet and Tramper 1991) and has a value of 0.0004 $mol.m^{-3}$.

Finally, the effect of the initial lactate concentration on the specific growth rate of *L. curvatus* was studied at different initial *pH* values. The results are shown in Fig. 3 and were firstly modelled using a linear relationship given by:

$$\mu_m = \mu_{opt3} \cdot (1 - \frac{P}{P_{inh}}) \qquad 9 \qquad (h^{-1})$$

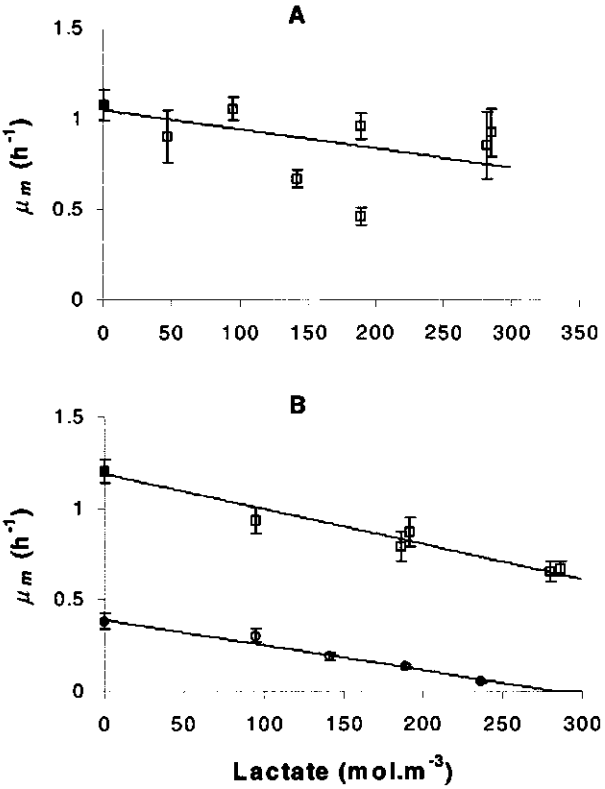

Fig. 3: Effect of the lactate concentration on the maximum specific growth rate of *L. curvatus* at an initial *pH* values of A: 7.0, B: 6.0 (□) and 5.0 (○). Solid lines are the linear least-square regression lines (parameter values given in Table 2). Error bars represent the 95% confidence intervals for the intra-experiment variation. The filled symbols represent the average value of a number of measurements in standard MRS with no added lactate (conc.= 0) with the error bar representing the 95% confidence interval calculated with the between experiment variation.

where P_{inh} (mol.m^{-3}) is the inhibitory lactate concentration for growth. At all three *pH* values the slope of the regression line (μ_{opt3}/P_{inh}) was significantly higher than zero, indicating that there was a significant effect of lactate. Furthermore, while P_{inh} strongly depended on the *pH*, the slopes of the regression lines were not statistically different at the different initial *pH* values.

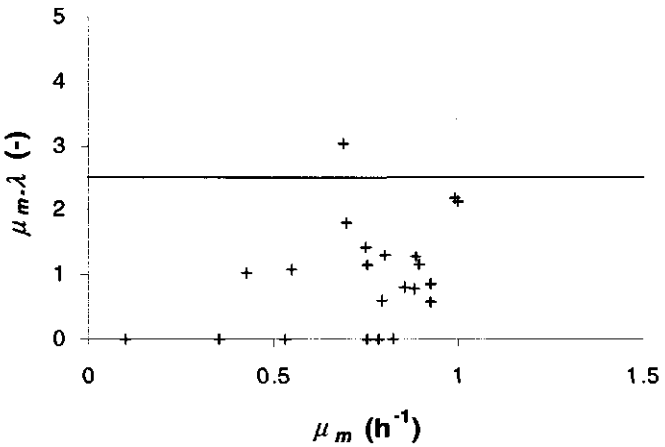

Fig. 4: $\mu_m \cdot \lambda$ as a function of the specific growth rate μ_m of *L. curvatus* for our data (□) and the data of Wijtzes et al. (1995) (+). The solid line represents the average value for our data.

Thus equation 9 was simplified to:

$$\mu_m = \mu_{opt3} - b_2 \cdot P \qquad 10 \qquad (h^{-1})$$

where the slope, b_2 ($m^3.mol^{-1}.h^{-1}$), equals μ_{opt3}/P_{inh}. The values for μ_{opt3} and b_2 are given in Table 2. The average slope for all three initial *pH* values was 0.0014 ± 0.0008 $m^3.mol^{-1}.h^{-1}$

The lag time, λ (h), was modelled as the inverse of the maximum specific growth rate (Simpson et al. 1989, Zwietering et al. 1994) as shown in Fig. 4, where $\mu_m \cdot \lambda$ is plotted as a function of μ_m. For comparison the datum points of Wijtzes et al. (1995) measured at 29 °C are also shown. Although these authors found a correlation between $\mu_m \cdot \lambda$ and μ_m, such a correlation was not clear for our data. Thus, $\mu_m \cdot \lambda$ was assumed constant at a calculated value of $c_{\lambda Lc}$=2.51±0.34 hours. This value is significantly higher then the average value of 1.20±0.35 found by Wijtzes et al. (1995). It remains unknown whether this is due to the earlier mentioned small differences in the experimental protocol. In addition, large variations are generally found in the lag time.

Table 3: Yield and maintenance parameters and number of datum points, n, used. It is assumed one cell is equivalent to one colony forming unit (cfu).

	Parameter	n	Value	95% confidence interval	
L. curvatus	Y_{XS} (cell.mol^{-1})	13	$7.0 \cdot 10^{13}$	$4.2 \cdot 10^{13}$	$9.8 \cdot 10^{13}$
	m_S (mol.cell^{-1}.s^{-1})	-	$6.5 \cdot 10^{-20}$ [a]	-	-
	Y_{XP} (cell.mol^{-1})	13	$3.3 \cdot 10^{13}$	$1.3 \cdot 10^{13}$	$5.3 \cdot 10^{13}$
	m_P (mol.cell^{-1}.s^{-1})	-	$1.3 \cdot 10^{-19}$ [a]	-	-
E. cloacae	Y_{XS} (cell.mol^{-1})	36	$8.6 \cdot 10^{13}$	$5.3 \cdot 10^{13}$	$11.9 \cdot 10^{13}$
	m_S (mol.cell^{-1}.s^{-1})	-	$2.5 \cdot 10^{-20}$ [b]	-	-

[a] : Value estimated from the maintenance requirements for ATP of *L. casei* (Roels 1983)
[b] : Value from *E. aerogenes* (Roels 1983).

For a number of experiments for *L. curvatus* the glucose and lactate concentrations were determined. From these experiments the yield of cells on glucose was estimated according to:

$$Y_{XS} = \frac{X(t_e) - X(0)}{S(0) - S(t_e)} \qquad 11 \qquad (\text{cell.mol}^{-1})$$

where Y_{XS} (cell.mol^{-1}) is the yield of cells on glucose, and t_e (h) is the time of the first measured point in the stationary phase. Likewise, the yield of cells on lactic acid was calculated according to:

$$Y_{XP} = \frac{X(t_e) - X(0)}{P(t_e) - P(0)} \qquad 12 \qquad (\text{cell.mol}^{-1})$$

where Y_{XP} (cell.mol^{-1}) is the yield of cells on lactic acid. The maintenance coefficients, m_S and m_P (mol.cell^{-1}.s^{-1}) were estimated from literature. Yield and maintenance coefficients are given in Table 3.

4.2. Modelling the growth of E. cloacae

The effect of the *pH* on the maximum specific growth rate of *E. cloacae* is shown in Fig. 5, where equation 7 and the modified Ratkowsky equation [equation 13] (Ratkowsky et al. 1982) were fitted through the datum points and the results are shown Table 4. The Ratkowsky equation modified for the effect of *pH* and without the square root of the specific growth rate is given by:

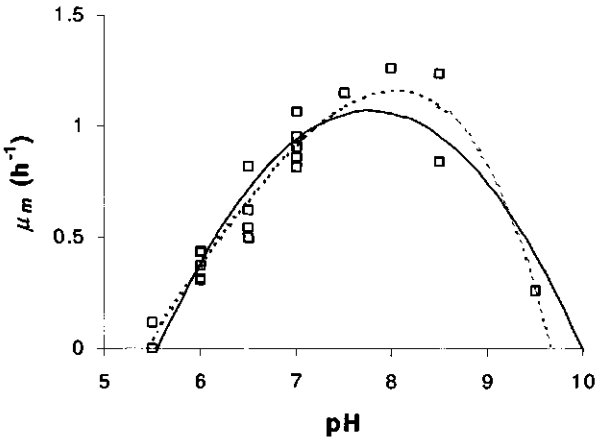

Fig. 5: Maximum specific growth rate of *E. cloacae* as a function of the *pH*. Symbols represent the experimental data, the solid line represents the fit using equation 7 and the broken line the fit using equation 13. Parameter values for the fitted lines are given in Table 4.

Table 4: Predicted and fitted parameter values for the specific growth rate of *E. cloacae* as a function of *pH* using Eqs. (7) and (13).

	Equation 7			Equation 13		
Parameter	Value	95% Conf. interval		Value	95% Conf. interval	
pH_{min}	5.56	5.41	5.70	5.44	5.23	5.65
pH_{max}	9.99	9.61	10.37	9.66	9.46	9.85
μ_m (h^{-1})	1.07	0.97	1.17	-	-	-
b_3 (h^{-1})	-	-	-	0.76	0.37	1.16
b_4 (-)	-	-	-	0.55	0.08	1.01

$$\mu_m = b_3 \cdot (pH - pH_{min}) \cdot (1 - e^{-b_4 \cdot (pH_{max} - pH)}) \qquad 13 \qquad (h^{-1})$$

where b_3 (h^{-1}) and b_4 (-) are regression parameters. Although equation 13 described the datum points slightly better than equation 7, this was not statistically significant on the basis of an *F*-test ($f = 1.03$, $F_{16}^{17} = 2.3$). More datum points at *pH* values of 8

and higher are required to study which model is the best. In this study equation 7 was retained because it has less parameters, is more robust and easier to use.

The effect of the glucose concentration in the range of 0-111 mol.m^{-3} is shown in Fig. 6. The slope of the shown regression line was not statistically different from zero (Table 5). The results were comparable to those obtained for *L. curvatus*. Thus, also for *E. cloacae* Monod kinetics (equation 3) with a very low Monod constant, K_S = 0.0004 mol.m^{-3} (general value of *E. coli* on glucose, van 't Riet and Tramper 1991) was assumed. As discussed for *L. curvatus*, even if no glucose was added the growth rate did not decrease as compared to the situation with 111 mol.m^{-3}. In addition to the small amounts of consumable sugars present in the added yeast and meat extract, this may have also been due to other compounds present in the medium, for example citrate, which *E. cloacae* can use as a substrate.

In Fig. 7 the effect of the lactate concentration on the maximum specific growth rate of *E. cloacae* is shown at different initial *pH* values. Equation 10 was fitted through the datum points and the resulting lines are shown in Fig. 7. Estimated parameter values are given in Table 5. Only at *pH*=7 a slight influence of the lactate concentration could be observed. However, at a lactate concentration as high as 94 mol.m^{-3} the *pH* is generally below 5. Thus, the effect of lactate on the growth of *E. cloacae* was negligible compared to the effect of the accompanying decrease in *pH*.

For *E. cloacae* the lag time, λ (hours), was modelled as the inverse of the maximum specific growth rate. As can be seen in Fig. 8 no correlation was observed between $\mu_m \cdot \lambda$ and μ_m. The average value of $\mu_m \cdot \lambda$ was $c_{\lambda Ec}$=2.46±0.38 h.

For a number of experiments with *E. cloacae* the glucose concentrations were measured. Using equation 11 the yield of cells on glucose, Y_{XS}, was determined. The maintenance coefficient, m_S, was obtained from literature (Roels 1983) and is shown together with the yield of cells on glucose in Table 3.

Table 5: Intercept and slope of the least-square regression lines shown in Fig. 6 and parameters of equation 10, μ_{opt3} and b_2 obtained for the least-square regression fit shown in Fig. 7.

Experiment	Parameter	Value	95% confidence interval	
Glucose	intercept (h^{-1})	0.89	0.72	1.06
	slope ($m^3.mol^{-1}.h^{-1}$)	0.000010	-0.0020	0.0020
Lactate *pH* 7	μ_{opt3} (h^{-1})	0.97	0.88	1.06
	b_2 ($m^3.mol^{-1}.h^{-1}$)	0.00099	0.00020	0.0016
Lactate *pH* 6.5	μ_{opt3} (h^{-1})	0.62	0.46	0.79
	b_2 ($m^3.mol^{-1}.h^{-1}$)	0.00030	-0.0014	0.0020
Lactate *pH* 6	μ_{opt3} (h^{-1})	0.38	0.33	0.43
	b_2 ($m^3.mol^{-1}.h^{-1}$)	0.00030	-0.00010	0.00070

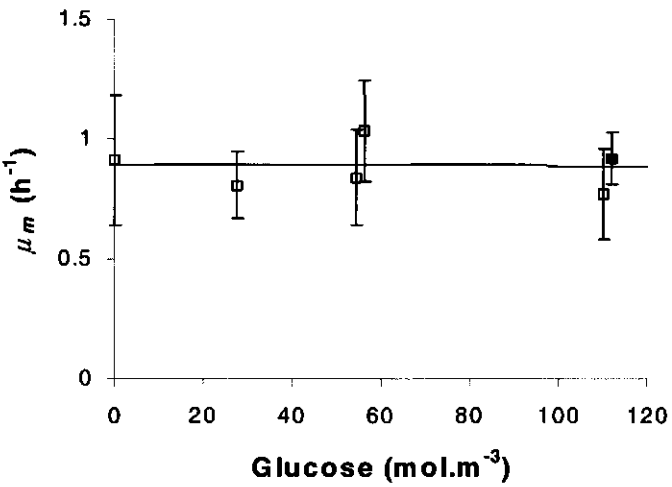

Fig. 6: Effect of the glucose concentration on the maximum specific growth rate of *E. cloacae*. The open squares represent the datum points obtained in reconstituted medium with the error bars representing the 95% confidence intervals for the intra-experiment variation. The filled square represents the average value of 6 measurements in standard MRS at *pH* 7.0 with the error bar representing the 95% confidence interval calculated with the between experiment variation. The line represents the least-square regression line.

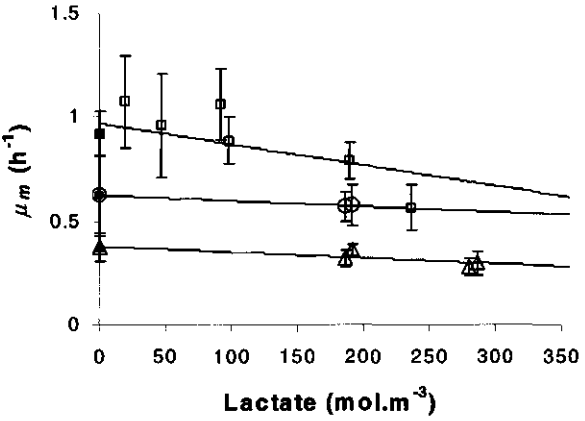

Fig. 7: Maximum specific growth rate of *E. cloacae* as a function of the lactate concentration at initial *pH* values of (□) *pH*=7.0, (O) *pH*=6.5, (Δ) *pH*=6.0. Solid lines are the linear least-square regression lines (parameter values given in Table 5). Error bars represent the 95% confidence intervals for the intra-experiment variation. The filled symbols represent the average value of a number of measurements in standard MRS with no added lactate with the error bar representing the 95% confidence interval calculated with the between experiment variation.

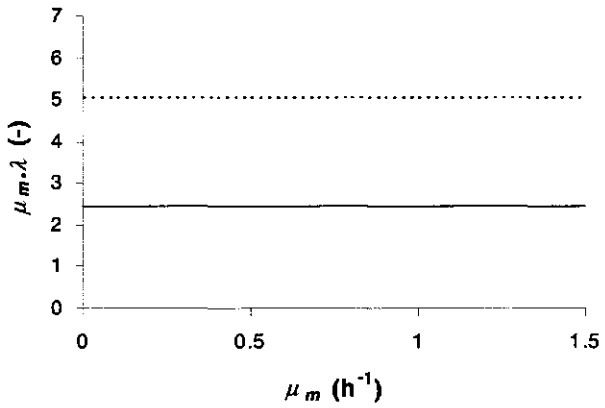

Fig. 8: $\mu_m \cdot \lambda$ as a function of the maximum specific growth rate μ_m for *E. cloacae*. The solid line represents the mean value while the dashed line represent the upper 95% prediction interval (the lower value equals zero).

4.3. Overall model performance

In Fig. 9 the measured value of Z *(=log[X(t)])*, $Z_{measured}$, is shown as a function of the predicted value of Z (Z_{model}) for both organisms. Z_{model} was obtained by solving equations 1, 2, 3 and 4. All individual datum points of all growth curves were used.

To evaluate the performance of the model, the variance of the model predictions was compared to the variance of the Gompertz model, with for each experiment 3 separate parameter values. In the overall model, for *L. curvatus* 4 parameters (Y_{XS}, Y_{XP}, b_2, $c_{\lambda Lc}$) were used for fitting the model to the experimental data, whereas for *E. cloacae* 5 parameters (μ_{opt}, pH_{min}, pH_{max}, Y_{XS}, $c_{\lambda Ec}$) were used. For the individual Gompertz models the number of parameters was equal to the number of accepted experiments multiplied with three being 144 for *L. curvatus* and 168 for *E.cloacae*. The variance, s^2, was estimated according to:

$$s^2 = \frac{\sum (Z_{measured} - Z_{model})^2}{df} \qquad 14$$

where Z_{model} are the values predicted by either the overall model or the Gompertz model and *df* is the degrees of freedom. The summation is over all experiments. The results are shown in Table 6. For the overall model (Table 6, model I) a variance of 0.534 was calculated for *L. curvatus* and of 0.714 for *E.cloacae*. For the individual Gompertz models, variances of 0.247 and 0.323 were obtained for *L. curvatus* and *E. cloacae*, respectively. On the basis of an *F* test it can be concluded that the variance of the overall model was significantly higher than the variance of the individual Gompertz models as shown in Table 6.

Part of this higher variance may have been due to the large spread in lag times (Fig. 4 and 8). When the lag times as estimated for each growth curve by the Gompertz equation were used (Table 6, model IIa) instead of the predicted values, the variance was reduced to 0.341 and 0.611 for *L. curvatus* and *E. cloacae*, respectively. For both organisms, especially for *L. curvatus*, the rather high variance of the overall model can thus be partly explained from the rather large spread in lag times. However, the variance was still significantly higher than the variance obtained from fitting all growth curves separately with the Gompertz

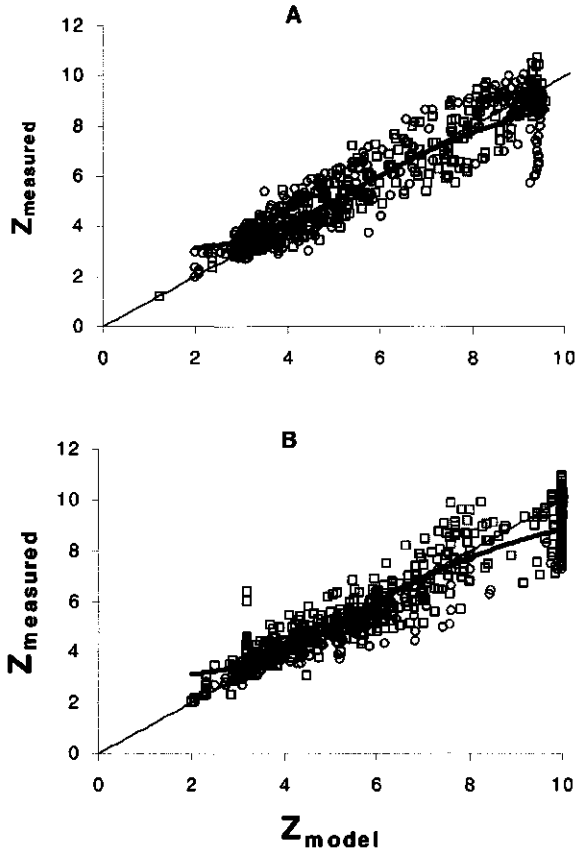

Fig. 9: Measured value of *Z=log(X(t))* as a function of the predicted value for *L. curvatus* (A) and *E. cloacae* (B). (□) experiments with a zero initial lactate concentration, (O) experiments with an initial lactate concentration higher than zero. The solid curve represents the error made by describing a sigmoidal curve with an exponential growth model.

model.

An additional cause for the higher variance may be the rather unreliable yield parameters (Table 3). The yield parameters determine the final concentration of microorganisms that can be reached. Consequently, the effect of the unreliable yields on the model deviation can be evaluated by considering only the points just

Table 6: Comparison of the performance of the overall model to the Gompertz model.

L. curvatus	Gompertz[a]	Model I[b]	Model IIa[c]	Model IIb[d]
Experiments	48	48	48	48
Degrees of freedom	600	740	693	556
(points-parameters)	(744-144)	(744-4)	(744-51)	(606-50)
Variance	0.247	0.534	0.341	0.301
f		2.170	1.385	1.227
F (p=0.05)		1.137	1.139	1.147
E. cloacae				
Experiments	56	56	56	56
Degrees of freedom	603	766	711	544
(Points-parameters)	(771-168)	(771-5)	(771-60)	(603-59)
Variance	0.323	0.714	0.611	0.358
f		2.211	1.892	1.108
F (p=0.05)		1.136	1.138	1.147

[a]: Data fitted by individual Gompertz models. For *L. curvatus* 48 experiments and for *E. cloacae* 56 experiments were used.

[b]: Data fitted by the overall model. For *L. curvatus* 4 parameters (Y_{XS}, Y_{XP}, b_2, $c_{\lambda Lc}$) and for *E. cloacae* 5 parameters (μ_{opt}, pH_{min}, pH_{max}, Y_{XS}, $c_{\lambda Ec}$) were used.

[c]: Lag time fitted for the individual experiments. Number of parameters is 4-1($c_{\lambda Lc}$)+48 for *L. curvatus* and 5-1($c_{\lambda Ec}$)+56 for *E. cloacae.*

[d]: Lag time fitted for individual experiments and the datum points at the final level not included. The number of parameters is reduced by one (Y_{XS}).

before the final level of microorganisms is reached being Z=9 (i.e. 10^9 cell.ml^{-1}) for *L. curvatus* and Z=9.9 (i.e. $8 \cdot 10^9$ cell.ml^{-1}) for *E. cloacae*. This is justified by the fact that, if interaction occurs, this will usually occur before the final level is reached. In this way the variance was further reduced to 0.301 and 0.358 for *L. curvatus* and *E. cloacae*, respectively. Therefore, for *L. curvatus* hardly any influence of the unreliable yields on the variance was observed, while for *E. cloacae* a considerable reduction of the variance was obtained. For *E. cloacae* the variance was no longer significantly different from the variance for the Gompertz

model. For *L. curvatus* the variance of the overall model was still significantly different from that for the Gompertz model. However, the difference is not very high (0.059).

Finally, description of a sigmoidal growth curve with an exponential model leads to systematic too low predictions in the area where the growth curve passes from the lag phase to the exponential phase and in systematic too high predictions in the area where the growth curve passes from the exponential to the stationary phase. Assuming the sigmoidal growth curve is perfectly described by the Gompertz equation and assuming that the inoculation density and final concentration are constant for all experiments, the systematic error can be shown to be solely a function of the predicted value of *Z* (Fig. 9). As can be seen in Fig. 9 this error is in general small and is largest at the low densities ($<10^3$ cell.ml^{-1}) and high densities ($>10^9$ cell.ml^{-1}).

5. Conclusions

In this work models were developed to describe the effect of glucose, lactate and *pH* on the growth of *L. curvatus* and *E. cloacae* in pure cultures. The aim of these models is to determine when interactions may occur in mixed cultures. For *L. curvatus* the maximum specific growth rate could be described by the next equation:

$$\mu_{mLc} = 4 \cdot \mu_{opt_{Lc}} \cdot \frac{S}{K_{S_{Lc}} + S} \cdot \frac{(pH - pH_{\min_{Lc}}) \cdot (pH_{\max_{Lc}} - pH)}{(pH_{\max_{Lc}} - pH_{\min_{Lc}})^2} - b_2 \cdot P \qquad 15 \quad (h^{-1})$$

For *E. cloacae* the growth rate was given by the next equation:

$$\mu_{mEc} = 4 \cdot \mu_{opt_{Ec}} \cdot \frac{S}{K_{S_{Ec}} + S} \cdot \frac{(pH - pH_{\min_{Ec}}) \cdot (pH_{\max_{Ec}} - pH)}{(pH_{\max_{Ec}} - pH_{\min_{Ec}})^2} \qquad 16 \quad (h^{-1})$$

For both organisms the lag time was modelled as proportional to the inverse of the growth rate. The theoretical minimum *pH* for growth was 5.6 and 4.3 for *E. cloacae* and *L. curvatus*, respectively, showing that *E. cloacae* was clearly more sensitive to a decrease in *pH* than *L. curvatus*. For both organisms no effect of glucose on the maximum specific growth rate could be detected and Monod

kinetics with a low Monod constant was assumed. For *L. curvatus* the effect of lactate on the maximum growth rate at different initial *pH* values could be described by a linear relationship. For *E. cloacae* an effect of lactate on the maximum growth rate could only be detected at *pH* 7, while at *pH* 6 and 6.5 no significant effect was observed. The decrease in maximum growth rate with increasing lactate concentrations at *pH* 7 was negligible compared to the effect of the accompanying decrease in *pH*.

From this study it may be concluded that, for the case *L. curvatus* is the dominant organism, the *pH* is the important parameter for determining the point of interaction. If the buffer capacity of the environment is very high also the produced lactate may become important. The glucose concentration will only be of importance at low initial concentration and in case *E. cloacae* is the dominant organism.

6. References

1. Baranyi,J., Roberts,T.A. 1995. Mathematics of predictive food microbiology. Int. J. Food Microbiol. 26: 199-218.
2. Beal,C., Spinnler,H.E., Corrieu,G. 1994. Comparison of growth, acidification and productivity of pure and mixed cultures of *Streptococcus salivarius* subsp. *thermophilus* 404 and *Lactobacillus delbrueckii* subsp. *bulgaricus* 398. Appl. Microbiol. Biotechnol. 41: 95-98.
3. Casla,D., Requena,T., Gomez,R. 1996. Antimicrobial activity of lactic acid bacteria isolated from goat's milk and artisanal cheeses: Characteristics of a bacteriocin produced by *Lactobacillus curvatus* IFPL105. J. Appl. Bacteriol. 81: 35-41.
4. Choi,S., Beuchat,L. 1994. Growth inhibition of *Listeria monocytogenes* by a bacteriocin of *Pediococcus acidilactici M* during fermentation of kimchi. Food Microbiol. 11: 301-307.
5. Driessen,F.M. 1981. Protocooperation of yoghurt bacteria in continuous cultures. In Mixed culture fermentations. M.E. Bushell and J.H. Slater, editors. 99-119.
6. Frederickson,A.G. 1977. Behaviour of mixed cultures of microorganisms. Ann. Rev. Microbiol. 31: 63-87.

7. Giraffa,G., Carminati,D., Tarelli,G.T. 1995. Inhibition of *Listeria monocytogenes* in milk by bacteriocin-producing *Enterococcus faecium* 7C5. J. Food Protect. 58: 621-623.
8. Gram,L., Melchiorsen,J. 1996. Interaction between spoilage bacteria *Pseudomonas* sp. and *Shewanella putrefaciens* in fish extracts and on fish tissue. J. Appl. Bacteriol. 80: 589-595.
9. Greer,G.G., Dilts,B.D. 1995. Lactic acid inhibition of the growth of spoilage bacteria and cold tolerant pathogens on pork. Int. J. Food Microbiol. 25: 141-151.
10. Ha,S.D., Ricke,S.C., Nisbet,D.J., Corrier,D.E., Deloach,J.R. 1994. Serine utilization as a potential competition mechanism between *Salmonella* and a chicken cecal bacterium. J. Food Protect. 57: 1074-1079.
11. Hansen,J.N. 1994. Nisin a model food preservative. Crit. Rev. Food Sci. Nutr. 34: 69-93.
12. Holt,J.G., Krieg,N.R., Bergey,D.H., Sneath,P.H.A., Mair,N.S., Sharp,M.E., Staley,J.T., Williams,S.T. 1984-1989. Bergey's manual of systematic bacteriology. Vol. 1-4, Williams and Wilkins, Baltimore, USA.
13. Houtsma,P.C., Kusters,B.J.M., de Wit,J.C., Rombouts,F.M., Zwietering,M.H. 1994. Modelling growth rates of *Listeria innocua* as a function of lactate concentration. Int. J. Food Microbiol. 24, 113-123.
14. Houtsma,P.C., Kant-Muermans,M.L., Rombouts, F.M., Zwietering,M.H. 1996. Model for the combined effects of temperature, *pH*, and sodium lactate on growth rates of *Listeria innocua* in broth and bologna-type sausages. Appl. Environ. Microbiol. 62: 1616-1622.
15. Juillard,V., Richard,J. 1994. Mixed cultures in milk of a proteinase-positive and a proteinase-negative variant of *Lactococcus lactis* subsp. *lactis*: Influence of initial percentage of proteinase-positive cells on the growth parameters of each strain and on the rate of acidification. Lait 74: 3-12.
16. Lambropoulou,K.A., Drosinos,E.H., Nychas,G.J.E. 1996. The effect of glucose supplementation on the spoilage microflora and chemical composition of minced beef stored aerobically or under a modified atmosphere at 4 degrees C. Int. J. Food Microbiol. 30: 281-291.
17. McMeekin,T.A., Olley,J., Ross,T., Ratkowsky,D.A. 1993. Predictive microbiology: Theory and application. Research Studies Press Ltd. Somerset, United Kingdom.

18. McMeekin,T.A., Ross,T. 1996. Shelf life prediction: status and future possibilities. Int. J. Food Microbiol. 33: 65-83.
19. Muermans,M.L.T., Stekelenburg,F.K., Zwietering,M.H., Huis in 't Veld,J.H.J. 1993. Modelling the microbial quality of meat. Food Control 4: 216-221.
20. Pirt,S.J., 1965. The maintenance energy of bacteria in growing cultures. Proc. R. Soc. London Ser B 163: 224-231.
21. Ratkowsky,D.A., Olley,J., McMeekin,T.A., Ball,J.A. 1982. Relationship between temperature and growth rate of bacterial cultures. J. Bacteriol. 149: 1-5.
22. van 't Riet,K. Tramper,J. 1991. Basic bioreactor design. Marcel Dekker Inc. New York, USA.
23. Robinson,T., Wimpenny,J., Earnshaw,R. 1994. Modelling the growth of *Clostridium sporogenes* in tomato juice contaminated with mould. Lett. Appl. Microbiol. 19: 129-133.
24. Roels,J.A. 1983. Energetics and kinetics in biotechnology. Elsevier Biomedical Press. Amsterdam, The Netherlands.
25. Ross,T., McMeekin,T.A. 1994. Predictive microbiology. Int. J. Food Microbiol. 23: 241-264.
26. Simpson,R., Li,K.Y., Torres,J.A. 1989. A management tool to improve the microbial quality of refrigerated foods, p155-168. In Proceedings of an international conference on technical innovations in freezing and refrigeration of fruits and vegetables, University of California Davis, USA, Publ. International Institute of Refrigeration.
27. Thomas,L.V., Wimpenny,J.W.T. 1996. Competition between *Salmonella* and *Pseudomonas* species growing in and on agar, as affected by *pH*, sodium chloride concentration and temperature. Int. J. Food Microbiol. 29: 361-370.
28. Wijtzes,T., de Wit,J.C., Huis in 't Veld,J.H.J., van 't Riet,K., Zwietering,M.H. 1995. Modelling bacterial growth of *Lactobacillus curvatus* as a function of acidity and temperature. Appl. Environ. Microbiol. 61: 2533-2539.
29. Zwietering,M.H., Cuppers,H.G.A.M., de Wit,J.C., van 't Riet,K. 1994. Evaluation of data transformations and validation of a model for the effect of temperature on bacterial growth. Appl. Environ. Microbiol. 60: 195-203.

Modelling the interactions between *Lactobacillus curvatus* and *Enterobacter cloacae*; Part: 2 Mixed cultures and shelf life predictions

Abstract

The modelling approach presented in this study can be used to predict when interactions between microorganisms in homogenous systems occur. It was tested for the interaction between *Lactobacillus curvatus* and *Enterobacter cloacae*. In this binary system, *L. curvatus* produces lactic acid, which decreases the *pH* in the system. The *pH* decrease was found to be the main limiting factor of growth of both *E. cloacae* and *L. curvatus*. This resulted in *E. cloacae* reaching its final concentration earlier when compared to its growth in pure culture. The models consisted of a set of first order ordinary differential equations describing the growth, consumption and productions rates of both microorganisms. The parameters for these equations were obtained from pure culture studies and from literature. These equations were solved using a combination of analytical and numerical methods. The prediction of growth in mixed culture using parameters from pure culture experiments and literature were close to the experimental data. Both model predictions and experimental validation indicated that interaction occurs when the concentration of *L. curvatus* reaches 10^8 cfu.ml^{-1}. At that moment in time, the *pH* had decreased to inhibiting levels. These concentrations of microorganisms (10^8 cfu.ml^{-1}) do occur in fermented products where interactions obviously are important. In non fermented foods however, this level of microorganism indicate that spoilage has occurred or is about to start. Microbial interactions can therefore be neglected when predicting shelf life or safety of food.

Published: Int. J. Food Microbiol. 1999. 51:67-79
Authors: Malakar,P.K., Martens,D.E., Béal,C., Zwietering,M.H., van 't Riet,K.

1. Introduction

Microbial quality is determined by the number of microorganisms present in the food. If the microbial load reaches a certain limit the food is considered spoiled and unfit for human consumption. Predictive microbiology (McMeekin et al. 1993, McMeekin and Ross 1996) endeavours to quantify the growth responses of microorganisms to environmental conditions and hence is a useful tool in evaluating microbial shelf life. Empirical studies with pure cultures or cocktails of the same species are performed, where the growth rate is measured as functions of the physical and chemical characteristics of the food or the environment, the most important being the temperature, *pH*, water activity and gaseous atmosphere. The end result is a mathematical description of the growth process. This mathematical function can then be used as a base for predicting the increase or decrease of microorganisms in foods.

However, foods can support a complex microflora and interactions between the different species of microorganisms may affect their growth. One possible scenario is depicted in Fig. 1. The growth of pathogen B decreases when grown together with microorganism A, which in some cases can be of practical importance. We can assume for instance a spoilage level of 10^7 cfu.ml^{-1} of A and an acceptable safety level of 10^4 cfu.ml^{-1}of B. If interaction occurs below both these levels as indicated in Fig. 1, then the mathematical function describing the growth of B must take this interaction into account. If the interaction levels are over these limits, the food will be not be fit for consumption. It will either be spoiled (A>10^7 cfu.ml^{-1}) or unsafe (B>10^4 cfu.ml^{-1}) at the point of interaction and microbial interactions is then not of relevance when predicting shelf life.

The aim of this investigation was to quantitatively determine when interactions start to occur. In food microbiology, most of the studies on interactions were qualitative in nature (Stecchini et al. 1991, El-Gazzar et al. 1992, Winkowski et al. 1993 Rodriquez et al. 1994, Vescovo et al. 1996) and only sometimes aimed at elucidating the mechanism of interaction. We would like to take a step further and develop methods of quantitatively determining the levels of interaction (Fig. 1).

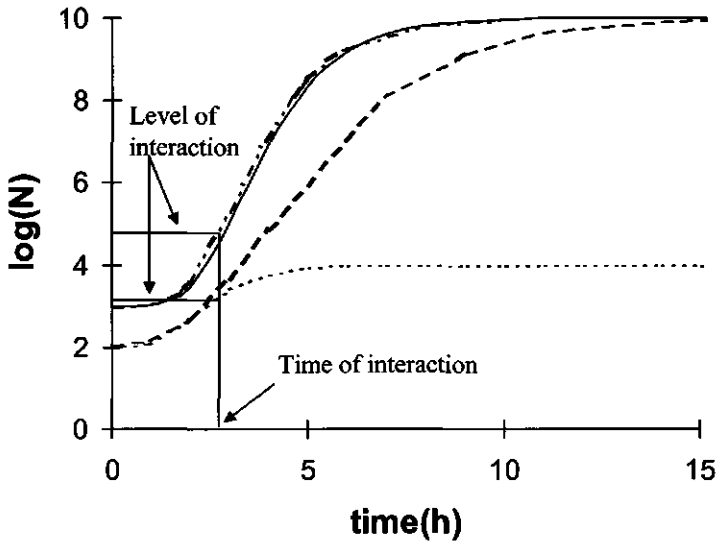

Fig. 1: Hypothetical simulation of growth of pure cultures of A (——) and B (— — —) compared with mixed cultures of A (— - - —) and B (- - - -). Interaction between A and B in the mixed culture decreases the growth of B. The level of interaction is the concentration of A at which the specific growth rate of B decreases by 10%.

Firstly by identifying the mechanism of interaction, secondly by defining when interaction happens and finally calculating the level of interaction. The time of interaction is defined as the time when the specific growth rates of the microorganisms in mixed culture deviates by 10% from their growth in pure culture. In Fig. 1 at the time of interaction, the difference in the predicted levels of microorganisms for pure and mixed culture growth is negligible. Therefore before this period is reached, models of pure culture growth can be used for predicting the growth of both pure and mixed cultures. In cases where the interaction levels are over the spoilage or safety limits, microbial interactions can clearly be neglected when modelling the growth of microorganisms, given the accuracy of microbial counts.

2. Theory

The model system chosen consisted of two microorganisms, *L. curvatus* and *E. cloacae* growing in a broth culture. The main carbon source for growth of both microorganisms was glucose. *L. curvatus* produces lactic acid, which lowers the *pH* of the broth culture. The *pH* decrease and lactic acid produced could inhibit the growth of both microorganisms. *L. curvatus* may also produce other inhibitory substances. However, these are secondary metabolites and they probably only play a minor role when compared to lactic acid (Martens et al. 1999).

2.1. Growth Kinetics

The following group of differential equations

$$\frac{dX_{Lc}}{dt} = \mu_{mLc} X_{Lc} \qquad (t>\lambda_{Lc}) \qquad 1 \qquad (\text{cell.m}^{-3}.\text{s}^{-1})$$

and

$$\frac{dX_{Ec}}{dt} = \mu_{mEc} X_{Ec} \qquad (t>\lambda_{Ec}) \qquad 2 \qquad (\text{cell.m}^{-3}.\text{s}^{-1})$$

was set up to represent this system, where the accumulation of *L. curvatus*, X_{Lc} (cell.m^{-3}) and *E. cloacae*, X_{Ec} (cell.m^{-3}) in the batch culture after the lag phase, is assumed to be proportional to the numbers of *L. curvatus* and *E. cloacae* present (first order kinetics). The constants of proportionality are the specific growth rates μ_{mLc} (s^{-1}) and μ_{mEc} (s^{-1}). These specific growth rates can change depending on the environmental conditions. The main factors of interaction are the glucose concentration S (mol.m^{-3}) the lactic acid concentration P (mol.m^{-3}) and the *pH* of the medium. In part one of this investigation, Martens et al. (1999) modelled the effects of S, P and *pH* on the specific growth rate of pure cultures of *L. curvatus* and *E. cloacae* at 30 °C. They concluded that the specific growth rate of *L. curvatus* could be described by

$$\mu_{mLc} = \mu_{opt_{Lc}} \left(\frac{S}{K_{S_{Lc}} + S} \right) \left(\frac{4(pH - pH_{\min_{Lc}})(pH_{\max_{Lc}} - pH)}{(pH_{\max_{Lc}} - pH_{\min_{Lc}})^2} \right) - b_2 P \qquad 3 \quad (\text{s}^{-1})$$

where the parameter $\mu_{opt_{Lc}}$ (s^{-1}) is the growth rate at optimal conditions. This occurs when S is much greater than $K_{S_{Lc}}$ ($mol.m^{-3}$), P is zero and the pH is equal to the mid point value of $pH_{\max_{Lc}}$ and $pH_{\min_{Lc}}$. $K_{S_{Lc}}$ is the Monod constant and b_2 ($m^3.mol^{-1}.s^{-1}$) is a regression parameter for the description of the effect of P on the specific growth rate of *L. curvatus*. Finally, $pH_{\min_{Lc}}$ is the minimal pH and $pH_{\max_{Lc}}$ the maximum pH at which no growth is observed.

In the case of *E. cloacae*, the specific growth rate can be described by

$$\mu_{mEc} = \mu_{opt_{Ec}} \left(\frac{S}{K_{S_{Ec}} + S} \right) \frac{4\left(pH - pH_{\min_{Ec}}\right)\left(pH_{\max_{Ec}} - pH\right)}{\left(pH_{\max_{Ec}} - pH_{\min_{Ec}}\right)^2} \qquad 4 \quad (s^{-1})$$

where the parameters $\mu_{opt_{Ec}}$, $K_{S_{Ec}}$, $pH_{\min_{Ec}}$ and $pH_{\max_{Ec}}$ have the same definitions as above. Equation 4 is similar to equation 3 except that lactic acid was found to have no significant effect on the specific growth rate of *E. cloacae* in the ranges at which the experiments were performed (Martens et al. 1999).

The rate of consumption of S in the broth culture (r_s) is also assumed to be proportional to the numbers of *L. curvatus* and *E. cloacae*. This model results in

$$r_{S_{Lc}} = \left(\frac{\mu_{mLc}}{Y_{XS_{Lc}}} + m_{Lc} \right) X_{Lc}(t) \qquad 5 \qquad (mol.m^{-3}.s^{-1})$$

and

$$r_{S_{Ec}} = \left(\frac{\mu_{mEc}}{Y_{XS_{Ec}}} + m_{Ec} \right) X_{Ec}(t) \qquad 6 \qquad (mol.m^{-3}.s^{-1})$$

where $r_{S_{Lc}}$ and $r_{S_{Ec}}$ are consumption rates, $Y_{XS_{Lc}}$ ($cell.mol^{-1}$) and $Y_{XS_{Ec}}$ ($cell.mol^{-1}$) are yield coefficients and m_{Lc} ($mol.cell^{-1}.s^{-1}$) and m_{Ec} ($mol.cell^{-1}.s^{-1}$) are non growth maintenance coefficients of *L. curvatus* and *E. cloacae*. The yield coefficient is the maximum amount of biomass produced from an amount of substrate consumed. These models state that the amount of S consumed is used for both growth and maintenance (Pirt 1975). In a batch culture, the absolute amount of S remaining in the culture is

$$\frac{dS}{dt} = -\left(r_{S_{Lc}} + r_{S_{Ec}}\right) \qquad 7 \qquad (\text{mol.m}^{-3}.\text{s}^{-1})$$

which is the total of the consumption rates of both microorganisms . The negative sign accounts for the consumption of *S*.

Lactic acid production by *Lactobacillus* species (equation 8) can also be modelled with a growth and non growth related term (Luedeking and Piret 1959). This model leads to

$$r_{P_{Lc}} = \left(\frac{\mu_{mLc}}{Y_{XP\,Lc}} + m_p\right) X_{Lc}(t) \qquad 8 \qquad (\text{mol.m}^{-3}.\text{s}^{-1})$$

where the yield value $Y_{XP\,Lc}$ (cell.mol^{-1}) is the maximum amount of biomass produced from an amount of lactic acid produced concurrently and the non growth term is represented by m_p (mol.cell^{-1}.s^{-1}) The absolute amount of *P* produced in time in the batch culture is

$$\frac{dP}{dt} = r_{P_{Lc}} \qquad 9 \qquad (\text{mol.m}^{-3}.\text{s}^{-1})$$

A point to note is that for solving equations 7 and 9, the yield and maintenance coefficients are assumed to be constant for the whole duration of growth. This assumption might not be valid just before the stationary phase as the degradation of the environment forces the microorganisms to adapt their metabolic activities (Nielsen and Villadsen 1992). For our purposes however, the assumption of constant coefficients is adequate because at 10 % deviation of specific growth rate, the conditions in the broth have not changed drastically yet. We would like to stress again that the objective of this research is to find the interaction level and not specifically describing the interaction process afterwards.

The *pH* of the broth can be correlated to the amount of *P* present, with the help of the titration curve

$$pH = \frac{pH_0 + a_1[P]}{1 + a_2[P]} \qquad 10 \qquad (-)$$

where the parameter pH_0 is the initial *pH* of the culture medium and a_1 (m^3.mol^{-1}) and a_2 (m^3.mol^{-1}) are regression parameters. Analytical solutions of equations 1, 2, 7 and 9 exist if the specific growth rates are constants and are presented in Table 1.

Table 1: Analytical solutions of the differential equations 1, 2, 7 and 9 for the case where the specific growth rate is constant.

Eq.	Analytical solution	units
1	$X_{Lc}(t) = X_{0_{Lc}} \exp(\mu_{mLc}(t - \lambda_{Lc}))$	cell.m^{-3}
2	$X_{Ec}(t) = X_{0_{Ec}} \exp(\mu_{mEc}(t - \lambda_{Ec}))$	cell.m^{-3}
7	$S_t = S_0 - \left(\frac{1}{\mu_{mLc}}\left(\frac{\mu_{mLc}}{Y_{XS_{Lc}}} + m_{Lc}\right)\left(X_{t_{Lc}} - X_{0_{Lc}}\right)\right) - \left(\frac{1}{\mu_{mEc}}\left(\frac{\mu_{mEc}}{Y_{XS_{Ec}}} + m_{Ec}\right)\left(X_{t_{Ec}} - X_{0_{Ec}}\right)\right)$	mol.m^{-3}
9	$P_t = P_0 + \left(\frac{1}{\mu_{mLc}}\left(\frac{\mu_{mLc}}{Y_{XP_{Lc}}} + m_P\right)\left(X_{t_{Lc}} - X_{0_{Lc}}\right)\right)$	mol.m^{-3}

$X_{0_{Lc}}$, $X_{0_{Ec}}$, S_0 and P_0 are initial concentrations. It is assumed one cell is equivalent to one colony forming unit (cfu).

Constant specific growth rate occurs (μ_m) during exponential growth and these solutions can then be used. However for prediction of growth until the stationary phase a numerical approach will have to be applied since μ_m starts to vary during this period. The parameters for the equations were determined either from pure culture studies of *L. curvatus* and *E. cloacae* or from literature (Roels 1983, van 't Riet and Tramper 1991, Wijtzes et al. 1995, Martens et al. 1999). These values are presented in Tables 2 and 3.

2.2. Time of interaction

The concentrations of *L. curvatus* and *E. cloacae* at the time of interaction can be calculated from our definition of when interaction occurs. We defined that this event takes place when the specific growth rate of *E. cloacae* in mixed culture deviates by 10 % from its growth in pure culture. This will then be 90 % of the maximum specific growth rate of *E. cloacae*, μ_{mEc} (dependent on the initial *pH*). Since the *pH* is the main factor for determining the point of interaction (Martens et al. 1999), the *pH* at which interaction occurs, pH_{int} is:

Table 2: Parameter values for equations 3 to 9 for *L. curvatus*

Parameter	Value	95% Confidence level	units
$\mu_{opt_{Lc}}{}^{w}$	1.06	1.01 - 1.11	h^{-1}
$K_{S_{Lc}}{}^{v}$	0.0004		$mol.m^{-3}$
$b_2{}^{m}$	$1.4 \cdot 10^{-3}$	$6 \cdot 10^{-4}$ - $2.2 \cdot 10^{-3}$	$m^3.mol^{-1}.h^{-1}$
$pH_{\min Lc}{}^{w}$	4.26	4.13 - 4.38	(-)
$pH_{\max Lc}{}^{w}$	9.77	9.53 - 10.01	(-)
$Y_{XS\,Lc}{}^{m}$	$7.0 \cdot 10^{13}$	$4.2 \cdot 10^{13}$ - $9.8 \cdot 10^{13}$	$cell.mol^{-1}$
$m_{Lc}{}^{r}$	$6.5 \cdot 10^{-20}$		$mol.cell^{-1}.s^{-1}$
$Y_{XP\,Lc}{}^{m}$	$3.3 \cdot 10^{13}$	$1.3 \cdot 10^{13}$ - $5.3 \cdot 10^{13}$	$cell.mol^{-1}$
$m_P{}^{r}$	$1.3 \cdot 10^{-19}$		$mol.cell^{-1}.s^{-1}$

^{m} : parameters values from Martens et al. (1999).

^{r} : values estimated from maintenance requirements for ATP of *L. casei*, Roels (1983).

^{v} : general value for glucose consumption of *E. coli*, van 't Riet and Tramper (1991).

^{w} : fitted parameters and predicted optimal growth rate at 30 °C from Wijtzes et al. (1995).

Table 3: Parameters for equations 3 to 7 for *E. cloacae*

Parameter	Value	95% Confidence level	units
$\mu_{opt_{Ec}}{}^{m}$	1.07	0.97 - 1.17	h^{-1}
$K_{S_{Ec}}{}^{v}$	0.0004		$mol.m^{-3}$
$pH_{\min Ec}{}^{m}$	5.56	5.41 - 5.70	
$pH_{\max Ec}{}^{m}$	9.99	9.61 - 10.37	
$Y_{XS\,Ec}{}^{m}$	$8.6 \cdot 10^{13}$	$5.3 \cdot 10^{13}$ - $11.9 \cdot 10^{13}$	$cell.mol^{-1}$
$m_{Ec}{}^{r1}$	$2.5 \cdot 10^{-20}$		$mol.cell^{-1}.s^{-1}$

^{m} : parameters values from Martens et al. (1999)

^{r1}: maintenance requirement of *E. aerogenes*, Roels (1983)

^{v} : general value for glucose consumption of *E. coli*, van 't Riet and Tramper (1991)

$$\left(pH_{int} - pH_{\min_{Ec}}\right)\left(pH_{\max_{Ec}} - pH_{int}\right) = \alpha_{int}\left(pH_0 - pH_{\min_{Ec}}\right)\left(pH_{\max_{Ec}} - pH_0\right) \qquad 11$$

where the parameter α_{int} is the percentage of the maximum specific growth rate for which interaction is defined. Equation 11 is a quadratic function giving only one solution of pH_{int} below the initial pH:

$$pH_{int}^2 - \left[pH_{\max_{Ec}} + pH_{\min_{Ec}}\right]pH_{int} + \begin{bmatrix}\alpha_{int}\left(pH_{\max_{Ec}} - pH_0\right)\left(pH_0 - pH_{\min_{Ec}}\right) \\ +\left(pH_{\max_{Ec}} pH_{\min_{Ec}}\right)\end{bmatrix} = 0$$

$$a = 1$$

$$b = -\left[pH_{\max_{Ec}} + pH_{\min_{Ec}}\right]$$

$$c = \left[\alpha_{int}\left(pH_{\max_{Ec}} - pH_0\right)\left(pH_0 - pH_{\min_{Ec}}\right) + pH_{\max_{Ec}} pH_{\min_{Ec}}\right]$$

$$pH_{int} = \frac{-b - \sqrt{b^2 - 4ac}}{2a} \qquad 12$$

In order to lower the initial pH of the broth to pH_{int}, a certain amount of lactic acid has to be produced by *L. curvatus*. This concentration of lactic acid at the time of interaction (P_{int}, mol.m^{-3}) can be found using

$$P_{int} = \frac{pH_{int} - pH_0}{a_1 - a_2 pH_{int}} \qquad 13 \qquad (\text{mol.m}^{-3})$$

which was derived from equation 10. Solving for P_{int}, there are two possible routes to obtaining the time of interaction t_{int} (s) and the population density of *L. curvatus* ($X_{int_{Lc}}$) and *E. cloacae* ($X_{int_{Ec}}$) at the moment of interaction. In the first route a numerical scheme can be used, where the calculations are stopped when the interaction point is reached (at concentration, P_{int}) and the interaction population densities and time noted down. The other possibility is to use an analytical solution.

2.2.1. Analytical solution

An analytical solution can be used if we make the following assumptions. *L. curvatus* is still growing at its maximum specific growth rate, μ_{mLc} when

interaction occurs and using this in equation 8, makes $\frac{\mu_{mLc}}{Y_{XPLc}} \rangle\rangle m_p$ as shown in equation 14

$$\frac{m_p}{\mu_{mLc}} Y_{XPLc} = 0.015 \qquad 14 \qquad (-)$$

Thus equation 8 and 9 can now be combined and simplified to

$$\frac{dP}{dt} = \left(\frac{\mu_{mLc}}{Y_{XPLc}} \right) X_{Lc}(t) \qquad 15 \qquad (\text{mol.m}^{-3}.\text{s}^{-1})$$

The assumption of a constant maximum specific growth rate of *L. curvatus* at the moment of interaction is valid because the growth of *L. curvatus* should not be inhibited by the *pH* yet as *L. curvatus* has a much lower $pH_{\min}$ than *E. cloacae*. Therefore, the time of interaction t_{int} calculated analytically and numerically should not differ substantially.

The population density of *L. curvatus* $X_{\text{int}_{Lc}}$ at the moment of interaction can now be calculated by integrating equation 1 (Table 1), which yields

$$X_{\text{int}_{Lc}} = X_{0_{Lc}} \exp(\mu_{mLc} t_g) \qquad 16 \qquad (\text{cell.m}^{-3})$$

where $X_{0_{Lc}}$ (cell.m^{-3}) is the initial inoculation density and t_g (s) is the time of growth of *L. curvatus*. The time of growth of *L. curvatus* is the time after lag until the time of interaction t_{int} (s). Substituting equation 16 in 15 and using the same integration interval as above yields

$$P_{\text{int}} = P_0 + \left(\frac{X_{\text{int}_{Lc}} - X_{0_{Lc}}}{Y_{XP_{Lc}}} \right) \qquad 17 \qquad (\text{mol.m}^{-3})$$

where P_0 and P_{int} (mol.m^{-3}) are the initial (P_0 =0) and interaction concentration of lactic acid. Note that we can neglect the initial population density of *L. curvatus*, $X_{0_{Lc}}$ in the numerator of equation 17 because it will be very small when compared to the interaction population density of *L. curvatus*, $X_{\text{int}_{Lc}}$. Solving for t_g from equations 16 and 17 yields

$$t_g = \frac{1}{\mu_{mLc}} \ln \left(\frac{P_{\text{int}} Y_{XP_{Lc}}}{X_{0_{Lc}}} \right) \qquad 18 \qquad (\text{s})$$

and the time of interaction is

$$t_{int} = t_g + \lambda_{Lc} \qquad 19 \qquad (s)$$

where λ_{Lc} (s) is the lagtime of *L. curvatus*.

If we now also calculate the population density of *E. cloacae* at the moment of interaction ($X_{int_{Ec}}$) analytically, there will be a discrepancy between the analytical and numerical solutions, since the maximum specific growth rate of *E. cloacae* in mixed culture deviates by 10%. If this discrepancy is shown to be small, we can still choose for the analytical solution. Integrating equation 2 from time after lag of *E. cloacae* to the time of interaction t_{int}, results in

$$X_{int_{Ec}} = X_{0_{Ec}} \exp(\mu_{mEc}(t_{int} - \lambda_{Ec})) \qquad 20 \qquad (cell.m^{-3})$$

where $X_{int_{Ec}}$ is the interaction population density, $X_{0_{Ec}}$ is the initial inoculation density and λ_{Ec} (s) is the lagtime of *E. cloacae*.

Equations 16, 18, 19 and 20 give a very quick method of estimating the time of interaction and numbers of *L. curvatus* and *E. cloacae* at the moment of interaction. In order to check the validity and describe the process of interaction even after the inhibition is more than 10%, equations 1 to 10 will also be solved numerically, taking into account dynamically changing conditions.

3. Material and methods

3.1. Experimental technique

Frozen cultures of *L. curvatus* and *E. cloacae* stored at -80 °C were thawed and pre-cultured at *pH* 5.8 and *pH* 7 respectively in MRS broth for 22 hours. Serial dilutions were then made to get the desired inoculum level for the start of the experiment.

Mixed experiments were carried out in 250 ml Erlenmeyers filled with 100 ml MRS broth (Merck). The initial *pH* of the MRS broth was adjusted to either *pH* 6 or *pH* 7 with 2N NaOH and the desired level of innoculum was then added to the Erlenmeyers. Concurrently, pure cultures of the inoculum were also prepared, each

Table 4. Regression parameters of titration curves to be used for equation 10

Parameter	initial *pH*	Value	95% Confidence level	units
a_1	7	0.038	0.033 - 0.044	$m^3.mol^{-1}$
a_2	7	0.015	0.013 - 0.016	$m^3.mol^{-1}$
a_1	6	0.029	0.027 - 0.032	$m^3.mol^{-1}$
a_2	6	0.011	0.010 - 0.012	$m^3.mol^{-1}$

having the same inoculum level as the mixed cultures. These cultures were then incubated at 30 °C.

Once every hour samples from both the pure and mixed cultures were taken. The concentration of microorganisms in $cfu.ml^{-1}$ was then determined using the pour plating method. *L. curvatus* was enumerated in MRS agar with acetic acid added to prevent the growth of *E. cloacae*. *E. cloacae* was enumerated on VBRG agar which did not support growth of *L. curvatus*. The *pH* of both the cultures was determined from 1 ml samples of the broth using a Schott *pH* electrode.

Titration experiments using DL-lactic acid (Janssen Chimica Belgium) as the titrant were performed on the MRS medium as used in the growth experiments. The regression parameters for the titration curves are presented in Table 4.

3.2. Computational technique

The differential equations, 1,2,7 and 9 were solved using a combination of analytical and numerical techniques. Firstly the duration of the lag phase was found by fitting the experimental data points of the pure cultures with the modified Gompertz model (Zwietering et al. 1990), using a constant μ_m calculated from equations 3 and 4 and initial conditions. These fitted lag times are presented in Table 5 and will be used for both pure and mixed culture predictions. This was because the aim of the investigation was to use only parameters of pure culture growth for predicting growth in mixed culture. The fit was done using the program TableCurve (TableCurve 2D for Windows V2.03). The main reason of determining the lag phase with an empirical fit is the large variability of the lag phase data.

Table 5: The fitted lag times of pure culture growth *L. curvatus* (λ_{Lc}) and *E. cloacae* (λ_{Ec}) used for simulations

Parameter	Initial *pH*	Value(h)	95% confidence level	Used in Fig.
λ_{Lc}	7	0.50	0.33 - 0.68	2
λ_{Ec}	7	2.00	1.61 - 2.39	2
λ_{Lc}	7	2.52	1.93 - 3.12	3
λ_{Ec}	7	2.49	1.77 - 3.22	3
λ_{Lc}	7	1.36	0.94 - 1.77	4
λ_{Ec}	7	1.41	0.84 - 1.97	4
λ_{Lc}	6	0.06	-0.48 - 0.59	5
λ_{Ec}	6	4.73	4.06 - 5.40	5
λ_{Lc}	6	0.00	-1.57 - 1.57	6
λ_{Ec}	6	9.88	8.90 - 10.86	6

Secondly the specific growth rate μ_m was assumed to be zero during the lag phase. When the lag phase ends, exponential growth occurs. To calculate the growth in this phase, time steps of 0.1 hour were selected and μ_m was assumed constant during each time step. For a constant μ_m during one time step, an analytical solution could be found for all the differential equations (Table 1). Using the initial values of the state variables, the values of all the state variables at the end of the first time step could be calculated. These values then become the initial conditions for the next time step and the above process was repeated until the *pH* equals the value of $pH_{\min}$ or S equals zero. The specific growth rate is now zero again and the maximum number of microorganisms in the culture is reached. These simulations were programmed in Matlab from Mathworks Inc.

4. Results and discussions

4.1. Qualitative description of interaction

Fig. 2 to 6 show that interactions can be clearly observed from the divergence of the growth curve of *E. cloacae* in the mixed culture when compared

to its growth in pure culture for various initial innoculum levels at an initial *pH* of 7 and 6. In Fig. 2 as the *pH* of the medium in the mixed culture begins to decrease after 5 hours, there is a gradual decrease of the specific growth rate of both microorganisms in the mixed culture. This trend is present in all the curves.

While there is no relevant difference between growth of *L. curvatus* in mixed and pure culture, *E. cloacae* in mixed culture approaches its final level much earlier when compared to *E. cloacae* in pure culture. Further decrease of *pH* in the mixed culture causes a decline in the number of *E. cloacae* and after 24 hours no *E. cloacae* is present anymore. The same trend can be seen in Fig. 3 to 6.

The main cause of interaction in the model system must be the decrease of *pH*. This is because glucose could still be detected at the end of the experiment at amounts much greater than K_S causing the term representing the effect of S to remain 1 (equation 3). The amounts of lactic acid produced at the moment of interaction P_{int} can be calculated with equation 11 and 13. At these concentrations, $4.01 \cdot 10^{-3}$ (M) at *pH* 7 and $1.36 \cdot 10^{-3}$ (M) at *pH* 6, the effect of P on the specific growth rate of *E. cloacae* is still negligible.

4.2. Point of interaction

From the data in Fig. 2 to 6 and Table 6, it can be concluded that the concentration of *L. curvatus* when interactions occur is about 10^8 cfu.ml^{-1} in all cases. At this concentration, *L. curvatus* has produced enough lactic acid to sufficiently bring the initial *pH* down to a level (pH_{int}) where growth of *E. cloacae* is inhibited. Also, at this *pH*, *L. curvatus* is not inhibited yet and the use of the analytical solution is justified as both methods give comparable values.

Using an analytical solution (equation 20) with a constant μ_{mEc} to estimate the number of *E. cloacae* at the moment of interaction is also satisfactory because the difference between the analytical and numerical approach is negligible. Real noticeable differences between the analytical and numerical values will occur when the specific growth rate of *E. cloacae* in the mixed culture decreases further.

Since the main mechanism of interaction is the lowering of *pH*, delaying *L. curvatus* from reaching this level will also delay the onset of *pH* decrease. This can

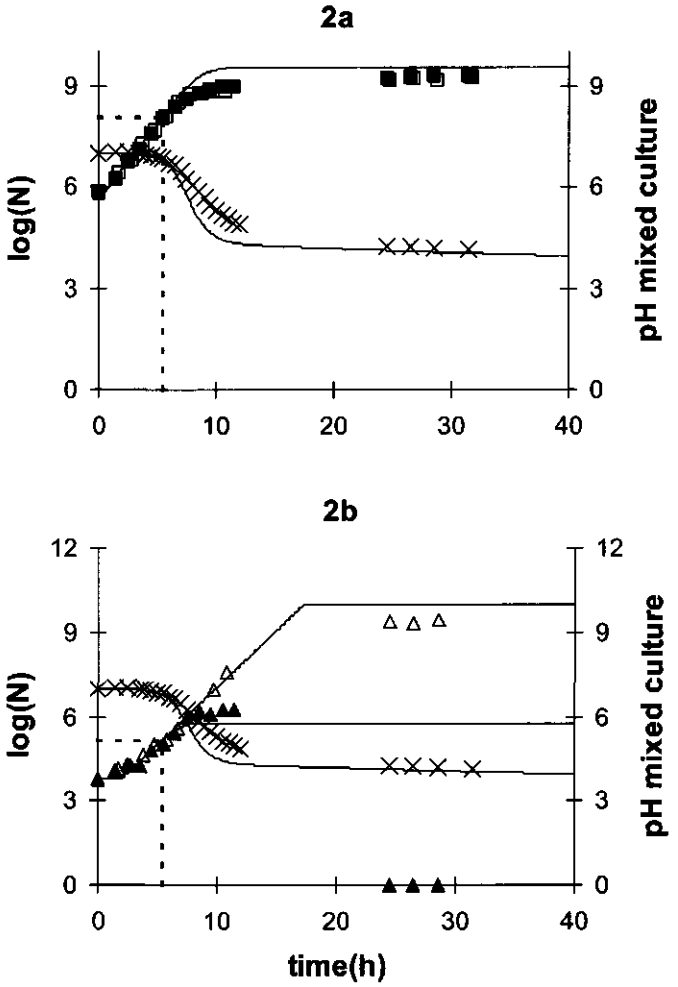

Fig. 2a and 2b: Growth of *L. curvatus* , 2a (initial innoculum of ~ 10^6 cfu.ml^{-1}) and *E. cloacae* 2b (initial innoculum of ~ 10^4 cfu.ml^{-1}) in pure and mixed cultures and the decrease of *pH* caused by the production of lactic acid by *L. curvatus* in the mixed cultures at an initial *pH* of 7. (▲ *E. cloacae* in mixed culture, Δ *E. cloacae* in pure culture, ■ *L. curvatus* in mixed culture, □ *L. curvatus* in pure culture, **X** *pH* in mixed culture. ▲ at 0.0 indicate the absence of *E. cloacae*, —— model predictions, ----- time and level of interaction).

Table 6: Calculated times of growth, and levels of interactions of *L. curvatus* ($t_{g_{Lc}}$, $X_{\text{int}_{Lc}}$) and *E. cloacae* ($t_{g_{Ec}}$, $X_{\text{int}_{Ec}}$) for various initial inoculum levels ($X_{0_{Lc}}$, $X_{0_{Ec}}$) at *pH* 7 and 6

Fig. no.	Initial *pH*	$\log X_{0_{Lc}}$	$\log X_{0_{Ec}}$	$t_{g_{Lc}}$ (h)	$\log X^{a}_{\text{int}_{Lc}}$	$\log X^{n}_{\text{int}_{Lc}}$	$t_{g_{Ec}}$ (h)	$\log X^{a}_{\text{int}_{Ec}}$	$\log X^{n}_{\text{int}_{Ec}}$
2	7	5.85	3.78	4.9	8.12	8.06	3.4	5.18	5.13
3	7	1.90	2.54	13.5	8.12	8.07	13.5	8.06	8.02
4	7	5.12	1.63	6.5	8.12	8.11	6.5	4.27	4.21
5	6	5.63	3.82	5.1	7.66	7.62	0.4	3.89	3.87
6	6	1.20	3.78	16.2	7.65	7.60	6.3	4.83	4.81

$X_{0_{Lc}}$, $X_{\text{int}_{Lc}}$, $X_{0_{Ec}}$, $X_{\text{int}_{Ec}}$ in cfu.ml^{-1}; *a*, analytical solution; *n*, numerical solution.

be seen by comparing Fig. 2 and 3, where the initial inoculum level of *L. curvatus* was decreased from 10^6 to 10^2 cfu.ml^{-1} while the number of *E. cloacae* was kept nearly the same. The time for interactions to occur subsequently increased from 5.4 hours to 16.0 hours while the level of *L. curvatus* when interactions occurred remained about 10^8 cfu.ml^{-1}. This was confirmed by the higher maximum concentration of *E. cloacae,* as it could now continue to grow at its intrinsic specific growth rate for a longer period of time.

The opposite effect can be observed by comparing Fig. 2 and 4 where the initial number of *E. cloacae* is decreased while the number of *L. curvatus* remained nearly the same. The time of interaction did not change much while the interaction level of *E. cloacae* decreased by nearly one log unit. Also the final level of *E. cloacae* was lower. The effects discussed above can also be seen in Fig. 5 and 6 where the initial *pH* was 6.

Further decreasing the concentration of *L. curvatus* while increasing that of *E. cloacae* will lead to a situation where the growth of *E. cloacae* would not be inhibited by the presence of *L. curvatus*. This is because *E. cloacae* would have reached its maximum concentration before the *pH* decreased to inhibitory levels. Two experiments were performed with 10^6 cfu.ml^{-1} of *E. cloacae* and 10^2 cfu.ml^{-1} of *L. curvatus* and there were no differences between the growth of *E. cloacae* in mixed and pure cultures (results not shown).

4.3. Model predictions

By solving the models numerically using parameters from pure culture experiments, both pure and mixed culture predictions were close to the actual data, except for some structural deviations (Fig. 2 to 6). Firstly, the inactivation kinetics of *E. cloacae* in the mixed culture was not taken into account. When *pH* of the broth reaches the minimum *pH* of growth ($pH_{\min_{Ec}}$) and below, the specific growth rate μ_{mEc} is predicted to be zero. This results in a prediction of a constant final concentration of *E. cloacae*. Since our main objective was to investigate the point of interaction, what happens after this moment was beyond the scope of the research. The point of interaction is however well predicted and occurs when the concentration of *L. curvatus* reaches 10^8 cfu.ml^{-1}.

Secondly, the decrease in growth rate at high concentrations of *L. curvatus* in most cases is faster than predicted. Also, the predicted *pH* decrease is more gradual when compared to the actual data points. As was introduced earlier, the models are not accurate anymore when conditions in the broth start to change rapidly. A likely reason for these observations is that the yield and maintenance coefficients of biomass on substrate and product are not constant but dependent on the *pH*.

The predicted growth of *E. cloacae* in pure cultures stops abruptly because according to the models, there is no more glucose remaining in the medium. This is not realistic because glucose can still be detected at the end of the experiments with pure culture growth. This suggests that another mechanism is taking place, which inhibits the growth of *E. cloacae* when high numbers are reached.

Lastly, the fitted lag times for the experiments at an initial *pH* of 6 differed by about 5 hours (Fig. 5, 6). This resulted in a large shift of the predicted point of interaction as shown in Fig. 6. This is inevitable because at lower *pH*, the lag times starts to show more variability partly because of adverse conditions.

It should be noted that the curves for the mixed and pure cultures in Fig. 2 to 6 are, with the exception of the lag time, predictions rather than empirical fits of the data (Berkman et al. 1990, Buchanan and Bagi 1997). The overall model gives a good prediction of the behavior of the organisms in both pure and mixed cultures over a large range of conditions. An empirical approach would require not only the

physical characteristics but also the effect of the initial number of microorganisms present and hence increase the numbers of parameters. The present methodology uses less parameters and gives a better qualitative and quantitative insight into the processes taking place in the mixed culture broth.

5. Conclusion

This research has shown quantitatively that interactions occur at around 10^8 $cfu.ml^{-1}$ and the main mechanism of interaction in our model system is the decrease of *pH*. A food would be considered spoiled at this level. This would not be the case for fermented foods where interactions are definitely important. Fermentation under controlled conditions is a natural way of ensuring food quality and food safety. Reliance on uncontrolled growth for quality and safety is however very dangerous and should not be considered good practice.

The general model set up proved to be simple and straightforward and was able to predict the onset of interaction. Further research will focus on colony growth of *L. curvatus* in solid medium. Here, local *pH* gradients in the colony can develop due to mass transfer restrictions and cause the growth of the microorganisms to deviate from growth in broth cultures. This phenomenon can be an important factor when considering the use of current models of predictive microbiology for predicting colony growth in solid media. This is because these models were developed from experiments in homogenous broth cultures.

6. Reference

1. Berkman,T., Bozoğlu,T.F., Özilgen 1990. Mixed culture growth kinetics of *Streptococcus thermophilus* and *Lactobacillus bulgaricus*. Enzyme Microb. Technol., 12: 138-140.
2. Buchanan,R.L., Bagi,L.K. 1997. Microbial competition: Effect of culture conditions on the suppression of *Listeria monocytogenes* Scott A by *Carnobacterium piscicola*. J. Food Protect. 3: 254-261

3. El-Gazzar,F.E., Bohner,H.F., Marth,E.H. 1992. Antagonism between *Listeria monocytogenes* and *Lactococci* during fermentation of products from ultrafiltered skim milk. J. Dairy Sci. 75: 43-50.
4. Luedeking,R., Piret,E.L. 1959. A kinetic study of the lactic acid fermentation. Batch process at controlled *pH*. J. Biochem. Microbiol. Technol. Engng. 1: 393-412.
5. Martens,D.E., Beal,C., Malakar,P.K., Zwietering,M.H., van 't Riet,K. 1999. Modelling the interactions between *Lactobacillus curvatus* and *Enterobacter cloacae*. I. Individual growth kinetics. Int. J. Food Microbiol. 51: 53-65.
6. McMeekin,T.A., Olley,J., Ross,T., Ratkowsky,D.A. 1993. Predictive microbiology: Theory and application. Research Studies Press Ltd. Somerset, United Kingdom.
7. McMeekin,T.A., Ross,T. 1996. Shelf life prediction: status and future possibilities. Int. J. Food Microbiol. 33: 65-83.
8. Nielsen,J., Villadsen,J. 1992. Modelling of microbial kinetics. Chem Engng. Sci. 47: 4225-4270
9. Pirt,S.J., 1975. Principles of Microbe and Cell Cultivation. Blackwell. London.
10. Rodriquez,J.M., Sobrino,O.J., Moreira,W.L., Cintas,L.M., Casaus,P., Ferna,M.F. 1994. Inhibition of *Yersinia enterocolitica* by *Lactobacillus-sake* strains. Meat Sci. 17: 305-313.
11. Roels,J.A. 1983. Energetics and kinetics in biotechnology. Elsevier Biomedical Press. Amsterdam, The Netherlands.
12. Stecchini,M.L., Sarais,I., Bertoldi,M. 1991. The influence of *Lactobacillus plantarum* culture inoculation on the fate of *Staphylococcus aureus* and *Salmonella typhimurium* in Montasio cheese. Int. J. Food Microbiol. 14: 99-110.
13. van 't Riet,K., Tramper,J. 1991. Basic bioreactor design. Marcel Dekker Inc. New York, US.
14. Vescovo,M., Torriani,S., Orsi,C., Macchiarolo,F., Scolari,G. 1996. Application of antimicrobial-producing lactic acid bacteria to control pathogens in ready-to-use vegetables. J Appl Bacteriol. 81: 113-119.
15. Wijtzes,T., de Wit,J.C., Huis in 't Veld,J.H.J., van 't Riet,K., Zwietering,M.H. 1995. Modelling bacterial growth of *Lactobacillus curvatus* as a function of acidity and temperature. Appl. Environ. Microbiol. 61: 2533-2539.
16. Winkowski,K., Crandall,A.D., Montville,T.J. 1993. Inhibition of *Listeria monocytogenes* by *Lactobacillus bavaricus* MN in beef systems at refrigeration temperatures. Appl. Environ. Microbiol. 59: 2552-2557.

17. Zwietering,M.H., Jongenburger,I., Rombouts,F.M., van 't Riet,K. 1990. Modeling of the bacterial growth curve. Appl. Environ. Microbiol. 56: 1875-1881.

Micro gradients in bacterial colonies: Use of fluorescence ratio imaging, a non- invasive technique

Abstract

Fluorescence ratio imaging is a non-invasive technique for studying the formation of micro-gradients in immobilized bacterial colonies. These gradients can be quantified easily when combined with the gel cassette system designed at the Institute of Food Research, Norwich, United Kingdom. Colonies of *Lactobacillus curvatus* were observed using this technique and relevant *pH* gradients were present when the colonies reached a diameter of about 100 μm. These *pH* gradients were due to production of lactic acid by *L. curvatus* cells in the colonies. The spatial resolution of the images was about 1.5 μm (scale of bacterial cells) and therefore very suitable for observing local effects in colonies which ranged in sizes from 1 to 500 μm.

1. Introduction

In microbiology, specifically predictive microbiology, there is a huge amount of data on growth of microorganisms in broth cultures (Pirt 1975, Zwietering et al. 1990, Nielsen and Villadsen 1992, McMeekin et al. 1993, Wijtzes et al. 1995). Here conditions are assumed to be homogenous throughout the culture media and any changes of the environment are transmitted to all the microorganisms instantaneously. Material is transported via convection and diffusion. In colony growth, the immobilized cells in the colony are subjected to more variable conditions as the mode of transport here is mainly diffusive, which is generally much slower than convection.

Localised gradients may arise in time. Along these gradients, microorganisms will vary in their growth rates (Wentland et al. 1996) and in some

Published: Int. J. Food Microbiol. 2000. 56:71-80
Authors: Malakar,P.K., Brocklehurst,T.F., Mackie,A.R., Wilson,P.D.G., Zwietering,M.H., van 't Riet,K.

cases stimulate their stress responses (Archer 1996) to cope with the adverse conditions. In broth cultures, similar conditions are present near the stationary phase, but if these stress responses are generated much earlier in solid systems, these may confer enhanced resistance on the microorganisms. Food manufacture involves the use of preservation systems and these will be more effective if the stress response (adaptation response) of the bacteria is not activated. With the modern consumer wanting foods which are minimally processed, this can be an important variable when considering strategies for controlling food safety.

The work done so far to investigate the existence of micro gradients in bacterial colonies has been performed with the help of micro electrodes. Wimpenny and Coombs (1983) have shown that there can be substantial gradients of oxygen tension in and around colonies of *Bacillus cereus*. Walker et al. (1997) have also shown that *pH* gradients occur in and around colonies of *Salmonella typhimurum*. Micro electrodes are invasive and colonies must be discarded after measurements have been taken. The measurement might even influence the gradient. The fluorescence ratioing technique used here enables us to observe colonies throughout their growth non-invasively and can be more representative of what actually happens in a colony in real time. It will also reinforce the concept that gradients do form in colonies.

The microorganism used in this study is *Lactobacillus curvatus*. It is a heterofermentative microorganism, which produces mainly lactic acid as an end product of metabolism, which decreases the *pH* of its surroundings. When immobilised, acid production is localised and lactic acid diffuses out of the colony. This phenomenon results in a continuum of growth characteristics throughout the colonies. In an isolated colony, a *pH* gradient would form in the colony in time and produce zones of different growth rates. Here, there is interaction in the colony itself (intra colony interaction) and the microorganisms at the leading edge of the colony grow the fastest as conditions here are most favourable.

At the other end of the continuum (high colony density), the acid produced by a colony would reach or affect its neighbour in a shorter time span when compared to an isolated colony. One consequence is that the surrounding medium

becomes saturated with lactic acid. The interactions between the colonies (inter colony interaction) results in growth which approaches that of broth cultures where the conditions are homogenous.

The main objective of this work was to investigate these two types of behaviour using fluorescence ratio imaging

2. Materials and methods

2.1. Preparation gel cassette

Fig. 1 shows the gel cassette used for this study. The cassette is of the same size as a glass microscope slide and has a depth of 2 mm (1a).

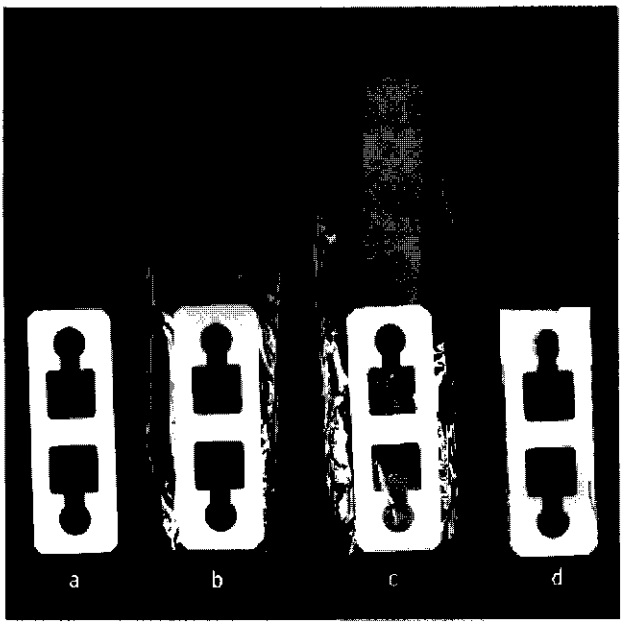

Fig. 1: Various stages in the preparation of a gel cassette for filling and inoculation. A gel cassette (1a) is placed in a PVC bag (1b) in which is placed a strip of baking paper (1c) to prevent the PVC bag from sticking to each other during autoclaving. 1d represents an autoclaved gel cassette, which has been filled with growth medium containing gelatine aseptically

At each end of the cassette there is a filling port for the introduction of the sample and a window for observation under a microscope. This cassette was then placed in a clear PVC bag (1b) after which a strip of baking paper was inserted (1c) to prevent the sides of the bag from sticking to each other during autoclaving. After autoclaving, the strip of baking paper was removed and the ends sealed with masking tape aseptically. Fig. 1d shows a cassette, which has been filled aseptically with gelatine using a syringe. The hole made by the syringe in the filling port was sealed using aseptic tape. The sample in the window of the cassette was sterile as no contamination was observed in all the cassettes used during this investigation.

2.2. Fluorescence ratio imaging

When a fluorophore is excited by suitable light source, its electrons gain energy and occupy higher energy levels. When returning to the ground state, from the first excited singlet state, energy can be emitted as light. This is called fluorescence, and it is always of lower energy or higher wavelength than the excitation light energy. This is because some or all of the excitation energy is also dissipated by non-radiative processes like heat. The competition between these two processes is environment dependent and fluorescence can be used as a probe to the immediate surroundings.

Fig. 2 shows typical spectra produced by measuring the fluorescent emission intensity at 555 nm as a function of excitation wavelength for Oregon Green™ (Molecular Probes, Leiden, Netherlands). These spectra were taken using a spectrophotometer (Perkin Elmer, Oak Brook, Illinois, USA). It is clear that some regions of the spectra are more sensitive to *pH* than others. By dividing the intensity at 510 nm by that at 440 nm (ratioing), it is possible to eliminate biases caused by the concentration of fluorophores, photo bleaching or illumination stability. If these ratios are then plotted against the *pH* of the sample, there will be a region where the correspondence between the ratios and the *pH* is linear. For Oregon Green™, this linear region is for the ranges of *pH* 6 to *pH* 3. A point to note is that the background fluorescence of the medium of interest must be accounted

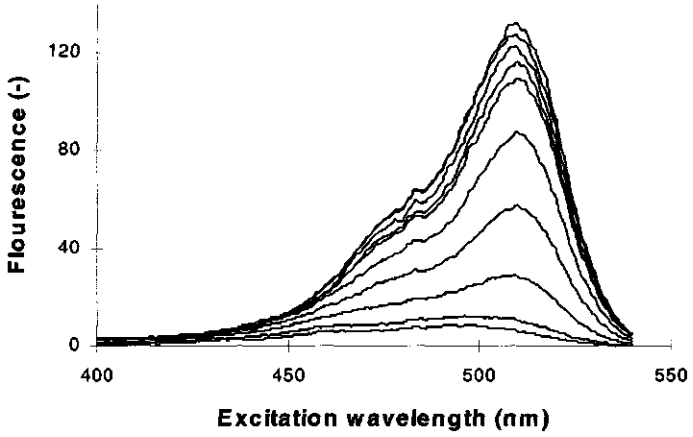

Fig. 2: Intensity of fluorescence measured at 555 nm from excitation light of wavelengths of 400 nm till 540 nm. The individual curves from top to bottom represent the *pH* range from *pH* 7.10, 6.67, 6.05, 5.48, 5.08,4.48, 4.07, 3.56, 2.98 and 2.76.

for to obtain accurate results. This can be done by subtracting it from the total fluorescence of the sample.

2.3. Calibration

For calibrating the microscope, a series of 10 ml samples containing equal volumes of MRS (Oxoid, Hampshire, UK, 104 $g.L^{-1}$) and bovine gelatine (Oxoid, Hampshire, UK, 200 $g.L^{-1}$) was prepared. A *pH* meter (Radiometer, Copenhagen, Denmark) was used to adjust the *pH* of this series with either 1 M NaOH or 5 M HCl (range, *pH* 6 to *pH* 3). Then about 0.5 ml of each sample was injected into one end of an empty and sterile gel cassette and the mixture allowed to set. This was done for all the samples in the series.

While the gel mixture was setting in the gel cassettes, Oregon Green™ was added to the remaining samples of the series (kept molten in 30 °C water bath) to a final concentration of about 1.25 $mg.L^{-1}$. This was done by diluting the stock

solution (5 mg Oregon Green™ in 2 ml 99.9% (w/v) ethanol) 10x and mixing 50 µl of this with 9.95 ml of sample.

When the gel mixture had set in one end of the cassette, about 0.5 ml of sample with Oregon Green™ at the corresponding *pH* was injected into the other end of the cassette. The final result is a cassette (at required *pH*) with one end containing sample with dye and the other without. The side of the cassette without the dye was used for measurement of the background fluorescence. The cassettes were then kept at 20 °C for further analysis.

2.4. Optical system

The optical system used was a fluorescence microscope (Nikon UK, Surrey, UK) with the following filters, excitation (440 ± 10 nm, 510 ± 11.5 nm), emission (535 ± 11.5 nm) and a dichroic mirror (540 nm, long pass). The light source was a mercury arc and the camera connected to the microscope was a cooled CCD device (SP eye, Photonic Science, Cambridge, UK).

The 1x and 5x objective lens were used for the calibration measurements. A plane in between the top and bottom of each window was chosen by adjusting the focusing at that window of the cassette. The area was then excited with light of the relevant wavelengths (440 and 510 nm) and the fluorescent intensity measured. The information from both windows was then processed with a macro of the image processing software (ImagePro, Media Cybernetics, Maryland, USA) and the ratios calculated after subtracting the background fluorescence.

In the growth experiments, the same procedure was used when the colonies were not yet visible. Once the colonies were visible, the widest part of the colony of interest was brought into focus. This gave information about the radius of the colony. A light transmission image was first taken and stored. Then the fluorescent images were taken and the ratios calculated. From these ratios, a 2D *pH* map of the area in focus could then be drawn. Superimposing the transmission image to the *pH* map gave the *pH* profile in and around the colony.

2.5. pH front experiments

The growth medium as prepared above was also used for the front experiment. The *pH* was first adjusted to *pH* 5.5 with 5 M HCl. Then 0.5 ml was introduced into one end of the gel cassette and allowed to set (blank). Oregon Green™ was then added to the growth medium to a concentration of 1.25 $mg.L^{-1}$ and 0.25 ml injected into the other end such that only half of the window was filled and allowed to solidify.

5 M lactic acid was added to a fresh batch of growth medium at an initial *pH* of 5.5 till the required *pH* for the start of the experiment. Oregon Green™ was then added and the mixture kept molten in a 30 °C water bath. Before the start of the *pH* front experiment, the *pH* of this liquid mixture was checked again with a *pH* meter. The *pH* of the mixture already in the cassette was also checked using the fluorescence microscope.

At the start of the experiment, 0.25 ml of the growth medium containing lactic acid and Oregon Green™ was introduced into the window of the gel cassette which was already half filled and allowed to set. This cassette was then placed under the microscope so that both halves were visible under a 1x objective. A clear boundary between the two halves was observed and a transmission image was taken. This served to fix the boundary for further analysis. Regular fluorescent measurements were then taken to track the diffusion of lactic acid.

2.6. Growth experiments

0.1 ml of stock culture of *L. curvatus* was thawed and resuscitated in 10 ml of MRS broth and incubated at 20 °C overnight. The composition of the growth medium (MRS, bovine gelatine) used for filling the gel cassette was the same as that used for calibrating the microscope. The only difference being that the mixing and filling was done aseptically. The initial *pH* was then adjusted aseptically to 5.5 and about 0.5 ml (without *L. curvatus*) was injected into one end of the gel cassette and the mixture allowed to set (blank).

The appropriate amount of the resuscitated *L. curvatus* was then inoculated aseptically into the growth medium and Oregon Green™ added to a final

concentration of 1.25 mg.L^{-1}. This mixture was then thoroughly mixed and about 0.5 ml injected into the other end of the gel cassette. The cassette was then placed in a 20 °C incubator for further analysis.

Duplicate cassettes containing 1000 cfu.ml^{-1}, 100 cfu.ml^{-1} and 5 cfu.ml^{-1} of *L. curvatus* were used for the experiments. Measurements of *pH* profiles in the cassettes were taken every 24 hours and continued for 240 hours.

3. Results and discussion

3.1. Calibration curve

Fig. 3 shows the calibration curve of the *pH* versus the fluorescence ratios (F_{510}/F_{440}) of the microscope used in this investigation. Note that these ratios are not quantitatively similar to those calculated from Fig. 2 as the optical system was different.

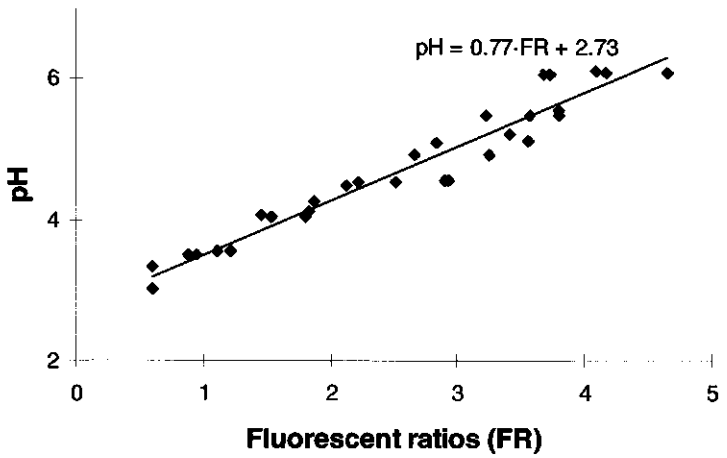

Fig. 3: Calibration curve for optical system used in this investigation. It shows the *pH* versus fluorescent ratio (FR) of the intensities at 440 nm and 510 nm. Linear regression was applied and the result presented in the upper right hand corner of the graph. (Valid from *pH* 3.0 to *pH* 6.0)

The intercept and its 95% confidence interval was 2.73 ± 0.20 *pH* units and the slope and its 95% confidence interval was 0.77 ± 0.07. This curve was valid from *pH* 3 to *pH* 6. This was sufficient for our purposes as *L. curvatus* grows very well at an initial *pH* of 6 and will acidify the medium through the production of lactic acid. The minimum *pH* of growth of *L. curvatus* is 4.26 (Wijtzes et al. 1995) and well within the range of the calibration curve.

3.2. Diffusion front experiment

The diffusion front experiment was performed to test the ability of the optical system in tracking the diffusion of lactic acid. Fig. 4 shows line graphs in the x-direction of 2D *pH* images taken at different time intervals. These *pH* images were converted from the fluorescent ones using the calibration curve above.

Initially, the left half of the gel cassette contained lactic acid at *pH* 3.5 while the other half was at *pH* 5.5 with no lactic acid present. Note that Fig. 4 shows

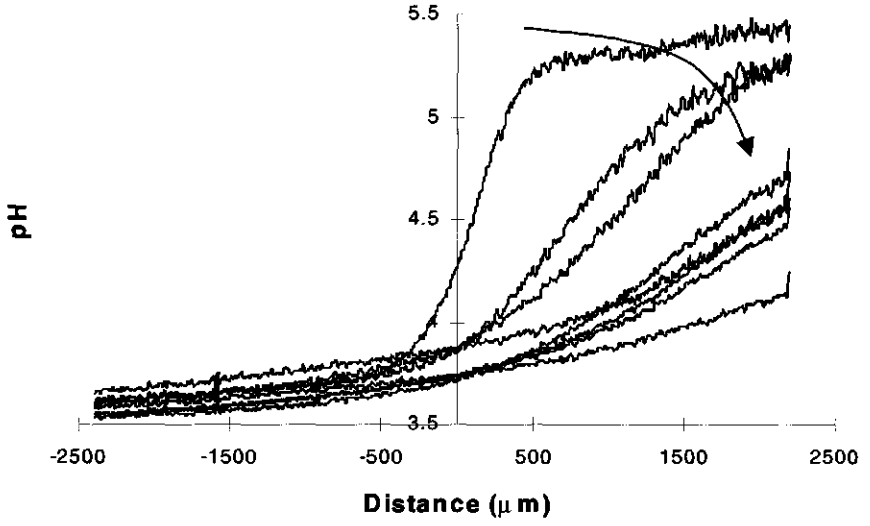

Fig. 4: Diffusion of lactic acid in gel cassette. The curves from top to bottom represent diffusion of lactic acid from 12, 27, 42, 57, 81, 96, 171 and 246 minutes.

the *pH* versus the distance and not the concentration of lactic acid versus the distance. The *pH* values can be translated to the equivalent concentration of lactic acid using a titration curve (results not shown). After 12 minutes, the front had already moved across the boundary and continued moving until at 250 minutes, where it had a flatter profile. This indicated that there was gradual acidification of the whole medium as lactic acid diffused from the left half of the window. The *pH* of the left side of Fig. 4 hardly changed since the pK_a of lactic acid is 3.86 and lactic acid strongly buffers around this *pH*.

The *pH* front image was taken with a 1x objective lens where every pixel is 6 microns by 6 microns. This gives very good resolution and since we will also be using a x5 objective lens (1 pixel = 1.32 microns), these lenses will be perfectly suitable for looking at what is happening inside an individual colony, which might range in diameter from 1 micron to 500 microns.

3.3. Growth experiments

3.3.1. Qualitative trends

Fig. 5a, 5b, 5c and 5d show the gel cassettes with different inoculation densities of *L. curvatus* (5 cfu.ml^{-1}, 10 cfu.ml^{-1}, 100 cfu.ml^{-1} and 1000 cfu.ml^{-1}). Each window with cells holds approximately 0.5 ml growth medium. Differences between the inoculation densities of 10 cfu.ml^{-1} and 5 cfu.ml^{-1} were small, and the 10 cfu.ml^{-1} cassette was excluded from further analysis

Fig. 6 shows the time course of colony diameter for the 3 inoculation densities. For the 5 cfu.ml^{-1} series, the data are from an individual colony revisited at each time point. For the 100 and 1000 cfu.ml^{-1} series, it was not possible to relocate the same individual colony, and the data presented are the mean diameters of an arbitrary selected 10 colonies. In Fig. 6, a number of features may be observed:

a) Firstly, the sizes of the colonies at the end of the experiment were different. In the gel cassette with 1000 cfu.ml^{-1}, growth appeared to stop after 71.5 hours, as the mean colony diameter remained constant. The mean diameter of the colonies was about 150 μm when growth entered the

stationary phase. The colonies in the gel cassette with 100 cfu.ml^{-1} were able to continue growing for longer and the colonies were still expanding after 186.5 hours. Here the average diameter after 239 hours was about 380 μm. In the gel cassette with only 5 cfu.ml^{-1}, the same trend was seen but the colonies were even larger. The diameter of the colony after 239 hours was about 430 μm.

b) There were two periods in time when growth in the different samples started to diverge. The first started at 40 hours and ended at 75 hours when the colony sizes were between 100 to 200 microns (taking lag into account

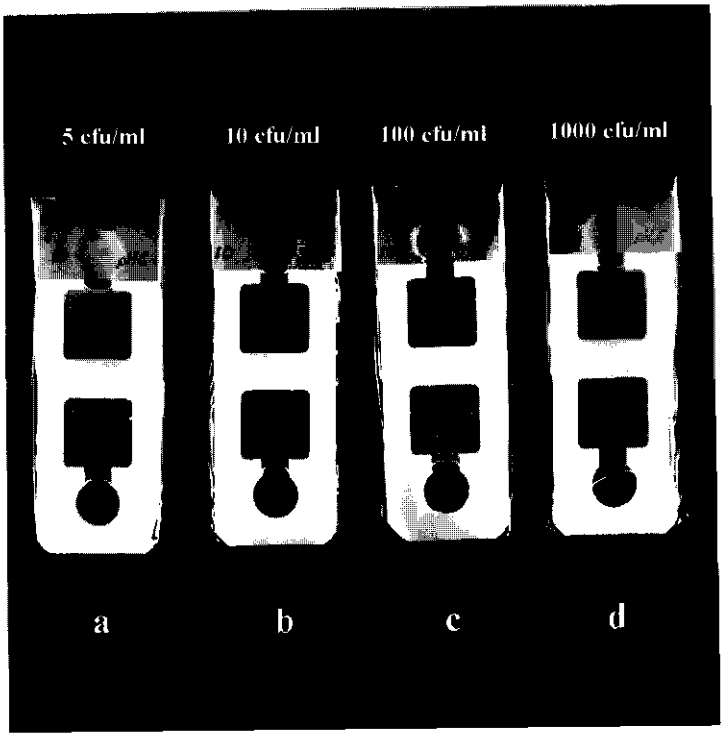

Fig. 5: Various inoculation densities of *L. curvatus* colonies introduced aseptically into a gel cassette. The upper window of the gel cassette was kept free of bacteria for measurement of background fluorescence of the growth medium. The colonies were approximately 5 days old.

for 5 cfu.ml^{-1} and 100 cfu.ml^{-1}). At 75 hours, there was a distinct difference in the size of the colony in the 1000 cfu.ml^{-1} sample when compared to the rest. The second period started at 75 hours and ended at 100 hours. This involved the colonies of the remaining two samples and at 100 hours, clearly three different colony sizes were present. This meant at those specific periods in time, some form of transition was occurring in the colonies

c) Lastly, there seemed to be a lag in the growth of the colonies in the gel cassettes with inoculation densities of 100 cfu.ml^{-1} and 5 cfu.ml^{-1} when compared to those in 1000 cfu.ml^{-1}. At 24 hours, no colonies could be detected in these gel cassettes, indicating that they were growing slower than those in the 1000 cfu.ml^{-1} gel cassette.

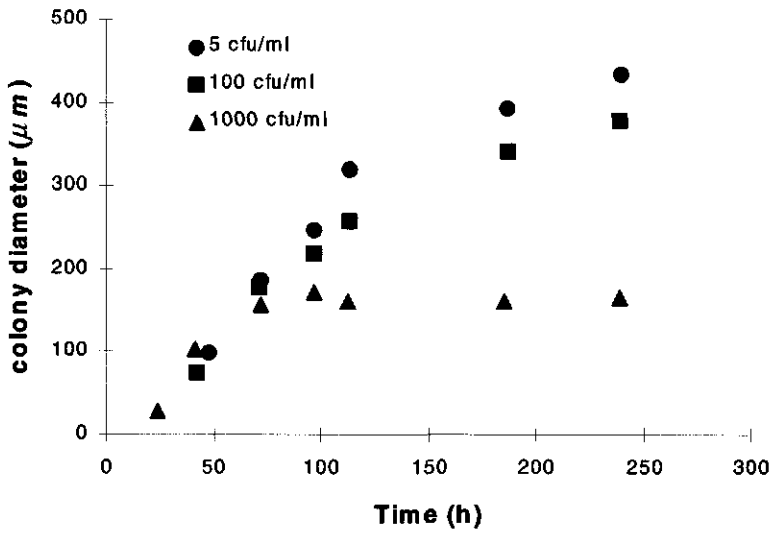

Fig. 6: Colony diameter of *L. curvatus* colonies at different initial inoculation densities at an initial *pH* of 5.5..

3.3.2. Interactions

The first and second trend can be explained by looking at the *pH* profile in and around the colonies. As was postulated in the introduction, there is a continuum of interactions possible when describing colony growth. Fig. 7 (1000 cfu.ml^{-1}) indicates an example of an inter colony type of interaction, Fig. 8 (100 cfu.ml^{-1}) an intermediate type and Fig. 9 (5 cfu.ml^{-1}) that of an intra colony type of interaction.

Fig. 7 shows line graphs of 2D maps of *pH* (*x* direction) in and around colonies of inoculation density of 1000 cfu.ml^{-1} for different time intervals. Here there were no significant changes of *pH* before 42 hours. However from this time onwards the colonies started to interact with each other, which can be seen by the divergence from the sizes of the colonies in the 100 cfu.ml^{-1} and 5 cfu.ml^{-1} samples (Fig. 6). Sizes are a measure of growth and this indicated that growth of the colonies was slowing down, mainly due to interaction between the colonies. Here the bulk medium was becoming saturated with lactic acid produced by these colonies. At 97 hours, saturation occurred and the *pH* had dropped to about 4.6 and

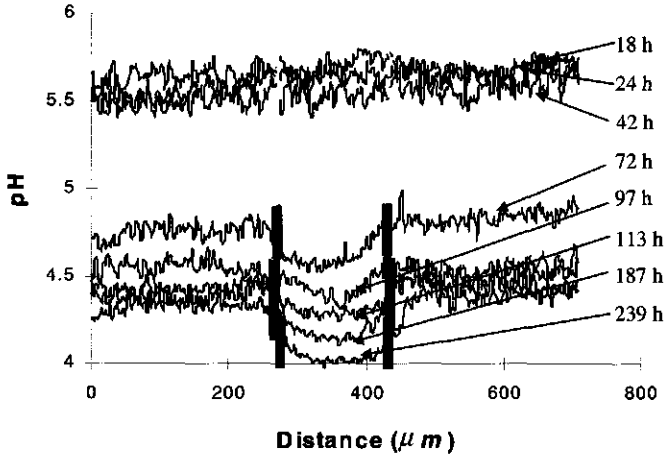

Fig. 7: *pH* profiles in and around colonies of *L. curvatus* at an inoculation density of 1000 cfu.ml^{-1}. Vertical bars indicate position of radius of colony.

growth had essentially stopped. The cells in the colonies must be in their stationary phase, as the colonies did not increase in size anymore. The further drop of *pH* indicated that the cells were still metabolically active.

In Fig. 8 (100 cfu.ml^{-1}) a combination of inter and intra colony type of interactions can be seen. There was no evidence of interactions between the individual colonies before 72 hours as the bulk *pH* was not significantly different from the start. However by this time, a gradient of about 0.5 *pH* units had formed inside a colony. This meant that there were already interactions between the cells in the colony although this decrease in *pH* will only slightly decrease the growth rate. After 72 hours the colonies began to interact with each other and the sizes of the colonies started to diverge from that in the sample with 5 cfu.ml^{-1} (Fig. 6). As a result of both inter and intra colony interaction, the *pH* outside and inside the colony dropped at regular intervals to a final level of 4.6 and 4.4 respectively.

Fig. 8 also shows that there were sharp declines in *pH* at the leading edge of the colony after 72 hours, which continued until 239 hours. The leading edge is a zone just before and after the colony radius. This is a consequence of the

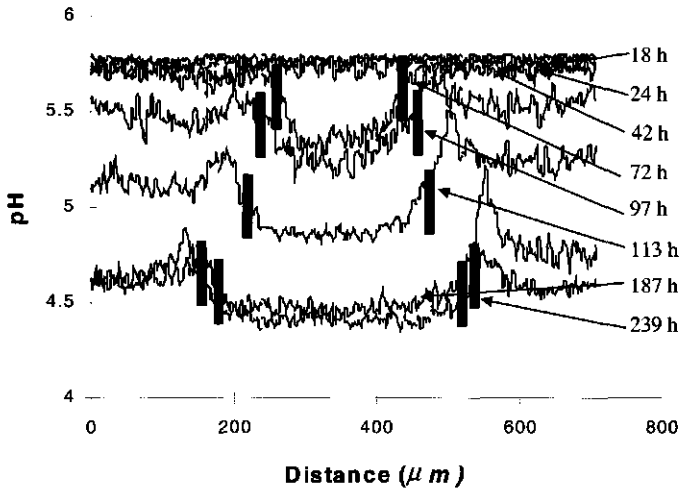

Fig. 8: *pH* profiles in and around colonies of *L. curvatus* at an inoculation density of 100 cfu.ml^{-1}. Vertical bars indicate position of radius of colony.

accumulation and production of lactic acid in the colony. As the colony increases in size, lactic acid that is produced takes longer to diffuse out and accumulates in the colony, resulting in a flat profile till the leading edge. At the leading edge however, there will be a boundary between a zone where there is production and one where there is no production of lactic acid. This sudden transition between production and no production of lactic acid produces the steep gradients in *pH* as shown in Fig. 8

This effect was even more evident in Fig. 9. Here there were only one or two colonies in the gel cassette. This effectively meant that the colonies do not interact at all with each other. A gradient of about 0.25 *pH* units was already formed after 48 hours (intra colony interaction) when the colony reached a size of about 100 μm.

The approximate volume of this colony should be in the order of 10^{-6} cm^3. From 72 hours onwards, there was a gradual flattening of the *pH* profile from the centre towards the leading edge with the steepest slope at the leading edge. This phenomenon was maintained until 239 hours. Since the colonies do not interact

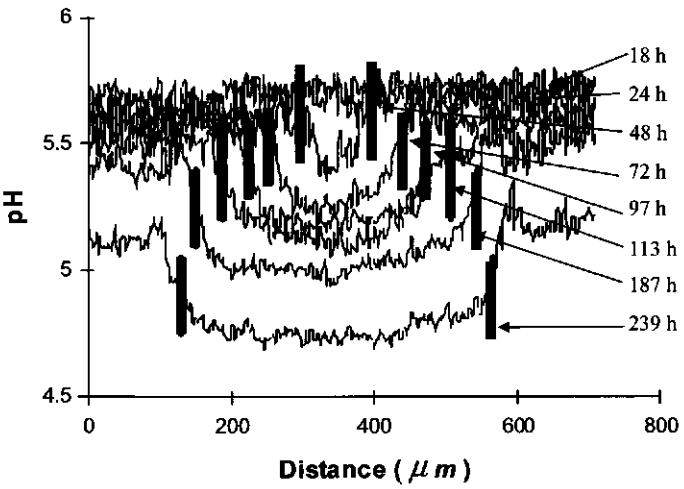

Fig. 9: *pH* profiles in and around colonies of *L. curvatus* at an inoculation density of 5 $cfu.ml^{-1}$. Vertical bars indicate position of radius of colony.

with each other, the decline of *pH* in the bulk medium was not as rapid as in Fig. 8. If the packing density of cells is in the region of 10^{11} cell.cm^{-3} (Pirt 1975, Grimson and Barker 1994), then intra colony interactions start to become important in colonies of about 10^5 cells where growth had proceeded from 1 cell to 10^5 cells.

This information can be of relevance when considering the use of growth models from broth cultures for predicting spoilage in solid systems. If a food system, as represented by a gel cassette is contaminated with about 100 cfu.ml^{-1} of bacteria, then deviation from these growth models would only occur at a level of 10^7 cfu.ml^{-1}. At these levels, foods are already spoiled and it would be reasonable to use the growth models up to the moment of spoilage. For lower initial numbers of microorganisms, this might not be the case. Intra colony interaction may decrease the growth rate and may trigger stress responses much earlier than predicted by broth models although it starts only after considerable outgrowth.

3.3.3. Lag

After 24 hours, colonies in the cassette with inoculum density of 1000 cfu.ml^{-1} reached sizes of 30 µm while none was observed in the gel cassettes with inoculation densities of 100 cfu.ml^{-1} and 5 cfu.ml^{-1}. This observation was strange because the *pH* in all the 3 samples was still at *pH* 5.5, the initial *pH*. If all the cells in the colonies of the 3 samples were growing exponentially at this *pH* and temperature, all these colonies should grow to about 30 µm at roughly the same time.

We performed an experiment to look for the causes of the lag. The 3 inoculum concentrations were grown in an anaerobic jar with a gaseous atmosphere containing 90 percent CO_2 and 10 percent H_2 Under these conditions, all the colonies grew to 30 µm at roughly the same time. One possible explanation for the observed lag and its absence in the 1000 cfu.ml^{-1} sample is that the colonies here produce enough CO_2 to saturate the gel, resulting in CO_2 enrichment. CO_2 enrichment is a recognised phenomenon encouraging the growth of lactic acid bacteria.

4. Conclusion

This study confirms that there is a continuum of growth phenomena when microorganisms are growing in solid medium. Growth of the colonies of *L. curvatus* approached that of a broth culture when the inoculation density was high. Inter colony interaction caused the saturation of the environment with lactic acid, which inhibited growth.

At lower inoculation densities, the colonies were able to grow bigger and inter colony interactions occurred much later. These bigger sizes resulted in the accumulation of lactic acid in the colony which produced zones of different growth rates. Deviations in solid systems from growth in homogenous systems are expected especially at low contamination levels (~ 10 cfu.ml^{-1}) and only after high outgrowths (factor 10^5).

The technique of fluorescence rationing is a useful non-invasive method for studying colony growth. It is simple to set up with the gel cassette system and measurements can be made in real time without disturbing the sample. Future work will concentrate on modelling the growth in the colonies coupled to the formation of the *pH* gradients.

5. Acknowledgements

The authors would like to thank the Netherlands Organisation for Scientific Research (NWO) for providing funds for this research at the Institute of Food Research, Norwich, United Kingdom. We would also like to thank UK Biotechnology and Biological Sciences Research Council (BBSRC) for providing funds for a further extension of this work at the Institute.

6. Reference

1. Archer,D.L. 1996. Preservation microbiology and safety: Evidence that stress enhances virulence and triggers adaptive mutations. Trends Food Sci. Technol. 7: 91-95.
2. Grimson,M.J., Barker,G.C. 1994. Continuum model for the spatiotemporal growth of bacterial colonies. Physical Review E. 49: 1680-1684.

3. McMeekin,T.A., Olley,J., Ross,T., Ratkowsky,D.A. 1993. Predictive microbiology: Theory and application. Research Studies Press Ltd. Somerset, United Kingdom.
4. Nielsen,J., Villadsen,J. 1992. Modelling of microbial kinetics. Chem. Engng. Sci. 47: 4225-4270.
5. Pirt,S.J., 1975. Principles of microbe and cell cultivation. Blackwell. London.
6. Walker,S.L., Brocklehurst,T.F., Wimpenny,J.W.T. 1997. The effects of growth dynamics upon *pH* gradient formation within and around subsurface colonies of *Salmonella typhimurum*. J. Appl. Microbiol. 82: 610-614.
7. Wentland,E.J., Stewart,P.S., Huang,C.T., McFeters,G.A. 1996. Spatial variations in growth rate within *Klebsiella pneumoniae* colonies and biofilms. Biotechnol. Prog. 12: 316-321.
8. Wijtzes,T., de Wit,J.C., Huis in 't Veld,J.H.J., van 't Riet,K., Zwietering,M.H. 1995. Modelling bacterial growth of *Lactobacillus curvatus* as a function of acidity and temperature. Appl. Environ. Microbiol. 61: 2533-2539.
9. Wimpenny,J.W.T., Coombs,J.P., 1983. Penetration of oxygen into bacterial colonies. J. Gen. Microbiol. 129: 1239-1242.
10. Zwietering,M.H., Jongenburger,I., Rombouts,F.M., van 't Riet,K. (1990). Modeling of the bacterial growth curve. Appl. Environ. Microbiol. 56: 1875-1881

Diffusion of lactic acid in a buffered gel system supporting growth of *Lactobacillus curvartus*

Abstract

The spatiotemporal behaviour of lactic acid in solid systems is of relevance for understanding of colony growth of lactic acid bacteria. Diffusion of lactic acid in a buffered gel system was investigated using fluorescent ratio imaging. The range of *pH* studied was from *pH* 5.5 to *pH* 3.8, which included the minimum *pH* of growth of *Lactobacillus curvatus* (*pH* 4.26). Diffusion of lactic acid in this *pH* range was found to be Fickian and the estimated effective diffusion coefficient of lactic acid at 20 °C was $2.81 \cdot 10^{-10}$ ($m^2.s^{-1}$) with a standard deviation of $0.21 \cdot 10^{-10}$ ($m^2.s^{-1}$)

This effective diffusion coefficient was estimated by fitting the one dimensional solution of the Fickian diffusion equation for infinite systems to a transformed experimental data set. The original data set as recorded by the fluorescent microscope consisted of concentration-distance curves at specific time intervals. This was transformed by realigning the distance scale of all the concentration-distance curves.

1. Introduction

Growth of bacteria in solid matrices is of importance in many food systems. Here bacteria grow as colonies and diffusion is the main mechanism of transfering nutrients into these colonies as well as getting rid of waste products of growth. Wimpenny et al. (1995) have shown that the size of a colony increases exponentially initially and then linearly, which they attributed to the effect of transport limitations. In the past two decades a lot of effort had been put into the development of empirical models of microbial growth as a tool for ensuring the safety and quality of foods. However these models do not take transport processes

due to diffusion into account as most of the data were collected from broth experiments.

We are currently interested in the colony growth of *L. curvatus*, a lactic acid bacterium, chosen as our model system for investigating growth in submerged solid systems. The diffusion of lactic acid (P) out of these bacterial colonies will be of importance to their growth and development. Accumulation of lactic acid and the concurrent decrease of pH in these colonies will slow down growth. Hence an important parameter in quantifying the growth will be the effective diffusion coefficient (D_p) of lactic acid. Here D_p is the diffusion of the total amount of the acid species present. It includes the contribution of the hydrogen ion, dissociated and associated species, which are at equilibrium. The time scale of this reaction (dissociation) is very small compared to growth and acid production, thus allowing the use of pH in growth modelling. This parameter will be estimated using a fluorescent imaging technique (Malakar et al. 2000) developed at the Institute of Food Research, Norwich, United Kingdom.

2. Theory

Fig. 1 shows the dimension of a window in the gel cassette system (Brocklehurst et al. 1995) in which the diffusion experiments were performed. Lactic acid initially confined in one half of the window is allowed to diffuse across to the other half. Here we consider only a one dimensional diffusion in the x-direction. We further assume that conditions at the impermeable boundaries at both ends of the window in the gel cassette do not change during the time of the experiment. This set of conditions would then describe diffusion in an infinite medium.

The minimum pH of growth of *L. curvatus* ($pH_{\min}$) is 4.26 (Wijtzes et al. 1995). The amount of lactic acid needed to acidify the growth medium of *L. curvatus*, at an initial pH of 6 to $pH_{\min}$ can be estimated from the titration curve of pH versus the concentration of lactic acid in a broth medium supporting growth of *L. curvatus* (Martens et al. 1999). This concentration of lactic acid is ~ 0.1M and it is likely that D_p will not depend on the concentration of lactic acid in the pH ranges that we

consider. Therefore we approximate the dynamics by assuming Fickian diffusion, which is given by equation 1,

$$\frac{\partial P}{\partial t} = D_p \frac{\partial^2 P}{\partial x^2} \qquad 1 \qquad (\text{mol.m}^{-3}.\text{s}^{-1})$$

where D_p is the effective diffusion coefficient.

2.1.Fickian diffusion

A standard method of solving equation 1 is using the Boltzmann transformation. Applying the appropriate initial and boundary conditions (Appendix 1), equation 1 can be solved to give the following form for the spatio temporal evolution of lactic acid,

$$\frac{P(x,t)}{P_0} = 0.5\left[1 - erf\left(\frac{x}{2\sqrt{D_p\, t}}\right)\right] \qquad 2 \qquad (-)$$

where $P(x,t)$ is the concentration of lactic acid at time t and distance x from the interface through which diffusion takes place, P_0 is the initial concentration of

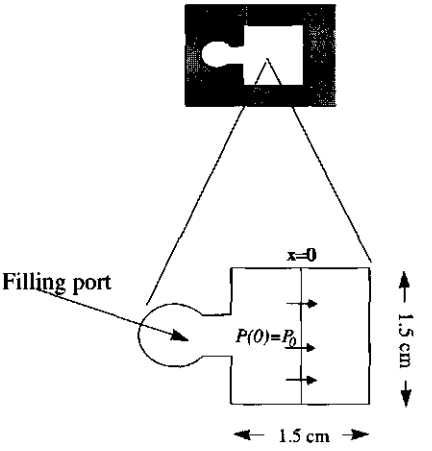

Fig. 1: Gel cassette window for the experimental determination of D_p, the effective diffusion coefficient of lactic acid.

lactic acid in one side of the interface and no lactic acid is initially present in the other side.

Fig. 2 shows the solution of equation 2 for a range of times using a diffusion coefficient of 10^{-10} $m^2.s^{-1}$. This diffusion coefficient is within the range of diffusion coefficients in liquid (Cussler 1997). The interface through which the diffusion takes place is located at the origin (x=0) and the normalized concentration of lactic acid ($P(x,t)/P_0$) at this point is 0.5. It is clear from Fig. 2 that concentrations at both boundaries of the gel cassette, which is located at ~7.5 mm from the interface will not have changed much during the time scale of the experiment (~ 2 hours).

In Fig. 2, only concentrations between ± 2.5 mm from the interface change rapidly. Therefore the assumption of an infinite medium is justified at this time scale of ~ 2 hours. These concentration-profiles can be compared with the experimental data to check the validity of the model i.e. diffusion of lactic acid in the buffered gel system, which supports the growth of *L. curvatus*, is Fickian and the effective diffusion coefficient is independent of the concentration of lactic acid.

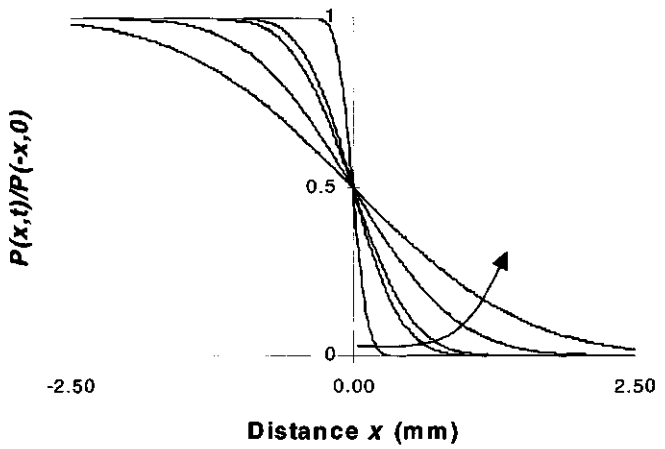

Fig. 2: Simulation of equation 2 with a D_p of 10^{-10} $m^2.s^{-1}$ at 1, 10, 15, 45 and 120 min. Curved arrow indicates increasing time.

3. Materials and methods

The experiments were performed in a gel cassette system (Fig. 1) developed at the Institute of Food Research, Norwich, UK. The preparation of the gel cassette, the calibration of the fluorescent microscope and the image analysis of fluorescence images have been described in detail by Malakar et al. (2000). The fluorescent dye used in this experiment was Oregon Green™ (Molecular Probes, Leiden, Netherlands), which has a linear range of fluorescent intensity versus *pH* between *pH* 3 and *pH* 6.

To prepare the buffered gelled medium, equal volumes of MRS (Sigma, 104 $g.L^{-1}$), and molten bovine gelatine (Sigma, 200 $g.L^{-1}$) were mixed together. MRS is a specially constituted growth media for *Lactobacillus* sp. A *pH* meter (Radiometer, Copenhagen) and 5 M HCl were used to adjust the *pH* of this mixture to an initial *pH* of 5.5. Oregon Green™ was then added to the mixture to a final concentration of about 1.25 $mg.L^{-1}$. The medium was then halved to give two portions, A and B.

Portion A was further acidified with 5 M lactic acid to lower the *pH* to 3.8. The volume of acid added to the mixture was about 0.03 % of the total, hence making very little change to the concentration of the growth media. This mixture containing lactic acid at *pH* 3.8 was then placed into one half of the gel cassette window with the help of a syringe and allowed to solidify at 20 °C. The *pH* range of diffusion of lactic acid studied was thus from *pH* 5.5 to 3.8.

At the start of the diffusion experiment, the other half of the gel cassette window was filled with portion B, which contained no lactic acid. Since this portion was still molten (25 °C), it was quite difficult to locate the exact position of the interface between the two halves at the beginning. Fluorescence images were only taken at the earliest time possible and at 15 minutes interval thereafter, and continued for 2 hours.

3.1. Titration

A titration experiment using lactic acid was performed on the medium without the fluorescence dye at an initial *pH* of 5.5. This was for the conversion of

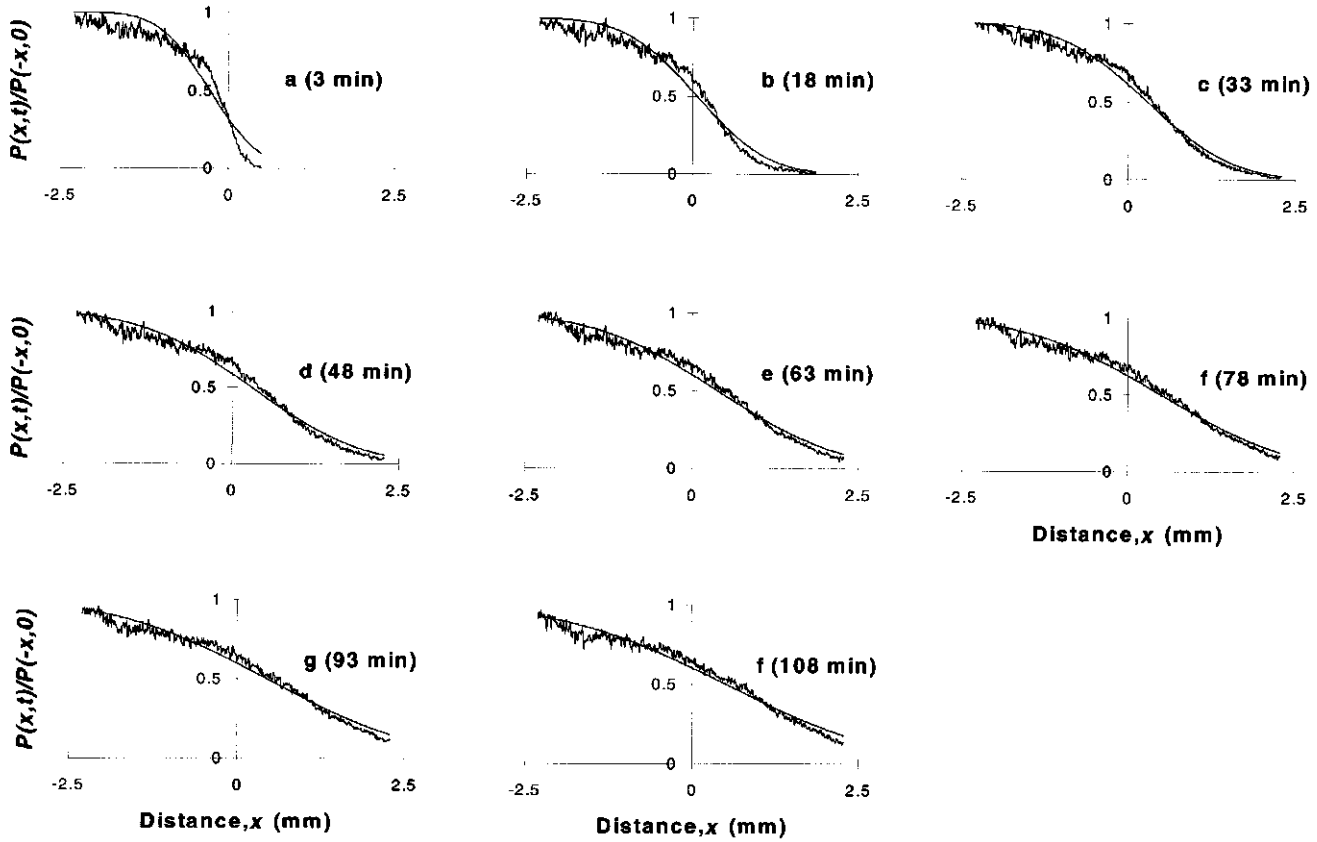

Fig. 4: Data and fitted (smooth line) curves of the individual diffusion front of lactic acid using equation 4.

decrease to *pH* 3.6 and onwards (pK_a of lactic acid, 3.86). Equation 3 was used to fit the titration data in Fig. 3a and the value of parameters a_1 and a_2 are 0.032 ± 0.0094 m^3 $mol^{-1}$and 0.011 ± 0.0024 m^3 mol^{-1} (95% confidence intervals). Buffering in the medium is probably caused by the protein components in the MRS. Increasing the amounts of MRS in the media caused the parameters a_1 and a_2 to change (results not shown), where more lactic acid was needed to obtain the same decrease in *pH*.

The titration curve was used to convert the *pH* fronts (Fig. 3b, *cf.* Fig. 4, chapter 4, page 69) recorded by the fluorescence microscope to the diffusion fronts of lactic acid (Fig. 3c). These fronts are in the form of concentration-distance curves. Note that the concentrations of lactic acid for the various times in Fig. 3c have been normalized. This was done by dividing the concentrations of lactic acid at all times with the initial concentration of lactic acid found in the left half of the gel cassette in Fig. 1.

The concentration-distance curves in Fig. 3c (at 3, 18, 33, 48, 63, 78, 93, 108 min) look symmetrical, and approach the asymptote at 1 and 0. Note also that the boundary of the concentration distance curves are situated at 7.5 mm from the origin. The assumption of no change of the initial concentration of lactic acid at the boundary is valid since the asymptotes are nearly reached at 2.5 mm from the origin for all the concentration-distance curves. The shapes of the concentration-distance curve in Fig. 3c are quite similar to those in Fig. 2, which was derived from the solution of the Fickian diffusion equation. However, the concentration and distance curves in Fig. 2 and 3 differ in the location of point of intersection. In Fig. 2 all the curves intersect at point 0.5 on the *y* axis, while in Fig. 3c there is no single point of intersection.

Even though these concentration profiles do not intersect at 0.5, it does not however rule out Fickian diffusion. We know we are dealing with a dilute system at the *pH* range considered and the gelatine concentration is only at 10%, not enough to cause deviations in diffusion phenomena. One possibility is that initially there may be a faster movement of the front due to the molten gelatine mixture on the right hand side of the gel cassette, making it difficult to locate the exact interface. Another possibility is slight movements of the stage of the microscope,

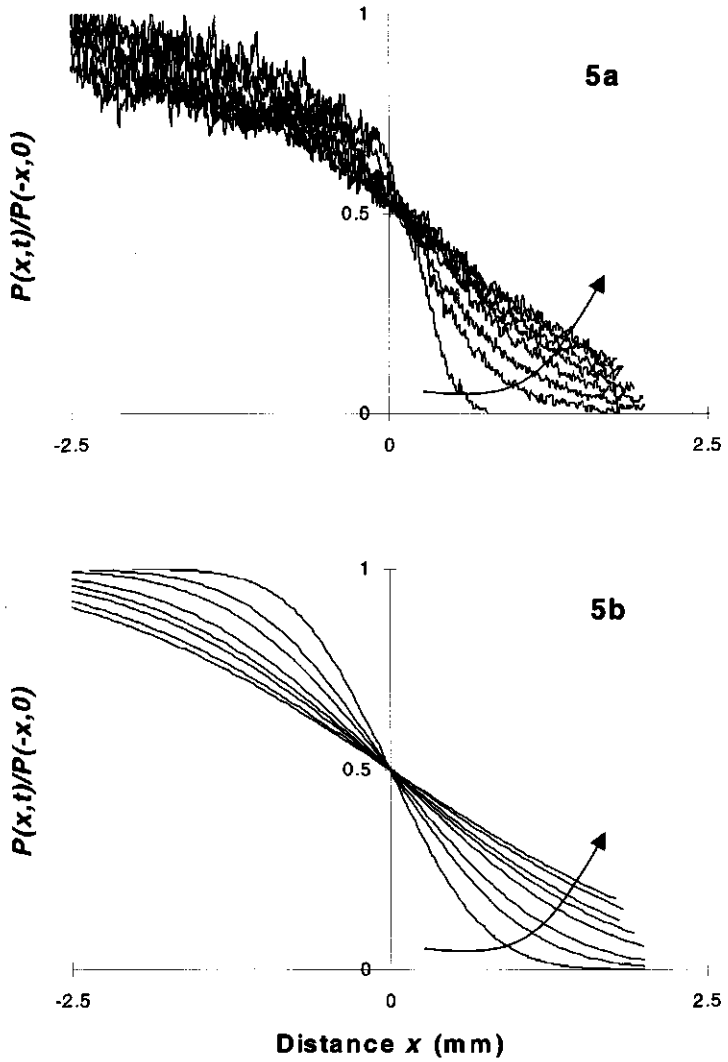

Fig. 5: Realigned diffusion fronts of lactic acid. Fig. 5a shows the transformed data and Fig. 5b shows the corresponding fitted curves. Curved arrow shows increasing time (3, 18, 33, 48, 63, 78, 93 and 108 min).

so that the frame of reference is changing all the time. Therefore a shift in the x axis (realignment) of the concentration-distance curves could be sufficient to transform the concentration-distance curves in Fig. 3c to resemble those in Fig. 2.

Table 1: Effective diffusion coefficient of lactic acid D_p realized by fitting equation 4 to the concentration and distance curves in Fig 4.

Time, t (min)	Fig. no.	D_p (10^{-10}m^2.s^{-1}) and 95 % conf. limit	h (mm) and 95 % conf. limit
3	4a	9.65 (8.72, 10.6)	-0.27 (-0.29, -0.25)
18	4b	3.25 (3.09, 3.41)	0.06 (0.05, 0.08)
33	4c	2.56 (2.47, 2.64)	0.28 (0.27, 0.29)
48	4d	2.83 (2.73, 2.92)	0.30 (0.28, 0.31)
63	4e	2.75 (2.66, 2.84)	0.37 (0.36, 0.39)
78	4f	2.60 (2.53, 2.68)	0.49 (0.47, 0.50)
93	4g	2.85 (2.76, 2.93)	0.45 (0.43, 0.47)
108	4h	2.83 (2.75, 2.92)	0.51 (0.49, 0.53)

Mean value $D_p = 3.67 \cdot 10^{-10}$ (std, $2.27 \cdot 10^{-10}$) m^2.s^{-1}.

Mean value without outlier, $D_p = 2.81 \cdot 10^{-10}$ (std, $0.21 \cdot 10^{-10}$) m^2.s^{-1}.

A shift in the axis is a plausible explanation for the dynamics of this dilute system. This transformation can be performed using equation 4. It is the same family of curves as equation 2 but has an added parameter h to account for the shift in the x axis.

4.1. Transformation

Fig. 4 shows the fit of the individual concentration-distance curves of Fig. 3c using equation 4. Except for the concentration-distance curve at 3 minutes this function fitted the data rather well. The concentration-distance curves in Fig. 3c were then realigned with the help of parameter h from the fit. This was done by adding or subtracting the value of h from the original data (x values) and plotting all the concentration-distance curves again.

This transformation resulted in the concentration-distance curves shown in Fig. 5a and 5b, where Fig. 5a shows the realigned raw data and Fig. 5b the fitted curves.

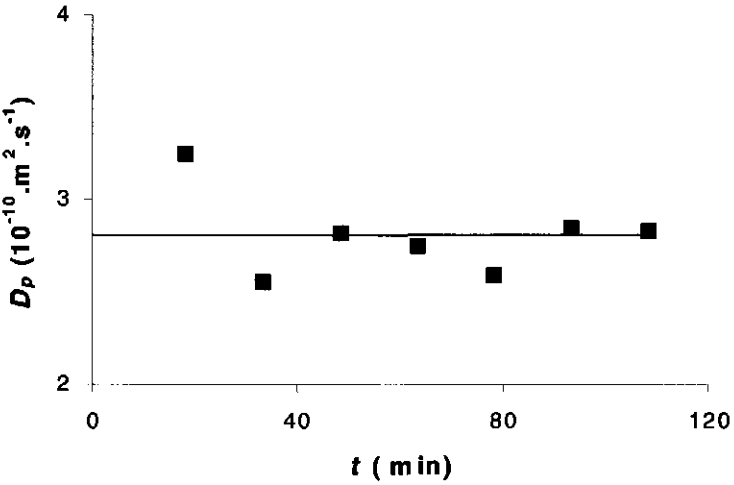

Fig. 6: Effective diffusion coefficient D_p estimated from the concentration distance curves from 18 to 108 minutes. The line indicates the mean.

All the curves have been shifted either to the left or right. These curves now resemble those in Fig. 2.

The values of the effective diffusion coefficient of lactic acid D_p from the fit are given in Table 1 and they ranged in value from 2.6 to $9.7 \cdot 10^{-10}$ ($m^2.s^{-1}$). The deviation at 3 minutes is a result of a transient. If we discount this value and take the arithmetic mean of the rest of the values (Fig. 6), we end up with a D_p of $2.81 \cdot 10^{-10}$ ($m^2.s^{-1}$) with standard deviation of $0.21 \cdot 10^{-10}$ ($m^2.s^{-1}$) at 20 °C. The diffusion coefficient of the fully ionised lactic acid at infinite dilution in water at 25 °C (Cussler 1997) is $1.74 \cdot 10^{-10}$ ($m^2.s^{-1}$) and therefore the order of magnitude of the estimated value of D_p is very reasonable.

The shift parameter h appears to increase with time. However this increase tends to a plateau at around 0.5 mm from the origin. This anomaly indicates that the experimental protocol should be improved, e.g. using a better method to locate the interface.

5. Conclusion

The estimated value of D_p and its standard deviation at 20 °C in the buffered gelled growth medium were $2.81 \cdot 10^{-10}$ ($m^2.s^{-1}$) and $0.21 \cdot 10^{-10}$ ($m^2.s^{-1}$). We assumed Fickian diffusion and the solution of the Fickian diffusion equation fitted the transformed data set well. This transformation involved realigning the distance scale of all the concentration-distance curves, which were recorded at a specific time interval.

6. Appendix 1

Using the Boltzmann transformation

$$\frac{\partial P}{\partial t} = D_p \frac{\partial^2 P}{\partial x^2} \qquad 5$$

can be transformed to an ordinary differential equation using

$$\eta = \frac{1}{2} \frac{x}{\sqrt{D_p t}} \qquad 6$$

and the differential of η with respect to x,

$$\frac{\partial P}{\partial x} = \frac{1}{2\sqrt{D_p t}} \frac{\partial P}{\partial \eta} \qquad 7$$

and the differential of η with respect to t,

$$\frac{\partial P}{\partial t} = -\frac{x}{4t\sqrt{D_p t}} \frac{\partial P}{\partial \eta} \qquad 8$$

and the second differential of equation 7,

$$D_p \frac{\partial}{\partial x}\left(\frac{\partial P}{\partial x}\right) = D_p \frac{\partial}{\partial x}\left(\frac{1}{2\sqrt{D_p t}} \frac{\partial P}{\partial \eta}\right) = \frac{1}{4t} \frac{\partial}{\partial \eta}\left(\frac{\partial P}{\partial \eta}\right) \qquad 9$$

and substituting equation 9 and 8 into equation 5 gives the required ordinary differential equation.

$$\frac{dP}{d\eta} = -\frac{1}{2\eta} \frac{d^2 P}{d\eta^2} \qquad 10$$

Using the initial conditions

$x<0,$	$t=0$	$P=P_0,$	results in	$\eta=-\infty$	$P=P_0$
$x>0,$	$t=0$	$P=0,$	results in	$\eta=+\infty$	$P=0$

and boundary conditions,

$x=-\infty$	$P=P_0,$	results in	$\eta=-\infty,$	$P=P_0$
$x=+\infty$	$P=0,$	results in	$\eta=+\infty,$	$P=0$

the ordinary differential equation in P and η (eq. 10) can be solved to give

$$P=\frac{1}{2}P_0[1-erf(\eta)] \qquad 11$$

and substituting for η results in

$$\frac{P(x,t)}{P_0}=0.5\left[1-erf\left(\frac{x}{2\sqrt{D_p t}}\right)\right] \qquad 12$$

7. Reference

1. Brocklehurst,T.F., Mackie,A.R., Steer,D.C., Wilson,P.D.R. 1995. Detection of microbial growth. U.K. Patent application. International Publication Number: WO 95/00661.
2. Crank,J. 1975. The mathematics of diffusion. Oxford university press.
3. Cussler,E.L. 1997. Diffusion mass transfer in fluid systems. Cambridge University Press.
4. Malakar,P.K., Brocklehurst,T.F., Mackie,A.R., Wilson,P.D.G., Zwietering,M.H., van 't Riet,K. 2000. Microgradients in bacterial colonies: use of fluorescence ratio imaging, a non-invasive technique. Int. J. Food Microbiol. 56: 71-80.
5. Martens,D.E., Beal,C., Malakar,P.K., Zwietering,M.H., van 't Riet,K. 1999. Modelling the interactions between *Lactobacillus curvatus* and *Enterobacter cloacae*. I. Individual growth kinetics. Int. J. Food Microbiol. 51: 53-65.
6. Wijtzes,T., de Wit,J.C., Huis in 't Veld, J.H.J., van 't Riet,K., Zwietering,M.H. 1995. Modelling bacterial growth of *Lactobacillus curvatus* as a function of acidity and temperature. Appl. Environ. Microbiol. 61:2533-2539.

7. Wimpenny,J.W.T., Leistner,L., Thomas,L.V., Mitchell,A.J., Katsaras,B., Peetz,P. 1995. Submerged bacterial colonies within food and model systems: their growth, distribution and interactions. Int. J. Food Microbiol. 28: 299-315.

Modelling the interactions of *Lactobacillus curvatus* colonies in solid medium: consequences for food quality and safety

Abstract

The growth process of *Lactobacillus curvatus* colonies was quantified by a coupled growth and diffusion equation incorporating a volumetric production rate of lactic acid. Analytical solutions were compared to numerical ones and both were able to predict the onset of interaction well. Interaction was assumed to occur when the volume averaged specific growth rate of the cells in a colony was 90 % of its initial maximum rate.

Growth of *L. curvatus* in solid medium is dependent on the number of cells in a colony. In colonies with populations of less than 10^5 cells, mass transfer limitation is not significant to the growth process. When the initial contamination level in the model solid system is relatively high, colonies are not able to grow to these sizes and growth can be described by broth cultures (no mass transfer limitation). Therefore in foods where the initial contamination level is high, it will be appropriate to use predictive models of broth cultures for estimating growth. However at very low initial contamination levels, large colonies can develop over time, where the growth characteristics deviate from growth in broth cultures. Nevertheless this deviation only occurs after a large outgrowth.

1. Introduction

The mathematical description of growth responses of microorganisms has a long history. In the recent two decades however a new family of these models has been developed for predicting food quality and safety. These are usually multidimensional empirical models for predicting growth of microorganisms. The independent variables are the environmental conditions of the food where these

microorganisms grow. As demands for minimally processed foods increase, these models will play an increasingly important role in ensuring the quality and safety of these foods.

These models are derived from experiments in liquid cultures where the environmental conditions are homogenous. However, there are many types of foods where this is not the case. One example is growth of microorganisms in sausages. Katsaras and Leistner (1991) showed that microorganisms grow in colonies or nests in these foods and micro gradients can occur in and around these colonies. The micro gradients are amongst others caused by diffusive transport of substrate into the colonies and metabolic products out of the colonies. Walker et al. (1997) managed to measure *pH* gradients in colonies of *Salmonella typhimurum* in their model solid system using microelectrodes, while Malakar et al. (2000) were able to detect *pH* gradients in colonies of *L. curvatus* using a fluorescence ratio imaging technique. In time, these micro gradients should produce variable specific growth rates in a colony.

These mass transfer effects can be important for predicting spoilage and safety. Outbreaks of *Escherichia coli* in hamburgers, an example of a solid matrix, point to the importance of understanding submerged colony growth. The strategy of controlling the growth of this pathogen in this heterogeneous system might be different from that of the free living species. The aim of this paper is to quantify these mass transfer effects in a model system. This model system consists of a homolactic bacterium, *L. curvatus,* growing in a nutrient medium, which has been solidified with agar.

2. Theory

In our model system, the solid matrix restricts the movement of individual cells or groups of cells of *L. curvatus* (non motile) and forces these cells to grow as individual colonies. The colony grows by addition of cells and we assumed a maximum closed packing density of 10^{17} cells.m^{-3} (Pirt 1975, Grimson and Barker 1994). This is a reasonable assumption, as these non-motile cells will use all available space to grow in this matrix. Furthermore, there will be diffusion of

substrate and metabolic end products in and out of the colony. The substrate used is glucose (S, mol.m^{-3}) and the main metabolic end product is lactic acid (P, mol.m^{-3}). The lactic acid produced lowers the pH.

2.1. Growth kinetics

The growth of an individual spherical colony after a lag period of λ, can be represented by the differential equation

$$\frac{d(nV)}{dt} = \mu_m \cdot (nV) \qquad (t>\lambda) \qquad 1 \qquad (\text{cell.s}^{-1})$$

where

$$\mu_m = f(P,S,pH)_{T,\ldots} \qquad 2 \qquad (\text{s}^{-1})$$

and n (cell.m^{-3}) is the packing density of cells, V (m^3) the volume of the colony and μ_m (s^{-1}) the local specific growth rate.

The specific growth rate of *L. curvatus* in broth culture μ_m, a function of the substrate (S), pH and lactic acid concentration (P) is described by equation 3 (Martens et al. 1999),

$$\mu_m = \mu_{opt}\left(\frac{S}{K_S + S}\right)\left(\frac{4(pH - pH_{\min})(pH_{\max} - pH)}{(pH_{\max} - pH_{\min})^2}\right) - (b_2 P) \qquad 3 \quad (\text{s}^{-1})$$

where μ_{opt} (s^{-1}) is the growth rate when conditions are optimal. This occurs when S is much greater than K_S (mol.m^{-3}), P is zero and the pH is equal to the mid point value of $pH_{\max}$ and $pH_{\min}$. The parameter K_S is the Monod constant, $pH_{\min}$ is the minimum pH and $pH_{\max}$ the maximum pH at which no growth is observed. Finally, b_2 (m^3.mol^{-1}.s^{-1}) is a regression parameter for the description of the direct effect of P on the specific growth rate of *L. curvatus*. The regression parameter b_2 was found to be independent of the initial pH of the broth culture. The numerical values of these parameters are given in Table 1

Apart from the direct effect, P also indirectly influences the specific growth rate by decreasing the pH. The pH can be empirically correlated to the amount of P present, with the help of the titration equation (Martens et al. 1999)

Table 1: Parameter values for equations 3, 5, 6 and 7 for *L. curvatus*

Eqn.	Parameter	Source	Value and units
1	n	g	10^{17} (cell.m^{-3}) or 10^{11} (cell.ml^{-1})
3	μ_{opt}	w	$2.94 \cdot 10^{-4}$ (s^{-1}) or 1.06 (h^{-1})
3	K_S	v	$4 \cdot 10^{-4}$ (mol.m^{-3})
3	b_2	m	$3.89 \cdot 10^{-7}$ (m^3.mol^{-1}.s^{-1}) or $1.40 \cdot 10^{-3}$ (m^3.mol^{-1}.h^{-1})
3	pH_{min}	w	4.26
3	pH_{max}	w	9.77
6	Y_{XP}	m	$3.3 \cdot 10^{13}$ (cell.mol^{-1})
6	m_p	r	$1.3 \cdot 10^{-19}$ (mol.cell^{-1}.s^{-1})
5,7	D_P	k	$2.81 \cdot 10^{-10}$ (m^2.s^{-1})

g : parameter value from Grimson and Barker (1994)

m : parameters values from Martens et al. (1999)

r : values estimated from maintenance requirements for ATP of *L. casei*, Roels (1983)

v : general value for glucose consumption of *E. coli*, van 't Riet and Tramper (1991)

w : parameters and predicted optimal growth rate at 30 °C, Wijtzes et al. (1995)

k : experimental data (Chapter 5)

Table 2: Regression parameters of titration curves (in MRS broth), at an initial *pH* 7 and 6 (Malakar et al. 1999).

Parameter	pH_0	Value	units
a_1	7	0.038	m^3.mol^{-1}
a_2	7	0.015	m^3.mol^{-1}
a_1	6	0.029	m^3.mol^{-1}
a_2	6	0.011	m^3.mol^{-1}

$$pH = \frac{pH_0 + a_1[P]}{1 + a_2[P]} \qquad 4$$

where the parameter pH_0 is the initial pH of the culture medium, a_1 ($m^3.mol^{-1}$) and a_2 ($m^3.mol^{-1}$) are regression parameters. These parameters are given in Table 2.

Equation 3 can be simplified by assuming the pH and the lactic acid produced (P) as the most important factors affecting growth. The low K_S value (Table 1) and abundant substrate available causes the term in equation 3 containing S to be unity. Since the pH is linked to the concentration of lactic acid (equation 4), modelling the concentration of lactic acid in the colony should be sufficient to describe the growth of the colony.

2.2. Diffusion

In our model system, these growth equations (equations 1-3) should also be applicable. However, we will have to account for diffusive transport in the growth process. Using Fick's second law for spherical shapes, accumulation of lactic acid inside a colony can be represented by

$$\frac{\partial P_i}{\partial t} = D_P\left(\frac{\partial^2 P_i}{\partial r^2} + \frac{2}{r}\frac{\partial P_i}{\partial r}\right) + q(r,t) \qquad r \le R_{col} \qquad 5 \qquad (mol.m^{-3}.s^{-1})$$

where the first expression on the right hand side is the diffusion term for spherical shapes and the second term represents the volumetric production rate q ($mol.m^{-3}.s^{-1}$) of the cells in the colony. The subscript i refers to inside the colony, D_p ($m^2.s^{-1}$) is the effective diffusion coefficient of lactic acid and R_{col} is the colony radius. The volumetric production rate can be adequately represented by

$$q = \left(\frac{\mu_m}{Y_{XP}} + m_p\right) n \qquad 6 \qquad (mol.m^{-3}.s^{-1})$$

which is the model of Luedeking and Piret (1959). It consists of a growth and non growth related term. The yield value Y_{XP} ($cell.mol^{-1}$) is the maximum amount of biomass produced given an amount of lactic acid produced concurrently and the non-growth term is represented by the maintenance coefficient m_P ($mol.cell^{-1}.s^{-1}$). Outside the colony, there is no production of lactic acid. Using Fick's second law for spherical shapes again results in

$$\frac{\partial P_o}{\partial t} = D_P\left(\frac{\partial^2 P_o}{\partial r^2} + \frac{2}{r}\frac{\partial P_o}{\partial r}\right) \qquad r > R_{col} \qquad 7 \qquad (\text{mol.m}^{-3}.\text{s}^{-1})$$

where we assume the effective diffusion coefficient of lactic acid (D_p) remains the same. The subscript *o* refers to outside the colony.

In their paper on submerged bacterial colonies, Wimpenny et al. (1995) show that a colony expands exponentially until a certain size is reached. Growth then proceeds linearly and comes to a stop. They postulated that this might be due to by-product inhibition. The coupled growth and diffusion equations above should be able to represent this. Qualitatively, when the colony expands to a certain size, lactic acid will start to accumulate in the centre, as diffusion cannot get rid of the lactic acid fast enough. Accumulation of lactic acid and the concurrent decrease in *pH* will result in a distribution of growth rates in the colony. Overall growth slows down and effectively stops when the *pH* in the whole colony and its surroundings is below the minimum *pH* of growth.

2.2.1. Boundary conditions

Equations 1, 5 and 7 with the help of equations 3, 4 and 6 can be solved using the appropriate initial and boundary conditions. We know foods harbour more than one colony. Lactic acid diffusing away from a colony might affect a neighbouring colony. So an appropriate boundary is at R_{bnd} , which is half of the distance between the centres of two neighbouring colonies as shown in Fig. 1 (Thomas et al. 1997).

Fig. 1 depicts an idealised geometry of colony distribution. Each of the colonies has a radius R_{col} and we assume that these colonies are homogeneously distributed in the sample. The boundaries of the living spaces are fixed at R_{bnd} by the initial inoculation density. This distance R_{bnd} can be calculated by assuming that the gel matrix is made up of identical cubes. Each cube contains a spherical colony in the centre. A higher inoculation density means that there will be more cubes present of smaller sizes and vice versa. The distance R_{bnd} is then one half of the cube root of the volume of each cube,

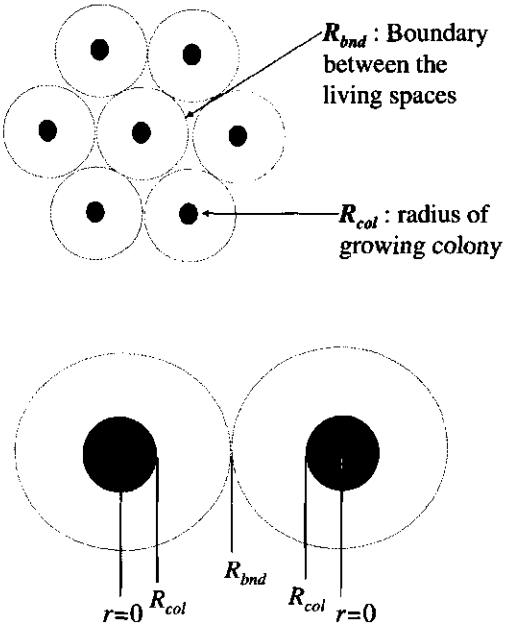

Fig. 1: A geometrical translation of the colony growth model. Each colony is sequestered in its own space, which is divided into two regions. The first is a zone of colony growth bounded by R_{col} (colony radius), which expands as new cells are added. The second is a zone of living space bounded by R_{bnd}, which is dependent on the initial inoculation density.

$$R_{bnd} = \frac{1}{2}\sqrt[3]{\frac{10^{-6}}{X_0}} \qquad 8 \qquad \text{(m)}$$

where X_0 (cfu.ml^{-1}) is the initial inoculation density. Each colony starts growth from one cell and in time the radius of the colony R_{col} can be calculated from the numbers of cells present because the packing density is known. We further assume that all the colonies behave similarly and the total number of cells in our system is just the summation of the number of cells in every individual colony.

The boundary conditions for equations 5 and 7 at the centre of the colony and at R_{bnd} are

$$\left(\frac{\partial P_t}{\partial r}\right)_{r=0} = 0 \qquad 9 \qquad \text{(mol.m}^{-3}\text{.m}^{-1}\text{)}$$

and

$$\left(\frac{\partial P_o}{\partial r}\right)_{r=R_{bnd}} = 0 \qquad 10 \qquad (\text{mol.m}^{-3}.\text{m}^{-1})$$

due to symmetry at these points (Crank, 1975). Additionally the concentration and flux at the common boundary at R_{col} are

$$P_i(R_{col}) = P_o(R_{col}) \qquad 11 \qquad (\text{mol.m}^{-3})$$

and

$$\left(\frac{\partial P_i}{\partial r}\right)_{R_{col}} = \left(\frac{\partial P_o}{\partial r}\right)_{R_{col}} \qquad 12 \qquad (\text{mol.m}^{-3}.\text{m}^{-1})$$

These boundary conditions and the zero initial concentration of lactic acid are sufficient to solve the coupled differential equations 1, 5 and 7.

2.2.2.Numerical solution

These equations will be solved using an implicit finite difference scheme with the appropriate time and distance discretisation to ensure a stable solution. Note that all parameters in the equations are constants and not functions of either distance or time.

2.2.3. Analytical solution

The numerical scheme is helpful because it can simulate the total growth period of *L. curvatus*. But on the other hand, it is not possible to get an intuitive feel of the growth of *L. curvatus* and a relative complex calculation scheme is necessary. An analytical solution should help because the function can be evaluated easily and characteristic numbers can be derived.

A possible analytical solution to the diffusion equations follows from a pseudo steady state approach. Diffusion gets rid of material rapidly at small distances and in this region, conditions change instantaneously. For a sphere of radius R, the relative amount of material that has diffused, E is a function of the dimensionless Fourier number Fo (Crank 1975).

$$E = 1 - \frac{6}{\pi^2}\exp\left(-\pi^2 Fo\right) \qquad 13$$

Using equations 13, the amount remaining is then only 23% for a *Fo* of 0.1. At a distance of 10 μm and a diffusion coefficient of 10^{-10} $m^2.s^{-1}$ this occurs in 0.1 seconds. At 1 mm and still using the same diffusion coefficient, it takes 17 minutes and at 1 cm it takes 27 hours. By comparing the time constants of diffusion and growth, we can define a region where a pseudo steady state condition is valid. Here during the time of growth (> time of diffusion), conditions remain essentially the same because most of the material has already diffused away.

Diffusion can be assumed to be much faster than growth by setting the characteristic time for diffusion (τ_D) to be 1/200 of the characteristic time of growth (τ_G). Using the equations in Table 3 and filling in the value of D_p given in Table 1, the distance R_{st} for which this condition is valid is ~ 200 μm. In this region we assume that a pseudo steady state exists. At this range at a certain time point, diffusion levels out production instantaneously. Using the pseudo steady state formalism equation 5 and 7 can be converted to

$$D_P\left(\frac{d^2P_i}{dr^2} + \frac{2}{r}\frac{dP_i}{dr}\right) = -q \qquad r \le R_{col} \qquad 14 \qquad (\text{mol.m}^{-3}.\text{s}^{-1})$$

Table 3: Time constants of growth and diffusion.

Time constants (s)	Using	References
$\tau_g = 3600$	$\frac{1}{\mu_m}$	Wijtzes et al. (1995)
$\tau_d = 18$	$\frac{D_P\tau_d}{R_{st}^2} = 0.1 = Fo$	Furusake (1989)

μ_m is the maximum specific growth rate of *L. curvatus* at 30 °C.

D_P is the effective diffusion coefficient of lactic acid.

R_{st} is the maximum distance where the time constant of diffusion (τ_d) is 1/200 of the time of growth (τ_g).

and

$$D_P\left(\frac{d^2P_o}{dr^2}+\frac{2}{r}\frac{dP_o}{dr}\right)=0 \qquad r > R_{col} \qquad 15 \qquad (\text{mol.m}^{-3}.\text{s}^{-1})$$

which are second order ordinary differential equations.

In order to solve these equations, the boundary condition

$$P_{r=\infty}=P_{t=0}=0 \qquad 16 \qquad (\text{mol.m}^{-3})$$

had to be used instead of the boundary condition depicted by equation 10. Initially, the concentration of P at the living space boundary R_{bnd} will not change at all (equation 10) and the analytical solution will be a good approximation. All other initial and boundary conditions remained the same. Note that the volumetric production rate (q) in equation 14 has further being simplified by assuming that it is a constant. This is valid as long as the amount of lactic acid produced is too little to cause a change in pH. If there is no change of pH, the specific growth rate remains unchanged also.

The general solutions of equations 1, 14 and 15 are presented in Table 4. They contain 4 unknowns a, b, c and d which are integration constants.

Table 4: Analytical solutions of the pseudo steady state condition.

eqn. no	Analytical solution	units
1	$N_t=\exp(\mu_m t_G)$	cell.colony^{-1}
14	$P_i=-\frac{q}{D_P}\frac{r^2}{6}-\frac{a}{r}+b$	mol.m^{-3}
15	$P_o=c-\frac{d}{r}$	mol.m^{-3}

N_t is the number of cells in a colony, which develops from 1 cell and t_G is time of growth after a lag period.

a, b, c and d are the integration constants.

μ_m is the maximum specific growth rate of *L. curvatus* at 30 °C.

q is the volumetric production rate of lactic acid.

D_p is the effective diffusion coefficient of lactic acid.

Applying the boundary condition and initial conditions (Appendix 1A) yields

$$P_i = \frac{q}{2D_P}\left(R_{col}^2 - \frac{r^2}{3}\right) \qquad r \le R_{col} \qquad 17 \qquad (\text{mol.m}^{-3})$$

and

$$P_o = \frac{1}{3}\frac{q}{D_P}\frac{R_{col}^3}{r} \qquad r > R_{col} \qquad 18 \qquad (\text{mol.m}^{-3})$$

where the concentration of lactic acid inside the colony increases with the square of the colony radius, while the concentration of lactic acid outside the colony increases with the cube of the colony radius.

Fig. 2 shows the results of using the above analytical solutions. The parameters q and D_P were kept constant but the radius of the colony R_{col} was increased for each curve. The vertical bars (at 10, 20, 30, 40, 50 μm) indicate the location of the colony radius. Qualitatively it shows that as the radius of the colony increases, the difference in concentrations between the centre and the radius also increases. The difference in concentration produces a set of varying local specific growth rates (μ_m) in the colony, which was postulated in the introduction. The

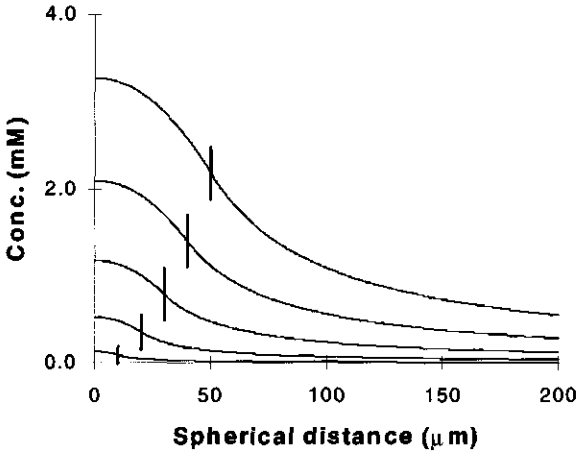

Fig. 2: Development of concentration profiles in an expanding colony (10, 20, 30, 40, 50 μm) and its surrounding using the pseudo steady state analytical solutions. The bars indicate the position of the colony radius.

validity of this pseudo steady state approach will be compared to the numerical approach.

2.3. Interactions

These analytical solutions can also give an easy and quick indication of the magnitude of the interaction time. The following dimensionless quantity

$$\frac{\overline{P}}{P\left(r = R_{col}\right)} = 1.2 \qquad 19$$

results from dividing the volume average concentration of lactic acid in a colony $\overline{P}$ by the concentration of lactic acid at R_{col} (Appendix 1B) and leads to

$$\overline{P} = 1.2\frac{q}{3D_p}R_{col}^2 \qquad 20 \quad (\text{mol.m}^{-3})$$

We next define interaction occurring when the specific growth rate is 90% of its initial maximum value (μ_m). The concentration of lactic acid P_{int} when this occurs can be calculated from equations 3 and 4 (Appendix 1B). Substituting for R_{col} (Appendix 1C) and P_{int} ($P_{\text{int}} \sim \overline{P}$) in equation 20 results in

$$P_{\text{int}} = 0.4\frac{q}{D_p}\left(\frac{0.75}{\pi}\frac{\exp\left(\mu_m t_a\right)}{n}\right)^{\frac{2}{3}} \qquad 21 \quad (\text{mol.m}^{-3})$$

and

$$t_a = \frac{1}{\mu_m}\left(\frac{3}{2}\ln\left(\frac{2.5}{q}P_{\text{int}}D_P\right) + \ln\left(\frac{4\pi n}{3}\right)\right) \qquad 22 \quad (\text{s})$$

where t_a is the time of interaction when lag is absent. Note that we are still using μ_m in equation 22, as no analytical solution is possible if μ_m changes. This is a valid assumption since μ_m has only changed by 10%. The required approximate time of interaction t_{int} with a lag period is

$$t_{\text{int}} = \lambda + t_a \qquad 23 \quad (\text{s})$$

where λ is the lag time.

3. Material and methods

3.1. Experimental technique

Frozen cultures of *L. curvatus* stored at -80 °C were thawed and pre-cultured at *pH* 5.8 (normal *pH* of MRS) in MRS (Oxoid) broth at 30 °C for 22 hours (start of the stationary phase). Serial dilutions were then made to obtain the desired initial inoculum density X_0 (cfu.ml^{-1}) for the start of the experiment. The initial inoculation densities were 1,10 and 100 cfu.ml^{-1} and the initial *pH* of the growth medium was poised at *pH* 6 and *pH* 7.

A 0.3%(w/v) MRS agar gel was prepared by dissolving the appropriate amount of MRS powder and 3 g of bacteriological agar in one litre demineralized water. A 0.3%(w/v) MRS agar gel was chosen because the colonies growing at this concentration were quite spherical in shape. Also, the inoculum could be introduced and mixed into the gel at around 35 °C before being dispensed into petri dishes. It still remains fluid at this temperature. A normal 1 %(w/v) agar has to be dispensed at about 50 °C and the *L. curvatus* cells might be heat stressed at these temperatures.

The MRS agar was then autoclaved and kept in a water bath at 50 °C. Prior to inoculation, the 0.3%(w/v) MRS agar was cooled down to 35 °C and the *pH* adjusted to the initial *pH* of the experiment adding either 5 M NaOH or HCl. An appropriate amount of X_0 was added and the agar solution stirred with a magnetic stirrer to make sure that the *L. curvatus* cells were well mixed and evenly distributed. An agar dispenser was subsequently used to distribute 35 ml of the medium in 90 mm petri dishes and allowed to solidify. In an experimental batch, about 24 petri dishes were used. The petri dishes were incubated at 30 °C for the duration of the experiment.

Sampling was done by stomaching. The contents of a petri dish was first weighed and made up to 100 g with peptone solution. The resulting solution was then stomached for 3 minutes. An appropriate amount of this solution was then serially diluted and pour-plated in standard MRS agar to enumerate the numbers of microrganisms.

4. Results and Discussion

4.1. Steady state assumptions

Fig. 3 shows a comparison between the pseudo steady state solution and the numerical solution for a colony of radius 1.6 and 20 μm. In Fig. 3a, the curves of the numerical solutions cluster together after 1 second showing that a pseudo steady state condition is reached fairly early. The pseudo steady state assumption is a valid one especially in the beginning, when R_{bnd} is very far away and the colonies are very small and do not interact with each other. Note that the change in concentration is in the order of μM when the colony radius is 1.6 μm, while at a radius of 20 μm the change is about a thousand fold, in the order of mM. These changes in the order of magnitude of the concentration are more important than the difference between the two calculation methods, when the colonies are small. At these concentrations, there will be no significant change in the *pH* (equation 4).

The main difference between the steady state analytical solution and the numerical solution can be attributed to the application of the boundary conditions at the centre of the colony (R_0) and at R_{bnd}. In the analytical solution, using reflective boundary conditions (equations 9,16) yields solutions where the integration constant *a* (Table 4) equals zero and the concentration of lactic acid at infinity also equals zero. The second condition, where the concentration of lactic acid at infinity is equal to zero implies that there is no interaction between the colonies.

We cannot use the pseudo steady state solution for the whole growth period because it is only valid until a certain radial distance from the centre of a colony (200 μm). However the steady state solutions are still very valuable for the initial, most relevant, stages of the growth process. It can tell us when interactions start to become important in colonies and whether this is significantly different from broth cultures. Interaction studies in homogeneous broth cultures of *L. curvatus* have already been carried out by Malakar et al. (1999). They also defined the onset of

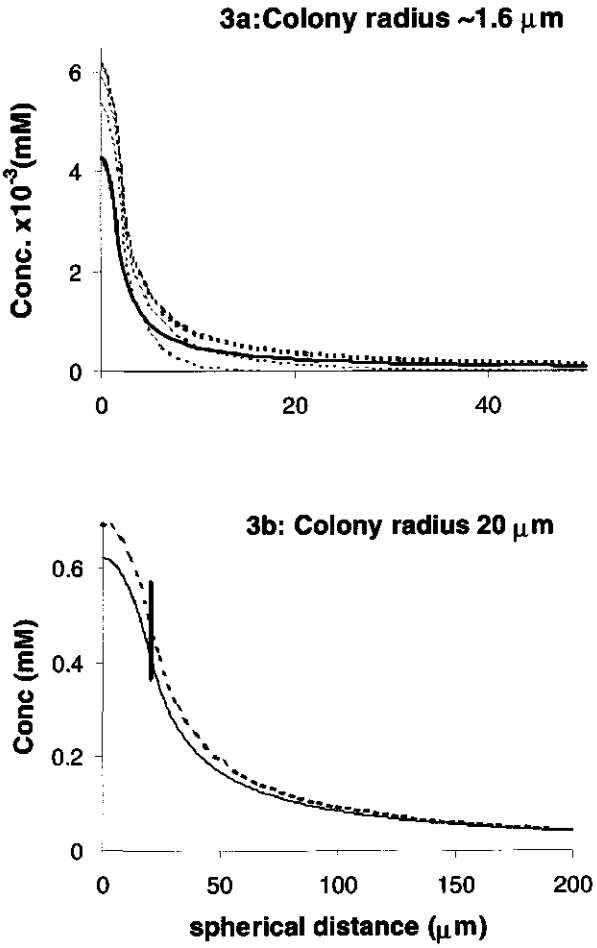

Fig. 3: Comparisons of concentration profiles produced using the pseudo steady state analytical solutions (——) and the numerical solutions (--------) for a colony of radius 1.6 and 20 μm. In Fig. 3a, the curves of the numerical solutions indicate concentration gradients at 0.1, 1, 60, 1800 and 2400 seconds. Here the colony consists of 2 cells (packing density 10^{17} cell.m^{-3}) after a doubling time of ~ 40 min. The order of magnitude of the concentration of lactic acid is μM in Fig. 3a and mM in Fig. 3b. The bar in 3b indicates the colony radius.

interaction as 10 % deviation of the specific growth rate from its maximum initial value.

4.2. Model predictions

Fig. 4 and 5 show the comparisons between growth of *L. curvatus* in broth and in agar for three different inoculation densities (1 cfu.ml^{-1}, 10 cfu.ml^{-1} and 100 cfu.ml^{-1}) at an initial *pH* of 6 and 7. The following trend can be seen in Fig. 4 and 5. As the inoculation density is decreased, growth in the agar samples starts to deviate from growth in the broth. This deviation is greatest in the sample with an inoculation density of ~ 1 cfu.ml^{-1}.

The model was able to describe these trends very well. It should be noted that these are not fits but real predictions using parameters from literature and from earlier experiments (Martens et al. 1999, Malakar et al. 1999). The lag time was the exception, as it was fitted using data from the 100 cfu.ml^{-1} experiments. There was very little difference between the analytical and numerical approaches for the first 20 hours of growth. Since this period also covers the growth phase when deviations start to occur in the agar samples, the analytical approach is a very useful tool, computationally simple, for indicating when interactions become important. The numerical solutions were able to predict the growth period till the end. Cells are just added to the edge of the colony as long as the conditions at that position are still favourable. In Fig. 4, the numerical solutions tended to overestimate the data points after 20 hours. This trend is more pronounced in Fig. 5.

One possible explanation could be the choice of the effective diffusion coefficient. We used a constant effective diffusion coefficient of $2.81 \cdot 10^{-10}$ ($m^2.s^{-1}$) for the simulations. Deceasing the effective diffusion coefficient to below 10^{-10} $m^2.s^{-1}$ causes the numerical solution to underestimate the data points after 20 hours (results not shown). The variability of effective diffusion coefficients in bacterial colonies has been reported by Mignot and Junter (1990).

Another interesting feature of Fig. 4 is the slight increase in lag time in the growth in solid medium (shifts to the right). The samples in the solid medium were inoculated at 35 °C and left to cool down to 30 °C before being placed into the 30

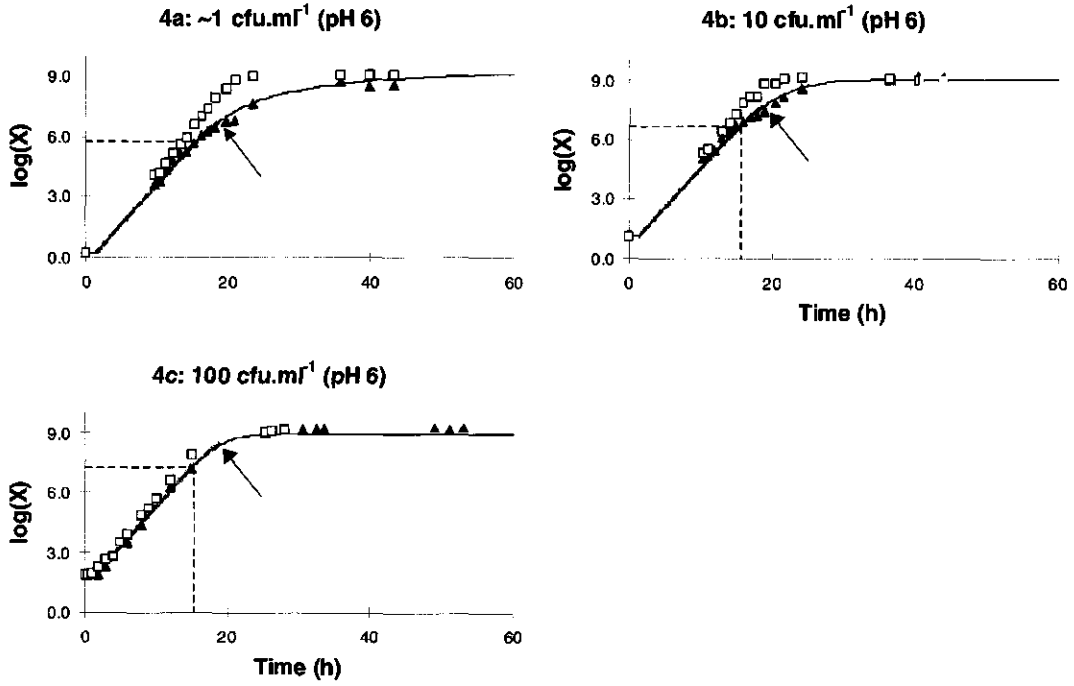

Fig. 4: Growth of *L. curvatus* at an initial *pH* of 6 in broth and in solid medium. Fig. 4a, 4b and 4c show growth data and predictions of the numerical and analytical solutions at an initial inoculation of 1, 10 and 100 cfu.ml^{-1}. The vertical and horizontal lines indicate the interaction time and interaction population density, calculated using equations 22 and 23. (▲ solid medium, □ broth, —— numerical solution, ------ analytical solution). The arrow indicates the population density for a colony of radius of 200 μm, which is the limit of the analytical solution. The analytical solution is superimposed by the numerical solution indicating minor differences between the two methods.

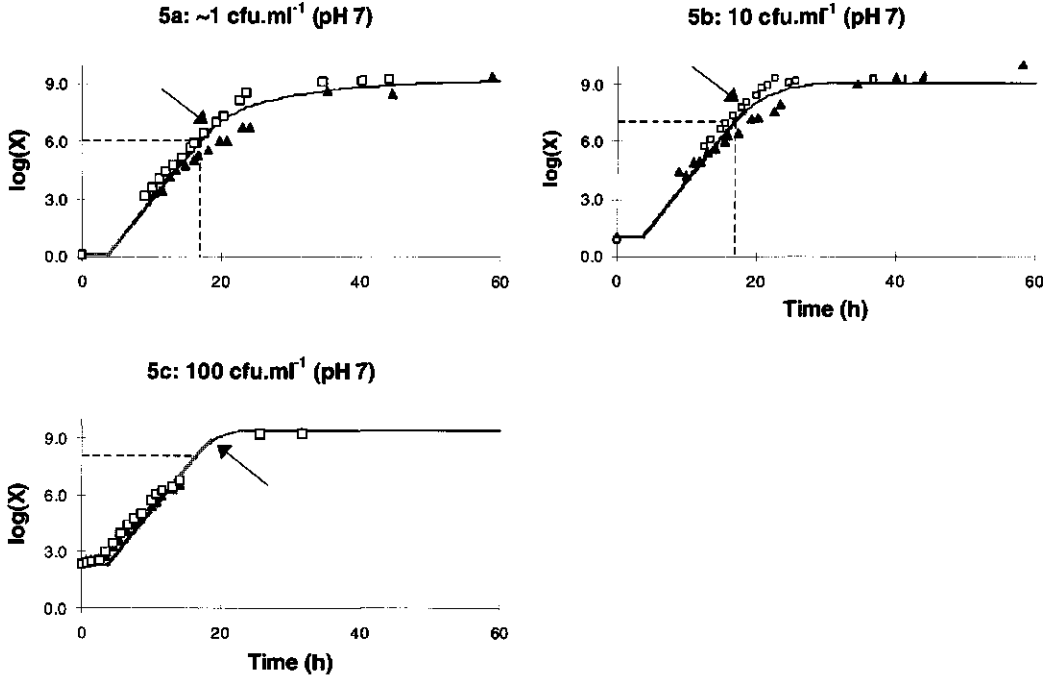

Fig. 5: Growth of *L. curvatus* at an initial *pH* of 7 in broth and in solid medium. Fig. 5a, 5b and 5c show growth data and predictions of the numerical and analytical solutions at an initial inoculation of 1, 10 and 100 cfu.ml^{-1}. The vertical and horizontal lines indicate the interaction time and interaction population density, calculated using equation 22 and 23. (▲ solid medium, □ broth, —— numerical solution, ------ analytical solution). The arrow indicates the population density for a colony of radius of 200 μm, which is the limit of the analytical solution. The analytical solution is superimposed by the numerical solution indicating minor differences between the two methods.

°C incubator. This was because this was the minimum temperature at which the agar mixture remained molten enough to allow for good mixing. This initial temperature shift maybe the source of the lag time. When inoculated at 50 °C and allowed to cool down to 30 °C, the lag time was even more pronounced (results not shown).

4.3. Interactions

For all the broth culture samples, the transition from the exponential phase to the stationary phase is quite sudden. This is because near the end of the exponential phase, many cells are present and a doubling of such a huge number of cells will only shorten the onset of the stationary phase. In the agar cultures, there is a more gradual transition from the exponential to the stationary phase in the samples with 10 cfu.ml^{-1} and 1 cfu.ml^{-1}. In these samples, the exponential phase ends much earlier due to the local accumulation of lactic acid in the colonies. The cells in the centre of the colony start to slow down their growth thus decreasing the volume averaged specific growth rate $\overline{\mu}_m$. The vertical lines in Fig. 4 show the predicted interaction times during which, the $\overline{\mu}_m$ is changed by 10 % (analytical solution, Table 6). This should signal the end of the exponential phase in the solid medium while in the broth culture growth was still exponential.

Table 6 compares the interaction times using the various solutions of the coupled growth and diffusion equations. The concentration of lactic acid at which growth is changed by 10% from its initial maximal rate is 8.5 and 16.8 mM for a medium at an initial *pH* of *pH* 6 and *pH* 7 (Appendix 1B). At these interaction concentrations of lactic acid, the *pH* has decreased to *pH* 5.7 and 6.1 respectively. The fourth column of Table 6 shows the estimated time of interaction (t_{int}^{a}) using equations 22 and 23. The utility of using equation 22 and 23 to estimate the interaction time is evident. These two equations give prompt estimation of the interaction time, while the interaction times for the pseudo steady state analytical (t_{int}^{b}) and numerical (t_{int}^{c}) solutions (column 5 and 6, Table 6) can only be estimated by running the associated Matlab programs.

where the unknown a must be zero or else no solution is possible (division by zero). The resulting concentration profile inside the colony is

$$P_i = -\frac{q}{D_p}\frac{r^2}{6} + b \qquad 25 \qquad (\text{mol.m}^{-3})$$

where b is a constant of integration. The concentration outside the colony (Table 4) is given by,

$$P_o = c - \frac{d}{r} \qquad 26 \qquad (\text{mol.m}^{-3})$$

where c and d are constants of integration. At a distance very far away from the colony, the concentration of lactic acid will still be zero (boundary condition at $r(\infty)$, equation 16), resulting in

$$P_o(r=\infty) = c - 0 = 0 \qquad 27 \qquad (\text{mol.m}^{-3})$$

and thus

$$c = 0 \qquad 28 \qquad (\text{mol.m}^{-3})$$

At the radius of the colony R_{col}, the fluxes

$$\left(\frac{dP_i}{dr}\right)_{r=R_{col}} = \left(\frac{dP_o}{dr}\right)_{r=R_{col}} \qquad 29 \qquad (\text{mol.m}^{-3}.\text{m}^{-1})$$

as they share a common boundary (equation 12), and this condition results in

$$-\frac{q}{3D_p}R_{col} = \frac{d}{R_{col}^2} \qquad 30 \qquad (\text{mol.m}^{-4})$$

and

$$d = -\frac{q}{3D_p}R_{col}^3 \qquad 31 \qquad (\text{mol.m}^{-2})$$

Using condition 11 at R_{col} gives

$$-\frac{q}{D_p}\frac{R_{col}^2}{6} + b = \frac{q}{3D_p}R_{col}^2 \qquad 32 \qquad (\text{mol.m}^{-3})$$

and

$$b = \frac{q}{2D_p}R_{col}^2 \qquad 33 \qquad (\text{mol.m}^{-3})$$

This completes the search for the values of the unknowns and yields

$$P_i = \frac{q}{2D_P}\left(R_{col}^2 - \frac{r^2}{3}\right) \qquad r \le R_{col} \qquad 34 \qquad (\text{mol.m}^{-3})$$

and

$$P_o = \frac{1}{3}\frac{q}{D_P}\frac{R_{col}^3}{r} \qquad r > R_{col} \qquad 35 \qquad (\text{mol.m}^{-3})$$

which describes the concentration of lactic acid from the centre of a colony till the distance R_{bnd}

6.2. Appendix 1B

The volume averaged concentration in the colony can be derived from

$$\overline{P} = \frac{\int_0^V P(r)dV}{V} \qquad 36 \qquad (\text{mol.m}^{-3})$$

and

$$\overline{P} = \frac{3\int_0^{R_{col}} P(r)r^2 dr}{R_{col}^3} \qquad 37 \qquad (\text{mol.m}^{-3})$$

and

$$\overline{P} = \frac{3\int_0^{R_{col}} \frac{q}{2D_P}\left(R_{col}^2 r^2 - \frac{r^4}{3}\right)dr}{R_{col}^3} \qquad 38 \qquad (\text{mol.m}^{-3})$$

which equals

$$\overline{P} = \frac{3}{2D_P}\frac{q}{R_{col}^3}\left[R_{col}^2\frac{r^3}{3} - \frac{r^5}{15}\right]_0^{R_{col}} \qquad 39 \qquad (\text{mol.m}^{-3})$$

resulting in

$$\overline{P} = \frac{2}{5}\frac{q}{D_p}R_{col}^2 \qquad 40 \qquad (\text{mol.m}^{-3})$$

The concentration of lactic acid at the R_{col} is

$$P\left(r = R_{col}\right) = \frac{1}{3}\frac{q}{D_p}R_{col}^2 \qquad 41 \qquad (\text{mol.m}^{-3})$$

and dividing this concentration by the volume averaged concentration yields

$$\frac{\overline{P}}{P\left(r = R_{col}\right)} = 1.2 \qquad 42 \quad (-)$$

which is a dimensionless quantity. Interactions occur when the specific growth rate μ_{int} is 90% of its initial value μ_m, given by

$$\mu_{int} = 0.9\mu_m \qquad 43 \quad (s^{-1})$$

Since the substrate term in the R.H.S of equation 3 is close to unity and b_2P is negligible, the pH is the most important factor decreasing the specific growth rate. Substituting the initial pH (pH_0) and interaction pH (pH_{int}) into equation 3 results in

$$\left(pH_{int} - pH_{min}\right)\left(pH_{max} - pH_{int}\right) = 0.9\left(pH_0 - pH_{min}\right)\left(pH_{max} - pH_0\right) \qquad 44$$

and solving for pH_{int} and substituting in equation 4 yields

$$P_{int} = \frac{pH_{int} - pH_0}{a_1 - a_2 pH_{int}} \qquad 45 \quad (mol.m^{-3})$$

Note that we assume μ_{int}, pH_{int} and P_{int} are approximately equal to their volume average counterpart since the specific growth rate has only changed by 10 %. If this is not assumed, then no analytical solution for the interaction time is possible

6.3. Appendix 1C

The radius of a colony developing from one cell can derived from

$$V_{col} = \frac{N}{n} = \frac{4}{3}\pi R_{col}^3 \qquad 46 \quad (m^3)$$

with

$$N = \exp(\mu_m t) \qquad 47 \quad (cell)$$

resulting in

$$R_{col} = \sqrt[3]{\frac{0.75}{\pi}\frac{\exp(\mu_m t)}{n}} \qquad 48 \quad (m)$$

where V_{col} is the volume and N the number of cell in a colony and n is the packing density

6.4. Appendix 1D

The volume averaged specific growth rate can be derived from

$$\frac{\int_0^V \mu_m(r)dV}{V} = \bar{\mu}_m \qquad 49 \qquad (s^{-1})$$

and

$$V = \frac{4}{3}\pi r^3 \qquad 50 \qquad (m^3)$$

and

$$dV = 4\pi r^2 dr \qquad 51 \qquad (m^3)$$

which yields

$$\frac{3\int_0^{R_{col}} \mu_m(r)r^2 dr}{R_{col}^3} = \bar{\mu}_m \qquad 52 \qquad (s^{-1})$$

7. Reference

1. Crank,J. 1975. The mathematics of diffusion. Oxford university press.
2. Furusake,S. Intradiffusion effect on reactivity of immobilized microrganisms. In: Bioproducts & Bioprocess. (Fiechter, Okada, and Tanner, Eds.). Springer-Verlag, Berlin, Federal Republic of Germany. 1989. 71-85.
3. Grimson,M.J., Barker,G.C. 1994. Continuum model for the spatio temporal growth of bacterial colonies. Physical Review E. 49: 1680-1684.
4. Katsaras,K., Leistner,L. 1991. Distribution and development of bacterial colonies in fermented sausages. Biofouling. 5: 115-124.
5. Luedeking,R., Piret,E.L. 1959. A kinetic study of the lactic acid fermentation. Batch process at controlled *pH*. J. Biochem. Microbiol. Technol. Engng. 1:393-412.
6. Malakar,P.K., Martens,D.E., Zwietering,M.H., Beal,C., van 't Riet,K. 1999. Modelling the interactions between *Lactobacillus curvatus* and *Enterobacter cloacae*. II. Mixed cultures and shelf life predictions. Int. J. Food Microbiol. 51:67-79.

7. Malakar,P.K., Brockelhurst,T.F., Mackie,A.R., Wilson,P.D.G., Zwietering,M.H., van 't Riet,K. 2000. Microgradients in bacterial colonies: use of fluorescence ratio imaging, a non-invasive technique. Int. J. Food Microbiol. 56: 71-80.
8. Martens,D.E., Beal,C., Malakar,P.K., Zwietering,M.H., van 't Riet,K. (1999). Modelling the interactions between *Lactobacillus curvatus* and *Enterobacter cloacae*. I. Individual growth kinetics. Int. J. Food Microbiol. 51: 53-65.
9. Mignot,L., Junter,G.A. 1990. Diffusion in immobilized-cell agar layers: Influence of microbial burden and cell morphology on the diffusion coefficients of L-malic acid and glucose. Appl. Microbiol. Biotechnol. 32: 418-423.
10. Pirt,S.J. 1975. Principles of Microbe and Cell Cultivation. Blackwell. London.
11. van 't Riet,K., Tramper,J. 1991. Basic bioreactor design. Marcel Dekker Inc. New York, USA.
12. Roels,J.A. 1983. Energetics and kinetics in biotechnology. Elsevier Biomedical Press. Amsterdam, The Netherlands.
13. Thomas,L.V., Wimpenny,J.W.T., Barker,G.C. 1997. Spatial interactions between subsurface bacterial colonies in a model system: A territory model describing the inhibition of *Listeria monocytogenes* by a lactic acid bacterium. Microbiology 143: 2575-2582.
14. Walker,S.L., Brocklehurst,T.F., Wimpenny,J.W.T. 1997. The effects of growth dynamics upon *pH* gradient formation within and around subsurface colonies of *Salmonella typhimurum*. J. Appl. Microbiol. 82: 610-614.
15. Wijtzes,T., de Wit,J.C., Huis in 't Veld,J.H.J., van 't Riet,K., Zwietering,M.H. 1995. Modelling bacterial growth of *Lactobacillus curvatus* as a function of acidity and temperature. Appl. Environ. Microbiol. 61: 2533-2539.
16. Wimpenny,J.W.T., Leistner,L., Thomas,L.V., Mitchell,A.J., Katsaras,B., Peetz,P. (1995). Submerged bacterial colonies within food and model systems: their growth, distribution and interactions. Int. J. Food Microbiol. 28: 299-315.
17. Zwietering,M.H., Jongenburger,I., Rombouts,F.M., van 't Riet,K. (1990). Modeling of the bacterial growth curve. Appl. Environ. Microbiol. 56: 1875-1881.

GENERAL DISCUSSION

In the preceding chapters we investigated two of the possible forms of microbial interactions. The first type involved an indirect interaction between two populations of bacteria namely *Lactobacillus curvatus* and *Enterobacter cloacae*. The interaction was mediated by a chemical compound secreted by one population, which had an antagonistic effect on the other, resulting in a decrease of the growth rate of the target population (amensalism). This is an important class of interaction, which is relevant to the food industry. The second type of interaction involved the effect of structure of the food matrix on the growth rate of a bacterial population. This matrix causes the bacteria to grow as bacterial colonies. We quantified this effect through the diffusive transport of substrate and by-products of metabolism in and out of these bacterial colonies.

Modelling these types of interaction is relevant for predicting microbial food safety. It allows one to quantify the importance of these phenomena when predicting microbial growth. Suppression of pathogen growth in foods by antagonistic microorganism or physical structure can be a useful tool for improving shelf life of foods. Consumers will welcome additional shelf life without the aid of preservatives.

1. Interactions in broth cultures

In Chapters 1 and 2, we confirmed that interactions between *Lactobacillus curvatus* and *E. cloacae* occurred only at high population densities in broth media. 4 mM of lactic acid produced by 10^8 cfu.ml^{-1}of *Lactobacillus curvatus* caused a 10% decrease in the growth rate of *E. cloacae*. A purely empirical method was used by Buchanan and Bagi (1997) to model the decrease of the maximum population density of *Listeria monocytogenes* by *Carnobacterium piscicola*. We

preferred a mechanistic approach as it gave a better understanding of the dynamics of the process. Models generally used in the fermentation industry form the basis of this modelling approach. A set of coupled differential equations was used to model this interaction. The growth equation used was a simple lagged exponential growth model and the consumption of substrate and production of lactic acid was assumed proportional to the growth rate. The growth rate was modelled, as a function of the *pH*, substrate and lactic acid concentration. In this dynamic system, the *pH* was found to be rate limiting for growth.

An analytical solution to the set of coupled differential equations was found and these solutions compared well to the numerical solutions in the initial most relevant region of food storage. The analytical solution for predicting the interaction population density of *Lactobacillus curvatus* in broth culture is,

$$X_{int} = X_0 \exp(\mu_m t_{int}) \qquad 1 \qquad (\text{cfu.ml}^{-1})$$

where the initial population density of *Lactobacillus curvatus* is X_0, (cfu.ml^{-1}), the maximum specific growth rate is μ_m (h^{-1}) and the time of interaction is t_{int}, (time after lag, h). When the initial concentration of lactic acid is zero and the initial population is negligible to the interaction population,

$$X_{int} = P_{int} Y_{XP} \qquad 2 \qquad (\text{cfu.ml}^{-1})$$

where P_{int} (10^{-3}M) is the concentration of lactic acid produced by *Lactobacillus curvatus,* which decreases the maximum specific growth rate of *E. cloacae* by 10% and the yield coefficient Y_{XP} (cfu.ml^{-1}) is the maximum amount of biomass produced from an amount of lactic acid produced concurrently. The key parameters in this set of equations are P_{int} and Y_{xp}. We can use these two parameters to give, a preliminary estimate of the order of magnitude of the population densities of the antagonistic and target microorganism at the point when interaction occurs. If these densities are considerably below the spoilage level, the potential of the antagonistic microorganism can be fully exploited as a protective culture. Secondly, it will be possible to rank the effectiveness of compounds secreted by the antagonistic microorganism for a specific pathogen.

Table 1 shows a list of compounds secreted by microorganisms, which can decrease the growth rate of *L. monocytogenes*. This pathogen is very important for the food industry, as it is able to grow at low temperatures. The yield data for these compounds is available in literature but the information concerning interaction concentration is scarce. In cases where this information is not available, we have used a value given by 10 % of the minimum inhibitory concentration (MIC) by assuming a linear relationship between the MIC and growth rate. This level of inhibition should allow for reduced growth, consistent with our definition of interaction in the introduction of this thesis. For organic acids, we have estimated the interaction concentration from the *pH* at which inhibition is defined to occur. Breidt and Fleming (1998) reported that the *pH* was the primary factor limiting the growth of *L. monocytogenes* in a co-culture growing with *Lactococcus lactis*. In their study the maximum growth rate of *L. monocytogenes* was 0.1 h^{-1} (at 10 °C) and we define the interaction *pH* as the *pH* when the growth rate was 90% of this value (*pH* 5.5). The interaction concentrations of these weak acids were then calculated from their titration curves in growth media (Wilson et al. 2000). The range of Y_{XP} values in Table 1 varied by about 4 orders of magnitude, from 10^{13} to 10^{17} cell.mol^{-1}. The interaction concentrations (P_{int}) varied by about 6 orders of magnitude from 0.5 μM to 0.6 M.

Column 7 of Table 1 shows the results of using equation 2. Except for the last entry, the order of magnitude of the interaction density is generally greater than 10^8 cfu.ml^{-1}. Typically, using antagonistic microorganisms to make food safe is a good strategy if performed under controlled conditions, which maximizes the growth rate and production of the inhibitor. The end product is fermented foods with the required qualities. In fact, without refrigeration, fermentation is one of the best methods of making foods shelf stable. Note that the initial innoculum density of the antagonistic microorganism can also be an important parameter in protective cultures. The ratio of the initial inoculum density of the antagonistic microorganism to the pathogen must be sufficient enough to prevent the outgrowth of the pathogen. Using equation 1, the log increase of the pathogen can be coupled

to the log increase of the antagonistic organism, if the lag times of the organisms are zero or equal. This leads to

$$\log\left(\frac{X_p}{X_{p0}}\right)=\frac{\mu_p}{\mu_a}\log\left(\frac{X_a}{X_{a0}}\right) \qquad 3 \qquad (-)$$

where X_p and X_a are population densities at a certain point in time, X_{p0} and X_{a0} are initial population density and μ_p and μ_a are growth rates of the pathogen and antagonist. The importance of X_{a0} and X_{p0} increases when the doubling time of the antagonistic microorganism is about the same order of magnitude as the pathogen and the log increase of both is about equal.

There are of course many other products of microbial metabolism, which can interact with the target microorganism. However to be effective, both the yield value (Y_{XP}) and the interaction concentration will have to decrease by orders of magnitude. The antagonistic microorganism will have to be more efficient in producing the chemical compound, which should also be more lethal to the target microorganism.

In Table 1, only penicillin produced by *P. chrysogenum* would seem to have this property. The interaction concentration of penicillin is about 3 orders of magnitude less than the other agents. Even though the Y_{XP} value of *P. chrysogenum* is of the same order of magnitude as the other agents, with the exception of *Lactococcus lactis*, this is enough to lower its interaction population density to only 10^4 cfu.ml^{-1}. This population density is much less than the spoilage density of microorganism in food (10^6 cfu.ml^{-1}, Jay 2000).

However the potential of penicillin producing *P. chrysogenum* as a protective culture against *L. monocytogenes* is quite doubtful. This strain is a mutant strain, which has been optimised for industrial production in a fermentor over the last few decades. It is questionable whether the yield value can be sustained in real foods. Even more important, antibiotics are neither allowed nor desirable in foods, and do not have GRAS approval. Another possible candidate compound is nisin, which does have GRAS approval. However *Lactococcus lactis* does not produce this compound efficiently enough.

The analytical solutions have proven useful in order of magnitude

Table 1: Concentration of different chemical compounds produced by microorganisms, which decreases the growth rate of *L. monocytogenes* by 10 % (P_{int}) and the corresponding interaction population density of these microorgansims (X_{int}). The yield of these chemical compounds is Y_{XP}.

Inhibitor	Microorganism	P_{int} [b]	Source	Y_{XP} (cell.mol^{-1})	Source	X_{int} [c] (cfu.ml^{-1})
ethanol	*Saccharomyces uvarum*	0.1M	Oh and Marshal (1993)	$1.2 \cdot 10^{13}$	Atkinson and Mavituna (1983)	$1.2 \cdot 10^{9}$
nisin	*Lactococcus lactis*	0.3 µM	Harris et al. (1991)	$6.8 \cdot 10^{17}$	Matsusaki et al. (1996)	$2.0 \cdot 10^{8}$
lactic acid	*Lactobacillus plantarum*	19.4 mM	a	$6.4 \cdot 10^{13}$	Passos et al. (1994)	$1.2 \cdot 10^{9}$
lactic acid	*Lactobacillus delbruecki*	19.4 mM	a	$1.2 \cdot 10^{13}$	Luedeking and Piret (1959)	$2.3 \cdot 10^{8}$
acetic acid	*Escherichia coli*	27.3 mM	a	$2.4 \cdot 10^{14}$	Farmer and Liao (1997)	$6.5 \cdot 10^{9}$
citric acid	*Aspergilus niger*	8.8 mM	a	$1.4 \cdot 10^{14}$	McIntyre and McNeil (1997)	$1.2 \cdot 10^{9}$
penicilin	*Penicillium chrysogenum*	0.14 µM	Garrod et al. (1973)	$4.0 \cdot 10^{14}$	Zangirolami et al. (1997)	$5.6 \cdot 10^{4}$

a: Interaction *pH* of *L. monocytogenes* was *pH* 5.5, which was calculated from data given in Breidt and Fleming (1998). The equivalent interaction concentration was calculated from titration curves of these acids in TSB growth media (Wilson et al. 2000)

b: P_{int} is the concentration at which the growth rate of *L. monocytogenes* is inhibited by 10%.

c: X_{int} is $Y_{XP}P_{int}$ the concentration of the antagonistic organism at the time of interaction (10% inhibition)

Table 2: Interaction population density of antagonistic microorganisms (X_{int}) in foods and the relative increase or decrease of the target microorganisms (I_x) when this occurs. Included are the chemical compounds, which mediate the interaction.

Antagonist	X_{int} (cfu.ml^{-1})	Target	I_x (-)	Food type	Compound	Source
Pseudomonas sp	10^8	*Shewanella putrefaciens*	10	Fish	siderophores	Gram and Melchiorsen (1996)
Pediococcus acidilactici	10^7	*Listeria monocytogenes*	10^{-1}	Wieners	pediosin AcH	Degnan et al. (1992)
Lactobacillus plantarum	10^{10}	*Staphyloccus aureus*	10	Montasio cheese	bacteriocin	Stecchini et al. (1991(
Pediococcus pentosaceus	10^9	*Listeria monocytogenes*	1	milk	*pH*, other factors	Raccach and Geshell (1993(
Lactobacillus hilgardii	10^8	*Pediococcus pentosaceus*	$10^{0.5}$	wine	peroxide, *pH*	Rodriguez and Nadra (1995)
Rahnella aquatilis	10^7	*Listeria monocytogenes*	10	min. processed endive	unknown	Carlin et al. (1996)

I_x: the ratio of interaction target population density to the initial target population density.

calculations of interaction density. There are indications that protective cultures with the right qualities can exist. Table 2 shows some of the published data on interactions in real foods. The data demonstrates the general trend indicated by the analytical solutions. The population densities of the antagonistic microorganisms at the time of interaction are between 10^7 to 10^{10} cfu.ml^{-1}. Ross and McMeekin (1994) have also cited this general trend of interaction only at high population densities in mixed cultures.

2. Interactions in solid medium

Homogenous broth studies are only valid for predicting behaviour of bacterial populations under certain constraints. In this environment, bacterial populations are able to grow unhindered until an overall deficiency of a key metabolic component occurs or when a certain level of waste product is produced. Heterogeneous environments present microorganisms with alternative challenges. Metabolic activities of bacterial populations create gradients and further growth of the bacterial population is dependent on location e.g. with respect to a source of nutrient. In this thesis we only considered colony growth, which is caused by the structure of the food matrix. Bacterial cells are typically 1 to 2 microns in size. In this range molecular diffusion will play an important part in transporting substrates to the cells as well as transporting waste products away. But as a bacterial colony increases in size, diffusion may not be able to cope with the demands of the cells at the centre of a colony. Wimpenny et al. (1995) have shown that the size of a colony increases exponentially initially and then linearly and have attributed this to the effect of transport limitations.

In Chapter 6 of this thesis, we derived an analytical solution to the diffusion of lactic inside and outside a bacterial colony made up of *Lactobacillus curvatus* cells. The diffusion of lactic acid and the concurrent decrease of *pH* is rate limiting for growth. Subject to certain constraints, the intra and extra colonial concentration profile of lactic acid is given by,

$$P_{col} = \frac{q_{col}}{2D_P}\left(R_{col}^2 - \frac{r^2}{3}\right) \qquad r \le R_{col} \qquad 4 \qquad \text{mol.m}^{-3}$$

and

$$P_{out} = \frac{1}{3}\frac{q_{col}}{D_p}\frac{R_{col}^3}{r} \qquad r > R_{col} \qquad 5 \qquad \text{mol.m}^{-3}$$

where P_{col} and P_{out} (mol.m^{-3}) are the concentration of lactic acid inside and outside a colony, q_{col} (mol.s^{-1}.m^{-3}) is the volumetric production rate of lactic acid, D_p (m^2.s^{-1}) is the effective diffusion coefficient of lactic acid and R_{col} (m) is the colony radius. These analytical solutions are only valid within a spherical distance from the centre of a colony and when interactions between colonies are still negligible. This spherical distance is estimated by comparing the characteristic time of mass transport with the characteristic time of growth (Chapter 6).

Even under these constraints, the analytical solutions can be used to give insight concerning the effect of initial innoculum density of an antagonistic microorganism on its own growth and also on the growth of a target microorganism. Initial innoculum density determines the spatial distribution of colonies and depending on the distances of separation between colonies, intra colony interactions and inter colony interactions can have important consequences for growth. The analytical solutions also give an indication of the importance of the magnitude of the diffusion parameter when comparing growth in broth and in colonies.

In Chapter 6 we defined distance of separation between colonies to be

$$R_{bnd} = \frac{1}{2}\sqrt[3]{\frac{10^{-6}}{X_0}} \qquad 6 \qquad \text{(m)}$$

where X_0 (cfu.ml^{-1}) is initial inoculation density (assumed homogenous). Increasing the density causes colonies to be closer together and vice versa. When the colonies are closer together, they should start interacting with each other (inter colony interaction) sooner, due to the rapid increase in the concentration of lactic acid in the system. The lactic acid produced by one colony will start to influence growth of neighbouring colonies. Smaller colonies are formed and growth in colonies approaches broth culture growth where all bacterial cells interact instantaneously due to homogenous conditions. If colonies are further away they can grow bigger before they start interacting with each other, and intra colony

interactions become more prominent. Here inhibition of growth within the colony will occur earlier when compared to inhibition of growth in homogeneous broth conditions.

2.1. Intra colony interactions

We can visualize intra colony interaction by comparing the interaction times in a colony and in broth. The interaction time for growth in a colony (Chapter 6), which develops from one cell, is

$$t_{\text{int}} = \frac{1}{\mu_m}\left(\frac{3}{2}\ln\left(\frac{2.5}{q_{col}}P_{\text{int}}D_P\right)+\ln\left(\frac{4\pi n}{3}\right)\right) \qquad 7 \qquad \text{(h)}$$

where n is the packing density of a colony. This function is only relevant when inter colony interaction is negligible. The interaction time for broth culture (Chapter 2) is

$$t_{\text{int}} = \frac{1}{\mu_m}\ln\left(\frac{P_{\text{int}}Y_{XP}}{X_0}\frac{1}{10^6}\right) \qquad 8 \qquad \text{(h)}$$

Note that in equation 8, the initial inoculation density, X_0 (cfu.ml^{-1}) can be an important parameter when compared to equation 7. The interaction times (t_{int}) for growth in a colony and growth in broth, initiated by 1 cfu.ml^{-1} (X_0) are 14 hours and 22 hours. At 1 cfu.ml^{-1} the distance of separation between colonies (R_{bnd}) is 0.5 cm and inter colony interaction should be minimal, as the size of a colony at the time of interaction is ~ 90 μm. The values of the parameters in equations 7 and 8 are given in Chapters 2, 3 and 5 and 6 (the initial pH is 6, the specific growth rate, μ_m is 0.9 h^{-1}, the effective diffusion coefficient, D_p is $3\cdot10^{-10}$ m^2.s^{-1}, the volumetric production rate, q_{col} is 0.78 mol.m^{-3}.s^{-1}, the packing density, n is 10^{17} cell.m^{-3}, the interaction concentration, P_{int} is 8.52 mol.m^{-3} and the yield coefficient, Y_{XP} is $3.3\cdot10^{13}$ cell.mol^{-1}).

The discrepancy in interaction times is due to diffusive transport not being able to cope with the build up of lactic acid in the colony as the colony grows and increases in size. Localised concentration gradients develop, leading to a more rapid decrease in the overall growth of cells in a colony when compared to growth

Table 3: Interactions times (t_{int}) and interaction bacterial population densities in broth culture at various initial inoculation densties (X_0).

X_0 (cfu.ml^{-1})	t_{int} (h)	X_{int} (cfu.ml^{-1})
1	22	$3 \cdot 10^8$
10	19	$3 \cdot 10^8$
100	17	$3 \cdot 10^8$
1000	14	$3 \cdot 10^8$
10000	11	$3 \cdot 10^8$

Both t_{int} (utilizing equation 8) and X_{int} (utilizing equation 1) were calculated using a specific growth rate μ_m of 0.9 (h^{-1}).

in broth. Therefore interaction takes place earlier in colony growth. The steeper the concentration gradient in a colony, the greater is the discrepancy between the interaction times. Experimental evidence indicates that at inoculation densities of ~ 10 cfu.ml^{-1} differences exist between growth in broth and growth in colonies (Chapter 6, Fig. 4b, 5b). These differences become more pronounced as the inoculation density is decreased. However, the difference occurs only after a large outgrowth of a colony (more than 5 logs).

Equation 8 shows that the interaction time, t_{int} of a broth culture decreases as the inoculation density, X_0 increases. We expect the broth interaction time to approach the colony interaction time when inter colony interactions are not negligible anymore. Table 3 shows that this occurs above 1000 cfu.ml^{-1}. Experimental evidence indicates that at inoculation densities above 100 cfu.ml^{-1} colony growth can be approximated by broth culture growth (Chapter 6, Fig. 4c, 5c).

2.2. Inter colony interactions

As a colony increases in size and is in close proximity with its neighbours, inter colony inhibition will begin. The increasing amounts of lactic acid in the system and the concurrent decrease in *pH* will start to influence those colonies nearest to the source of the acid. Fig. 1 shows the decrease in the growth rate of *E.*

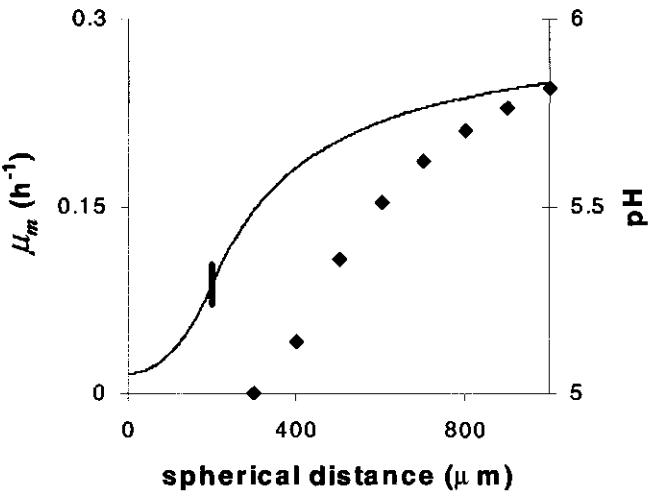

Fig. 1: The *pH* profile of a *Lactobacillus curvatus* colony of size 200 microns, which is indicated by the vertical bar and the growth rates of *E. cloacae* colonies (◆) at various distances from the centre of the *Lactobacillus curvatus* colony.

cloacae colonies, as a function of the distance from the centre of a *Lactobacillus curvatus* colony, when the initial *pH* was *pH* 6.

The *Lactobacillus curvatus* colony has a radius of about 200 microns and is made up of about 10^6 cells, calculated from a packing density of 10^{17} (cell.m^{-3}). The lactic acid concentration profile of this colony (eq. 4 and 5) was converted to a *pH* profile (secondary axis, Fig. 1) and used to calculate the growth rates of the *E. cloacae* colonies. These growth rates were calculated from the growth model of *E. cloacae* given in Chapter 2. Within a distance of 100 microns from the outer edge of the *Lactobacillus curvatus* colony, the growth rate of a colony of *E. cloacae* is zero because its minimum *pH* of growth is *pH* 5.56. We assume the colony diameter remains constant when the growth rate is zero.

Qualitatively, the diameters of *E. cloacae* colonies nearest to the source of lactic acid will be smallest when compared to those further away. Chapuis and Flandrois (1994) also observed this type of behaviour in a study on the interaction of *Micrococcus* spp. and *Pseudomonas aeruginosa*. They modelled the diameter of

Micrococcus spp. colonies as a function of the distance from colonies of *Pseudomonas. aeruginosa*, which produced enzymes that had a lytic effect on *Micrococcus* cells. The diameter a *Micrococcus* colony increased with increasing distance from the source of the enzyme.

Thomas et al. (1997) showed similar results using colonies of *L. monocytogenes,* which were inhibited by colonies of nisin producing *Lactococcus lactis*. These effects can also be seen in diffusion well experiments, where a zone of inhibition builds up around a colony producing an antimicrobial compound. In this zone, there are no colonies of the target microorgansim present.

2.3. Implications

Intra and inter colony interaction can be an important factor for ensuring safe foods, which depends on microbial interactions in solid medium. Here we rely on inter colony interaction of the antagonistic microorganism to prevent pathogenic microorgansim from proliferating in foods. If the distance between antagonistic colonies (R_{bnd}) is above a certain minimum (R_{safe}), the safety of these foods will be compromised because inter colony interaction will be delayed. A pathogenic colony may be able to grow unhindered and cause problems later.

The problem relating to R_{bnd} is a valid concern because mixing will be incomplete in some foods, resulting in a distribution of R_{bnd} for the antagonistic microorganisms. Instead of a homogenous distribution of colonies, in the non ideal case (inhomogeneous distribution), there are regions of space, which have sparse number of colonies. Therefore there is a finite probability that pathogenic colonies located in these sparse regions will be able to grow and become dangerous.

Thomas et al. (1997), using a Poisson distribution of separation distance between colonies of nisin producing *Lactococcus. lactis* and *L. monocytogenes* concluded that statistical variations lead to less inhibition of *L. monocytogenes* by nisin. To guarantee adequate safety, we must ensure that the probability of the existence of these sparse regions should be very small.

2.4. Effect of the magnitude of the diffusion coefficient

Another important feature of equations 4 and 5 is the influence of the effective diffusion coefficient of lactic acid, D_p and the volumetric production rate of lactic acid q_{col} in a colony. These two parameters are linked because D_p influences the concentration profile, which determines the growth rate and therefore the volumetric production rate q_{col}. Fig. 2a shows the of effect of increasing D_p from 10^{-10} to 10^{-9} $m^2.s^{-1}$ on the concentration profile and volumetric production rate for a colony, which grows from 1 cell to a colony of radius of 100 μm. The initial *pH* is *pH* 6. Note that we still make use of the analytical solutions but apply an updating process to allow for growth and for an increase in the diameter of a colony (Chapter 6). In Fig. 2a, the concentration profile of lactic acid becomes flatter as D_p increases from 10^{-10} to 10^{-9} $m^2.s^{-1}$. Accumulation of lactic acid at the centre of the colony is less and the difference in the concentration of lactic acid between the centre and the edge of a colony is only 1.3 mM when D_p is 10^{-9} $m^2.s^{-1}$.

Another consequence of increasing the effective diffusion coefficient, D_p is an increase in the volumetric production rate of lactic acid, q_{col}. Fig. 2b shows the variation of D_p to q_{col}, where q_{col} tends to a constant value as D_p is increased. This asymptotic value is the initial volumetric production rate of the colony. As diffusion gets rid of the lactic acid more effectively, the resulting decrease of *pH* in the colony is less, allowing the cells in a growing colony to maintain their growth rates. This in turn keeps the volumetric production rate q_{col} at a higher level. Therefore as D_p increases, growth in a colony approaches growth in a broth culture. In both situations, all the cells in a colony and in a broth are able to grow at their initial maximal rates. Of course the growth rate will decrease when the overall *pH* becomes inhibitory in both cases.

A decrease of an order of magnitude in D_p ($10^{-9} \rightarrow 10^{-10}$ $m^2.s^{-1}$) ensures a steeper concentration profile, resulting in earlier intra colony interaction. Therefore growth in a colony will now be significantly different from growth in a broth when colonies are smaller in size. Temperature causes fluctuation in the

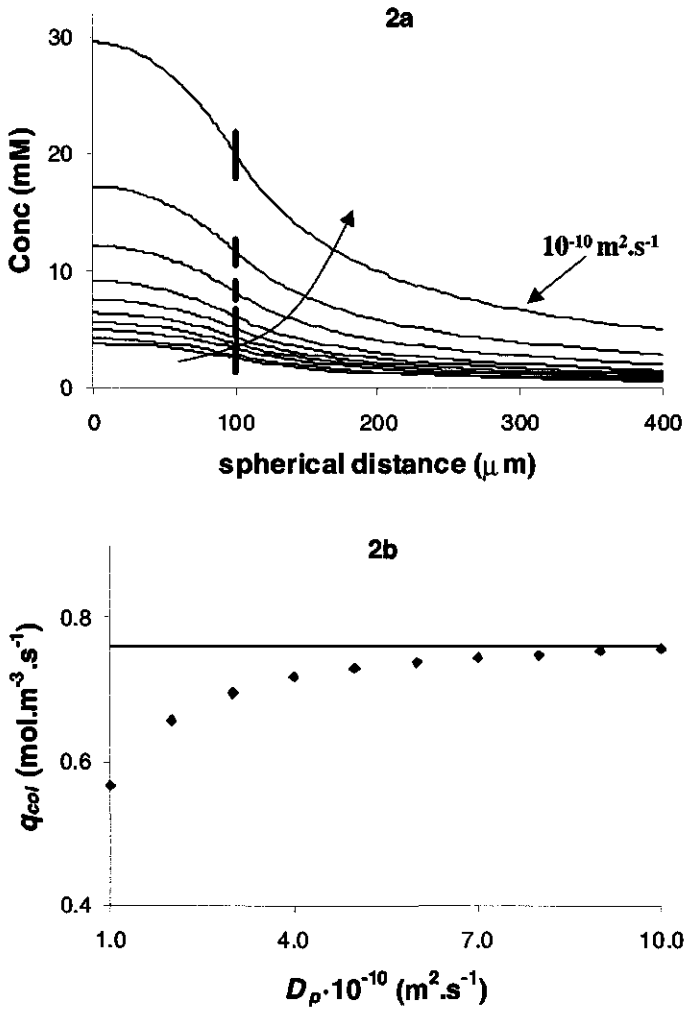

Fig. 2: The influence of the effective diffusion coefficient, D_p (at 1, 2, 3, 4, 5, 6, 7, 8, 9, and $10 \cdot 10^{-10}$ $m^2.s^{-1}$) on the concentration profile of lactic acid inside and outside a colony (radius 100 μm) and on the volumetric production rate, q_{col} of the colony. In Fig 2a, the concentration gradient becomes steeper as D_p decreases (arrow indicates decreasing D_p and vertical bar is the colony radius). In Fig. 2b, the production rate increases asymptotically (——) as D_p increases.

Table 4: The specific growth rate of *Lactobacillus curvatus* at *pH* 6 and the effective diffusion coefficient of lactic acid at different temperatures.

T (°C)	μ_m (h^{-1})	D_p [a] (10^{-10} $m^2.s^{-1}$)
5	0.06	1.88
10	0.15	2.16
20	0.45	2.81
30	0.92	3.59

μ_m: from Wijtzes et al. (1995), *a:* Arrhenius equation with activation energy (E_a) of 18.1 $kJ.mol^{-1}$ (Chu et al. 1992).

effective diffusion coefficient D_p and it is possible for colony growth to be significantly different from growth in broth at lower temperatures. However this effect could be offset by the decrease in growth rate at lower temperatures. Table 4 shows the values of D_p and the specific growth rate μ_m of *Lactobacillus curvatus* for a range of temperatures.

At fridge temperatures (5 °C), D_p is of the same order of magnitude as that at 30 °C. Since the effective diffusion coefficient is of the same order of magnitude and the growth rate has decreased by almost an order of magnitude, colony growth can be represented by broth culture growth at lower temperatures for even more conditions. The time constant of growth at 5 °C is ~17 hours compared to ~1 hour at 30 °C, thus allowing less significant build up of lactic acid (Chapter 6) in the colony at lower temperatures.

2.5. Effect of buffer capacity

Foods have various degrees of buffering capacity. Generally foods with high protein contents will have higher buffering capacity due to the many carboxyl and ammonium groups on the amino acid fragments. In this thesis, we have used the titration curve

$$pH = \frac{pH_0 + a_1[P]}{1 + a_2[P]} \qquad 9$$

to represent the buffering capacity of the growth medium, where P ($mol.m^{-3}$) is the concentration of lactic acid, pH_0 is the initial pH of the medium and a_1 ($m^3.mol^{-1}$) and a_2 ($m^3.mol^{-1}$) are fit parameters. Decreasing a_1 and a_2 increases the buffering capacity, as more lactic acid will be needed to give a change in pH. Therefore in systems where the buffering capacity is increased, we would expect the effect of mass transport limitation to be diminished. The pH gradients will be more gradual, leading to similarities with broth culture growth. Differences between colony and broth culture growth will only occur at very low initial inoculation densities and only after larger outgrowth. We can therefore use broth culture growth to represent colony growth for a bigger range of inoculation densities as the buffering capacity increases.

3. Final conclusion

Current thinking in microbial food safety and quality is based on acceptable levels of microorganisms and their metabolic products in foods. We have shown that microbial interactions in an amensal system only become important at population densties, which are above these safety levels. However this analysis does not apply to fermented foods. The methodology used can be easily adapted to model other types of bacterial interactions.

Colony growth is a response to food structure. In bacterial colonies, diffusion limitation acts as a constraint on growth. We have simulated colony growth and shown that these constraints only become important when colonies are allowed to reach certain sizes, which depends on the initial inoculation density. At inoculation densities above 100 $cfu.ml^{-1}$, broth culture growth is representative of colony growth. At lower densities it is representative for growth of at least 5 logs, so for most practical situations representative in the range of interest.

Microbial interactions and food structure are phenomena, which influence growth through changes in the intrinsic and possibly the extrinsic factors of foods. Modelling of bacterial interactions and effect of food structure gives insight into the dynamic nature of bacterial interactions to its environment.

4. Reference

1. Atkison,B., Mavituna,F. 1983. Biochemical Engineering and Biotechnology Handbook. The Nature Press, New York.
2. Breidt,F., Fleming, H.P. 1998. Modeling of the Competitive growth of *Listeria monocytogenes* and *Lactococcus lactis* in vegetable broth. Appl. Environ. Microbiol. 64: 3159-3165.
3. Buchanan,R.L., Bagi,L.K. 1997. Microbial competition: Effect of culture conditions on the suppression of *Listeria monocytogenes* Scott A by *Carnobacterium piscicola*. J. Food Protect. 3: 254-261.
4. Carlin,F., Nguyen-the,C., Morris,C.E. 1996. Influence of background microflora on *Listeria monocytogenes* on minimally processed fresh broad-leaved endive (*Cichorium endiva* var. *latifolia*). J. Food Protect. 59: 698-703.
5. Chapuis,C., Flandrois,J.P. 1994. Mathematical model of the interactions between *Micrococcus* spp. and *Pseudomonas aeruginosa* on agar surface. J. Appl. Bacteriol. 77: 727-732.
6. Chu,C.L., Spieß,W.E.L., Wolf,W. 1992. Diffusion of lactic acid in gels. Food Sci. Tech. 25: 470-475.
7. Degnan,A.J., Yousef,A.E., Luchansky,J.B. 1992. Use of *Pediococcus acidilactici* to control *Listeria monocytogenes* in temperature-abused vacuum-packaged wieners. J. Food Protect. 55: 98-103.
8. Farmer,W.R., Liao,J.C. 1997. Reduction of acetate production by *Escherichia coli*. Appl. Environ. Microbiol. 63: 3205-3210.
9. Garrod,L.P., Lambert,H.P., O'Grady,F., Waterworth,P.M. 1973. Antibiotic and chemotherapy. Churchill Livingstone, London.
10. Gram,L., Melchiorsen,J. 1996. Interaction between spoilage bacteria *Pseudomonas* sp. and *Shewanella putrefaciens* in fish extracts and on fish tissue. J. Appl. Bacteriol. 80: 589-595.
11. Harris,L.J., Fleming,H.P., Klaenhammer,T.R. 1991. Sensitivity and resistance of *Listeria monocytogenes* ATCC 19115, Scott A, and UAL500 to nisin. J. Food Protect. 54: 836-840.
12. Jay,J.M. 2000. Modern food microbiology. Aspen publishers, Inc. Maryland, USA.
13. Luedeking,R., Piret,E.L. 1959. A kinetic study of the lactic acid fermentation. Batch process at controlled *pH*. J. Biochem. Microbiol. Technol. Engng. 1: 393-412.

14. Matsusaki,H., Endo,N., Sonomoto,K., Ishizaki,A. 1996. Lantibiotic nisin Z fermentative production by *Lactococcus lactis* I0-1: relationship between production of the lantibiotic and lactate and cell growth. Appl. Microbiol. Biotechnol. 45: 36-40.
15. McIntyre,M., McNeil,B. 1997. Dissolved carbon dioxide effects on morphology, growth, and citrate production in *Aspergillus niger* A60. Enz. Microbiol. Tech. 20: 135-142.
16. Oh,D.H., Marshall,L. 1993. Antimicrobial activity of ethanol, glycerol monolaurate or lactic acid against *Listeria monocytogenes*. Int. J. Food Microbiol. 20: 239-246.
17. Passos,F.V., Fleming,H.P., Ollis, D.F., Felder,R.M., McFeeters,R.F. 1994. Kinetics and modeling of lactic acid production by *Lactobacillus plantarum*. Appl. Environ. Microbiol. 60: 2627-2638.
18. Raccach,M., Geshell,D.J. 1993. The inhibition of *Listeria monocytogenes* in milk by pediococci. Food Microbiol. 10: 181-186.
19. Rodriguez,A.V., Manca de Nadra,C.M. 1995. Effect of *pH* and hydrogen peroxide produced by *Lactobacillus hilgardii* on *Pediococcus pentosaceus* growth. FEMS Microbiol. Lett. 128: 59-62.
20. Ross, T., McMeekin, T.A. 1994. Predictive microbiology. Int. J. Food Microbiol. 23, 241-264.
21. Stecchini,M.L., Sarais,I., Bertoldi,M. 1991. The influence of *Lactobacillus plantarum* culture inoculation on the fate of *Staphylococcus aureus* and *Salmonella typhimurium* in Montasio cheese. Int. J. Food Microbiol. 14: 99-110.
22. Thomas,L.V., Wimpenny,J.W.T., Barker,G.C. 1997 Spatial interactions between subsurface bacterial colonies in a model system: A territory model describing the inhibition of *Listeria monocytogenes* by a nisin-producing lactic acid bacterium. Microbiology. 143: 2575-2582.
23. Wijtzes,T., de Wit,J.C., Huis in 't Veld,J.H.J., van 't Riet,K., Zwietering,M.H. 1995. Modelling bacterial growth of *Lactobacillus curvatus* as a function of acidity and temperature. Appl. Environ. Microbiol. 61: 2533-2539.
24. Wilson,P.D.G., Wilson,D.R., Waspe,C.R. 2000. Weak acids: dissociation in complex buffering systems and partitioning into oils. J. Sci. Food Agric. 80: 471-476.
25. Wimpenny,J.W.T., Leistner,L., Thomas,L.V., Mitchell,A.J., Katsaras,B., Peetz,P. 1995. Submerged bacterial colonies within food and model systems:their growth, distribution and interactions. Int. J. Food Microbiol. 28: 299-315.

26. Zangirolami,T.C., Johansen,C.L., Nielsen,J., Jorgensen,S.B. 1997. Simulation of penicillin production in fed-batch cultivations using a morphologically structured model. Biotech. Bioeng. 56: 593-604.

Summary

Current trends in the food retail market are foods, which combine easy preparation, minimum processing and have adequate shelf life. These foods must also be of high quality, have better flavour, texture, appearance and should be affordable. Another important factor is freshness and use of minimum artificial additives. And last but not least, it has to be safe, which in this thesis refers to microbial (bacterial) safety. These demands have lead to innovative food production methods as well as introducing new problems in ensuring microbial food safety.

Currently a packet of food produced in one factory can be distributed across a very wide area, which increases the possibility of spreading infections if the packet is contaminated with pathogens (disease causing bacteria). Also, the ingredients come from many different sources, compounding this problem. Improved hygienic practices and HACCP principles have been introduced to reduce or eliminate these sources of infections. Another tool is predictive microbiology, where microbial response of pathogens to the environment is quantified via mathematical models. The environment in these models is represented by the temperature, acidity, salt content, protective gaseous atmosphere and the presence of preservatives.

These models allow one to simulate the growth and destruction of pathogens computationally, and can be used to find the optimal conditions for eliminating or slowing down the growth of pathogens in foods. These simulations, combined with hygienic practices and HACCP principles offer food manufacturers a powerful set of tools to create the type of foods demanded by consumers. In developing these mathematical models, microbiologists use experimental procedures, where similar strains of pathogens are grown in a liquid environment. These experiments give

reproducible results, essential in developing mathematical models. However foods support a multitude of strains and may also be solid.

In this thesis we look into the possibilities of mixed growth in a liquid environment (different strains growing together) and growth in a non liquid environment, representative of growth in most foods. We compare these types of growth to the predictions given by the current mathematical models.

Mixed growth in a liquid environment produces significant differences from the predictions given by the current mathematical models (single strains). However, these differences only occur after the microbial population density reaches a relatively high level. These levels indicate that the food will already be spoiled, except for fermented foods, where high population densities are intended and essential for ensuring quality and microbial safety. In a non liquid environment, growth of microorganisms was similar to growth in a liquid environment, unless the initial contamination level was very low, in the region of 1 to 10 cells per gramme (equivalent to a unit volume of 1 ml). Even at these low contamination levels, these differences in growth only occur after large numbers of cells are present.

This research has shown that mixed growth and growth in non liquid environments do produce interesting growth phenomena. However in terms of the present advance in predictive microbiology, it is still valid to use the current mathematical models for prediction of growth and inactivation of pathogens in foods in most of the relevant ranges (before spoilage occurs).

Dutch Summary

Huidige trends in de levensmiddelenindustrie zijn levensmiddelen die gemakkelijke bereiding, minimale processing en een voldoende lange houdbaarheid combineren. Deze levensmiddelen moeten ook van goede kwaliteit zijn, een betere smaak, textuur, en uiterlijk hebben en moeten betaalbaar zijn. Een andere belangrijke factor is versheid en gebruik van een minimum aan kunstmatige toevoegingen. En bovendien moeten ze veilig zijn, waarbij veiligheid in dit proefschrift gericht is op microbiële (bacteriële) veiligheid. Deze criteria hebben geleid tot innovatieve levensmiddelenproductiesystemen, maar ook geleid tot het voorkomen van nieuwe problemen in het beheersen van de microbiële veiligheid.

Momenteel kunnen levensmiddelen gedistribueerd worden over erg grote afstanden, wat de mogelijkheid tot het veroorzaken van infecties vergroot als een levensmiddel besmet is met pathogenen (ziekteverwekkende bacteriën). Verder komen de ingrediënten van verschillende bronnen, wat dit probleem nog verder vergroot. Verbeterde hygiëne en HACCP principes zijn geïntroduceerd om deze bronnen van infectie te verminderen of the voorkomen. Een ander hulpmiddel is voorspellende microbiologie ("predictive microbiology"), waar de microbiële respons van pathogenen op hun omgeving wordt gekwantificeerd via wiskundige modellen. De omgeving in deze modellen wordt gerepresenteerd door de temperatuur, zuurgraad, zoutconcentratie, beschermende gasatmosfeer en de aanwezigheid van conserveringsmiddelen.

Deze modellen maken het mogelijk de groei en afsterving van micro-organismen te simuleren en kunnen gebruikt worden om de optimale condities te vinden voor het elimineren of het verlangzamen van de groei van pathogenen in levensmiddelen. Deze simulaties gecombineerd met hygiënische condities en het volgen van het HACCP-systeem, geven de levensmiddelenproducent een krachtige set van hulpmiddelen om levensmiddelen te ontwikkelen die gewenst worden door de

consument. Bij het afleiden van deze wiskundige modellen gebruiken microbiologen experimentele procedures waarbij relevante stammen van pathogenen gekweekt worden in een vloeibaar medium. Deze experimenten geven reproduceerbare resultaten, wat essentieel is voor het opstellen van wiskundige modellen. Levensmiddelen echter, maken de groei mogelijk van een groot scala aan stammen en kunnen ook niet vloeibaar zijn.

In dit proefschrift is onderzoek beschreven naar de fenomenen van mengculturen in vloeibare media (verschillende stammen simultaan gekweekt) en groei in niet vloeibare media, representatief voor groei in de meeste levensmiddelen. We vergelijken deze groeivormen met de voorspellingen van de huidige wiskundige modellen.

Gemengde groei in vloeibare media geeft relevante verschillen te zien met groei voorspeld door de huidige modellen (reine culturen). Echter, deze verschillen treden pas op nadat de microbiële populaties een relatief hoog niveau bereikt hebben. Deze niveaus geven aan dat de levensmiddelen al duidelijk aan het bederven zijn, behalve in het geval van gefermenteerde levensmiddelen, waar hoge aantallen gewenst zijn voor een goede kwaliteit en veiligheid. In niet vloeibare media is groei van micro-organismen gelijk aan groei in vloeibare media, behalve als de aanvangsbesmetting erg laag is, in de grootte-orde van 1 tot 10 cellen per gram (equivalent met een volume-eenheid van 1 ml). En zelf bij deze lage beginbesmettingen treedt dit verschil in groei pas op nadat er een groot aantal cellen aanwezig is.

Dit onderzoek laat zien dat groei in gemengde culturen en groei in niet vloeibare media interessante verschijnselen te zien geven. Echter voor de huidige voortgang in de voorspellende microbiologie blijft het gelegitimeerd de huidige wiskundige modellen voor de voorspelling van groei en afsterving van pathogenen in levensmiddelen te gebruiken in de meest relevante gebieden (voordat bederf intreedt).

Acknowledgments

I guess when all PhD students get to this section, they heave a sigh of relief. It has been a good learning experience and it is time to move on. I would never have got on this journey if it wasn't for the encouragement and support of Marjolyn. So, I dedicate this achievement to her, for her patience and understanding.

My supervisor Marcel, without whom this thesis would not have achieved its current form, is another big influence. Thank you for your comments, dedication and advice. Thank you also Klaas for letting me begin my studies at your department, even though there was no funding available then. I would also like to thank all the staff at Proceskunde for their help and for making life at the department such a pleasant one, especially Joyce and Hedy. Special thanks to Remko for his kind comments. And last but not least, to Ronald my roommate on the 6^{th} floor, for putting up with me.

Over at the IFR, I would like to thank Tim for inviting me to an interesting experience at his lab. Yvonne, thank you for helping with the job hunting. And to Gary Barker for his patience and understanding, when I took time off to complete this dissertation.

And finally to mum and dad, thank you for believing in me.

Curriculum Vitae

Born in Alor Star, Malaysia, 1962, Pradeep Malakar completed his secondary school education at Sultan Badlishah Secondary School, Kulim, Kedah, Malaysia. After receiving his Higher School Certificate in 1981, he enrolled for a Bachelor of Science course at the National University of Singapore in 1982. Majoring in Biology and Biochemistry he received his B.Sc. degree in 1985 and in 1993 was accepted for a Masters of Science course in Biotechnolgy at Wageningen Agricultural University. Majoring in Process Engineering, he completed his thesis dissertation on "Application of Expert Systems in Risk Analysis of Food" at the department of Process Engineering and received his M.Sc. degree in 1995.

From March 1996 until November 1999, he worked on this Ph.D. dissertation at the department of Process Engineering, Wageningen Agricultural University. In December 1999, he accepted a post doctoral fellowship at the department of Food Safety, Institute of Food Research, Norwich, United Kingdom, where he is currently based.